KEMPER ENGINEERING SERVICES, LLC

INTEGRATED ENGINEERING AND DESIGN

[redacted] | President
[redacted] | Principal Engineer
[redacted] | Senior Consultant

14 Jan 2018

[redacted]
President/CEO
Hydrospace Group
9559 Center Ave., Suite P
Rancho Cucamonga, CA 91730
Email: [redacted]

Ref: Preliminary evaluation of Cyclops viewport design at 5800 psi

Dear [redacted]

Based on the provided materials and our conversation, Kemper Engineering Services (KES) proposes the following estimate for services:

BACKGROUND: The Client (Hydrospace) has a hypothetical design for a submersible window. It uses PVHO-1 grade acrylic (PMMA) but does not use PVHO-1 geometry. The question posed by the Client is what benefit the domed "Cyclops" design has to a traditional conical frustum PVHO-1 design with the same seat profile. The pressure designated was 5800 psi. The window is shown below.

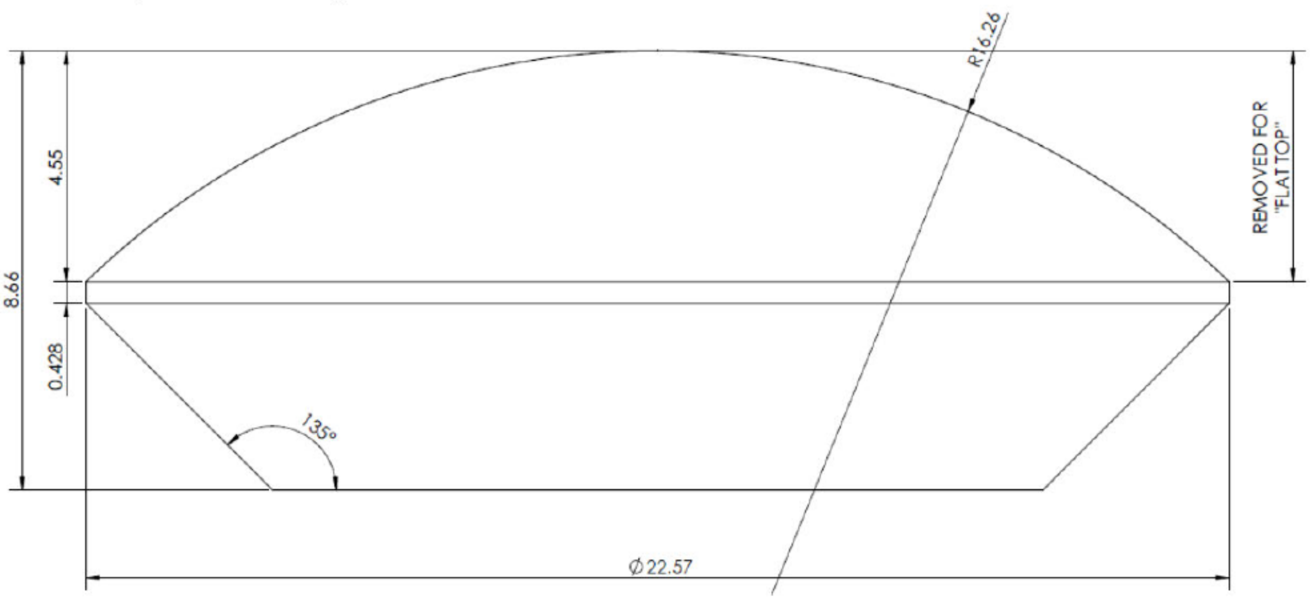

Fig. 1. Cyclops window design. Dimension are in inches. The "flat top" design is the same dimensions with the dome section removed.

METHOD: KES performed linear and nonlinear analysis. The material properties. included the stress-strain curve, is for 80F of MIL Grade 8184P acrylic. No material information was provided by the Client as this is a geometry comparison and not a design review of an actual submersible viewport. The effects of heat transfer, creep, and cyclic load are neglected in this preliminary assessment. The window seat is assumed and is only

P.O. Box 80674, Baton Rouge, LA | Tel. (225)923-2945 | Fax (225)930-0782 | www.kempereng.com | instagram: kempereng | WOSB & SDVOSB

provided to develop the boundary conditions for the viewport. Axi-symmetric modeling is used, with contact elements allowing the viewport to slide along the window seat. Nonlinear analysis is the primary focus since acrylic window is a polymer that does not behave in a purely linear manner under significant load. Linear analysis is conducted as part of a normal modeling process and is presented for reference purposes. More information is in the attached pages.

RESULTS: Given the results are above the nominal yield of 7500 psi, the strain is used to evaluate potential for failure. Axial (inwards) deflection is provided as another measure.

	Cyclops Viewport		**Flat top Viewport**	
Model	*Max Strain (in/in)*	*Deflection (in)*	*Max Strain (in/in)*	*Deflection (in)*
5800 psi Linear	0.12	0.203	0.16	0.394
5800 psi Nonlinear	0.44 (possible cyclic fail)	0.264	0.73 (catastrophic failure)	0.924
4000 psi Nonlinear	0.27 (no failure)	0.174	0.54 (failure)	0.453
2900 psi Nonlinear	0.16 (no failure)	0.123	0.33 (cyclic failure)	0.269

CONCLUSIONS: The preliminary conclusions based on the assumptions specified are as follows:

1. The Cyclops design provides more axial stiffness and generates less strain than the same seat dimensions without the domed portion.
2. The specified Cyclops design at 5800 psi indicates significant strain that is consistent with potential short cycle failure modes.
3. The specified Cyclops design at lower pressures indicate acceptable strain levels, with the 2900 psi load being most consistent with traditional PVHO windows operating within normal design conditions.
4. The “flat top” viewport design would be likely to fail at 2900 psi pressure and will fail at higher pressures.
5. Actual material data, the window seat design, and operational information would be needed to conduct a design review and performance prediction.

KES offers a full range of engineering services, including solid modeling, CAD, stress analysis, transient and dynamic analysis, fluid flow with heat transfer simulations, kinematic modeling, animations, and presentation support. While some of the services are not part of the current estimate, they are available if needed to better assist the Client in their needs.

Thank you for giving KES the opportunity to support this project.

Sincerely,

[redacted] ***P.E.***
Principal Engineer

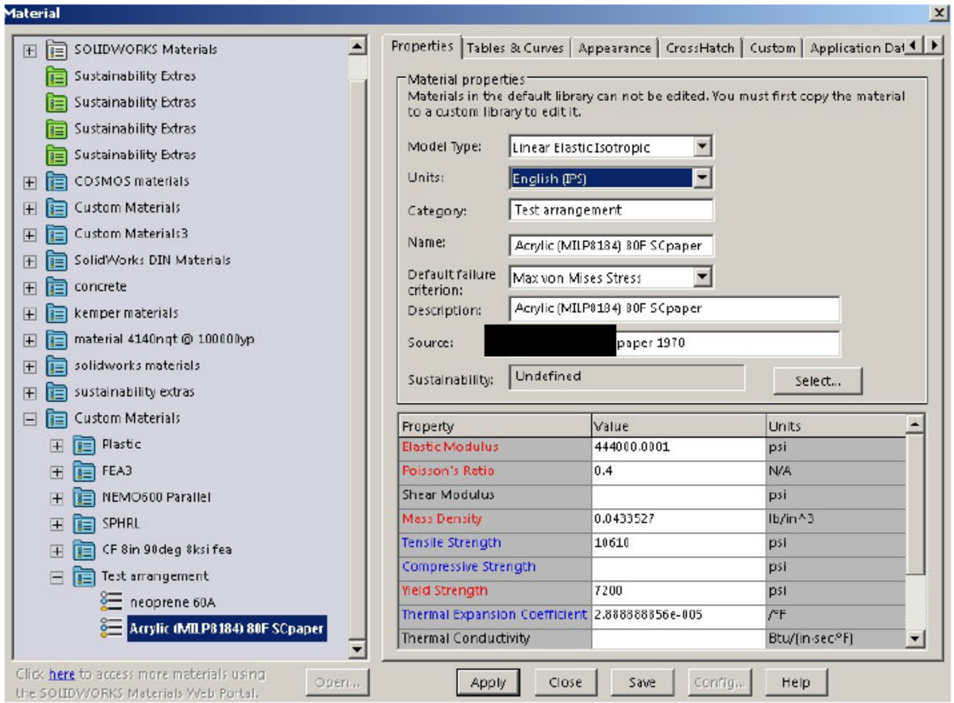

Fig. A1. Linear material specifications

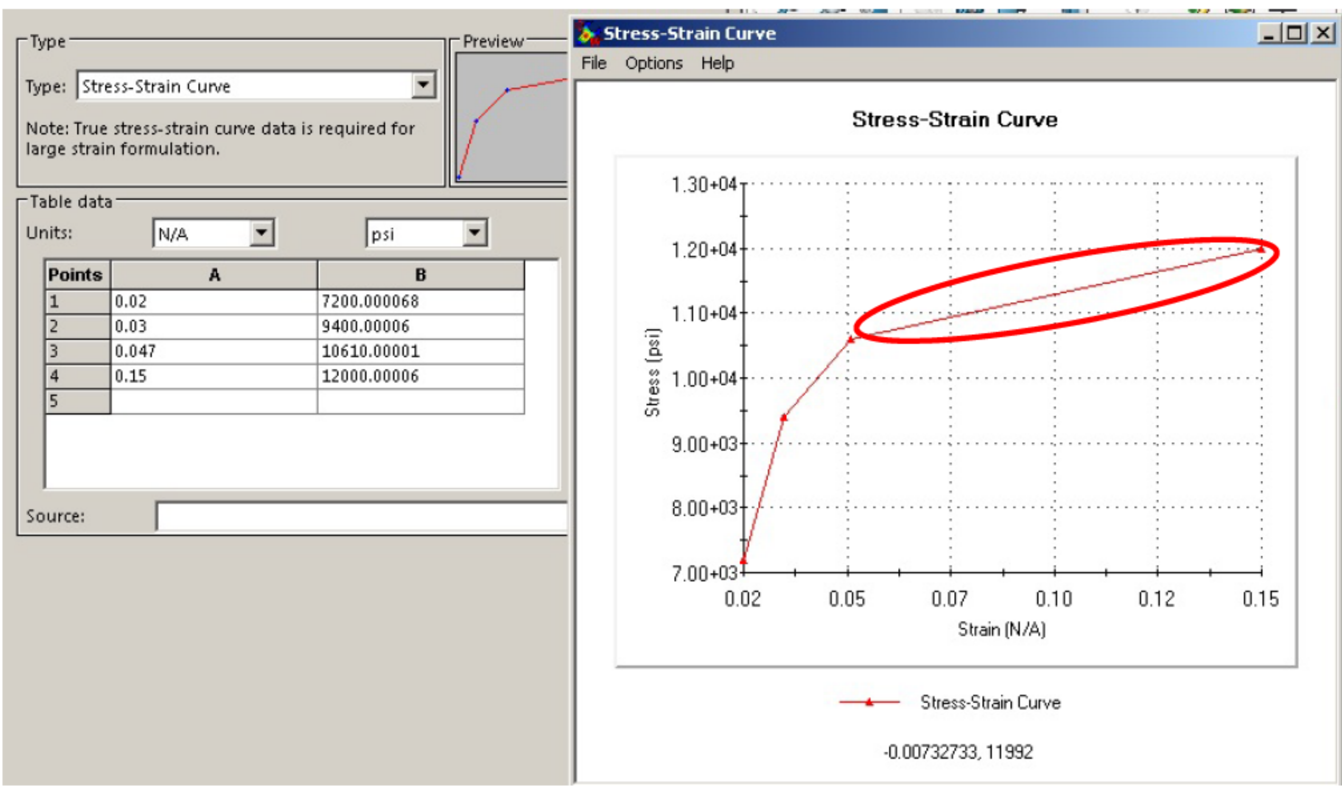

Fig. A2. Nonlinear curve used. This is for 80 degrees F, which is a mid-temperature from maximum surface ambient conditions and temperature at depth. The maximum strain is 0.05. The last segment (circled in red) is above ultimate strength to allow greater strain rate for an implicit nonlinear analysis to approximate a localized failure mode and allowing it to propagate.

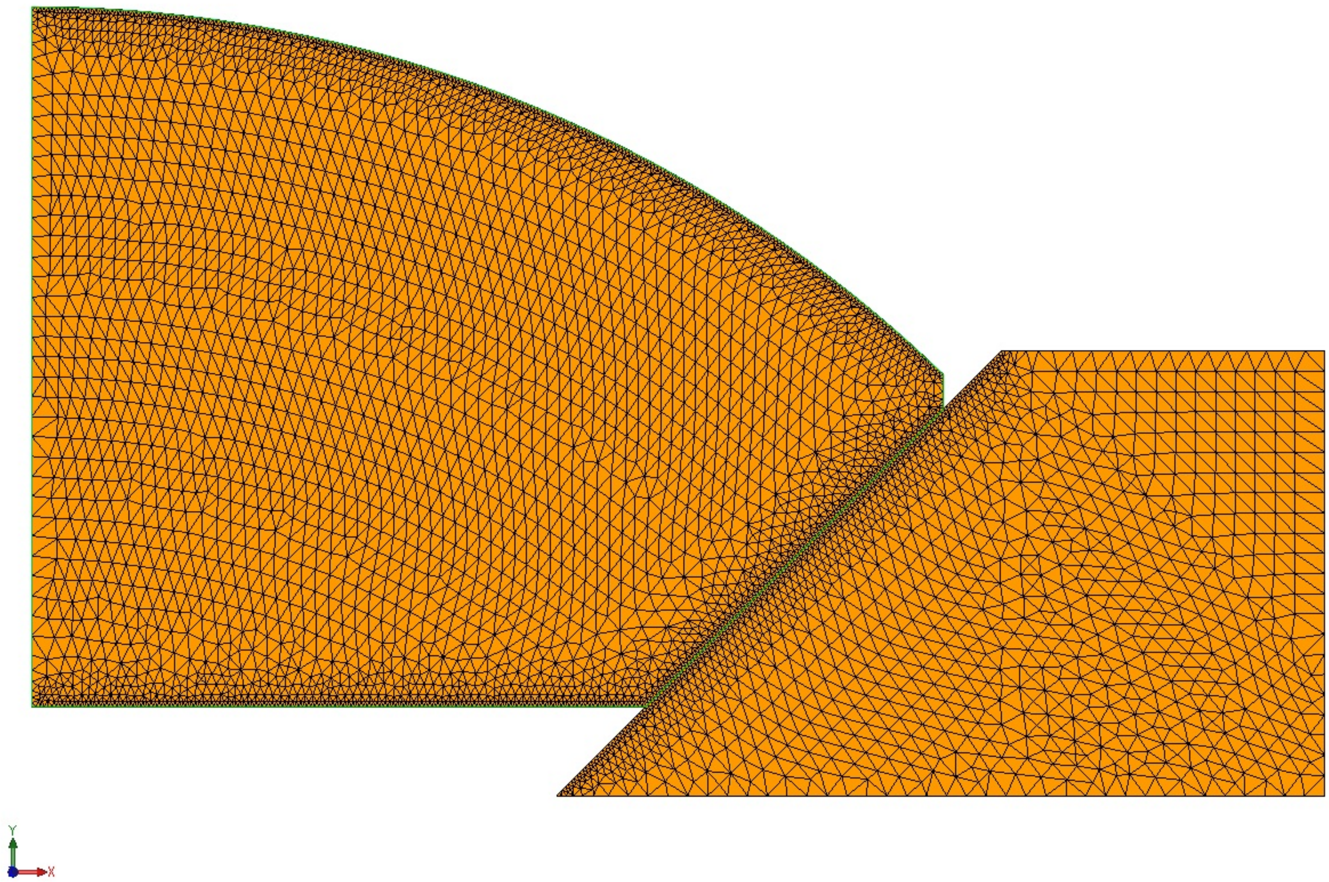

Fig. B1. Mesh for the cyclops geometry. Contact elements allow the window to slide against the fixed window seat.

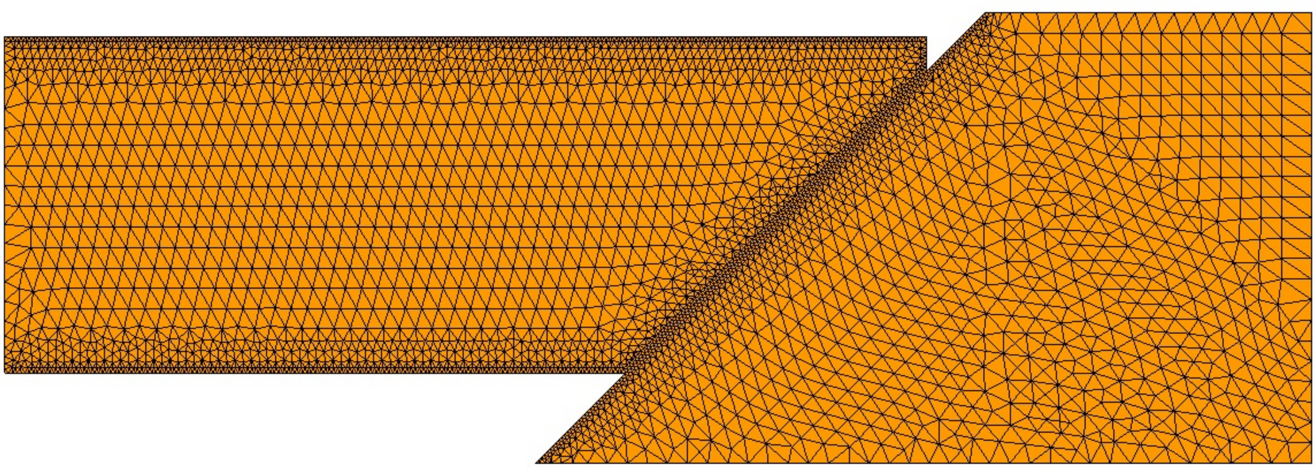

Fig. B2. Mesh for the truncated window geometry. It removes all of the material at the curved upper portion. All other dimensions are the same.

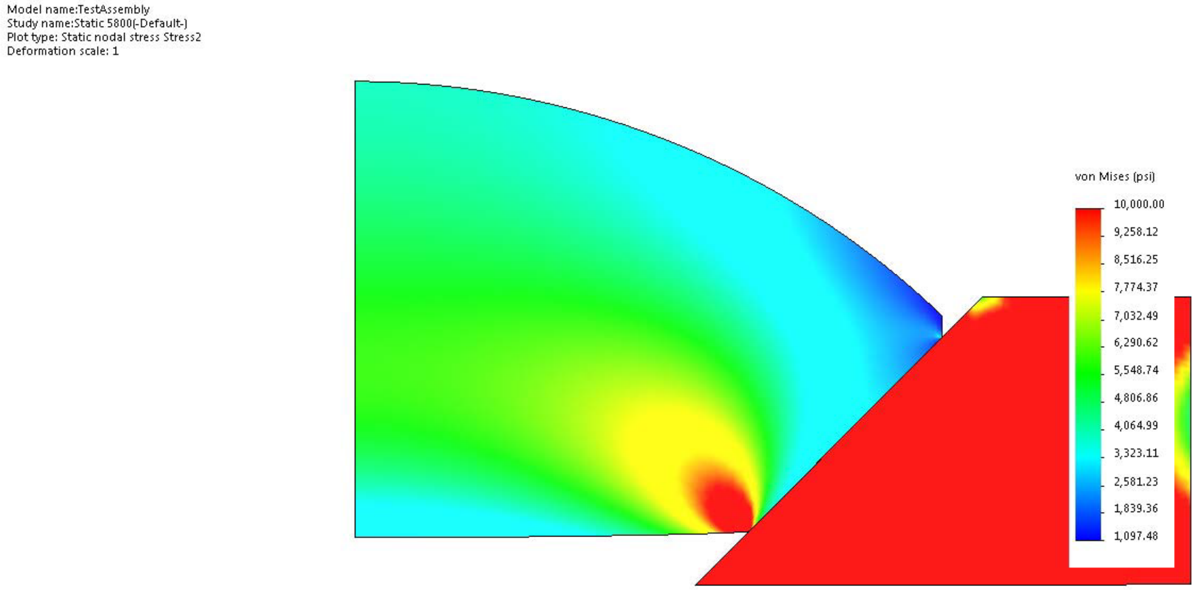

Fig. C1. Linear analysis, 5800 psi. Von mises is proportional to strain.

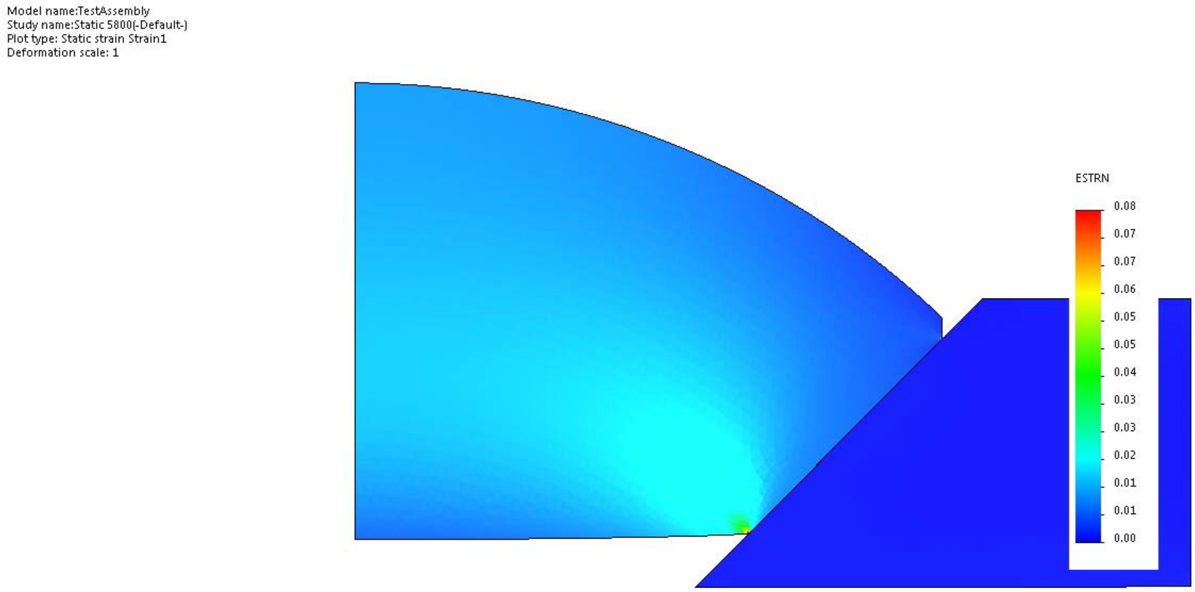

Fig. C2. Linear analysis, 5800 psi. Strain limited to 0.08 for consistency for comparison to other results. Maximum strain is 0.12.

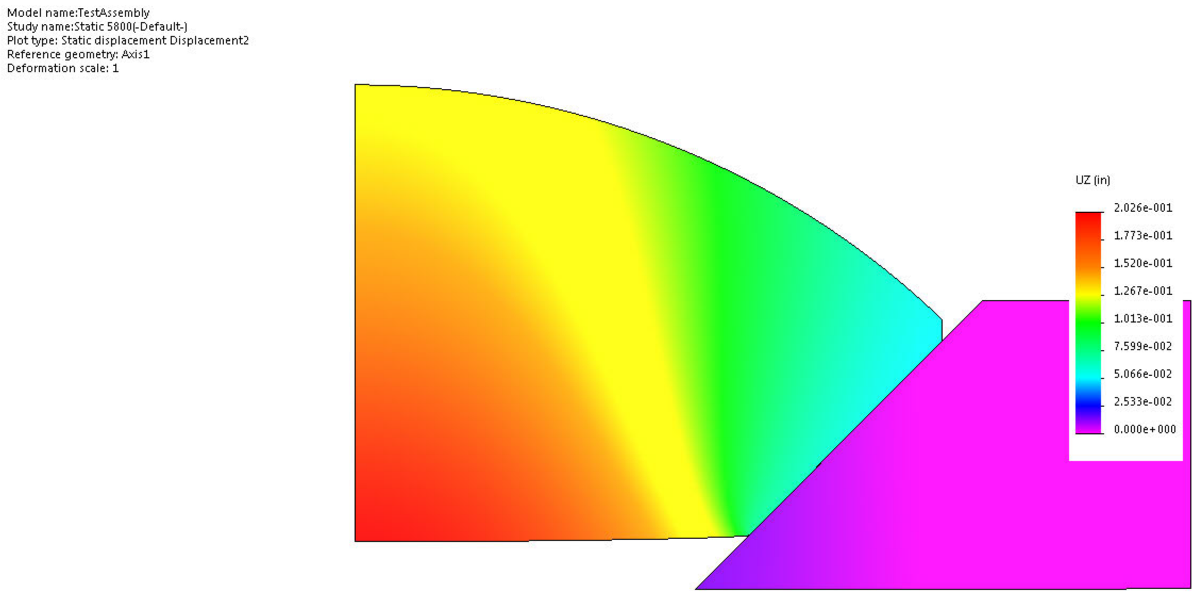

Fig. C3. Linear analysis, 5800 psi. Downwards displacement. Linear analysis is unsuitable for analyzing acrylic windows, but is being used for a purpose of comparison to the work by others.

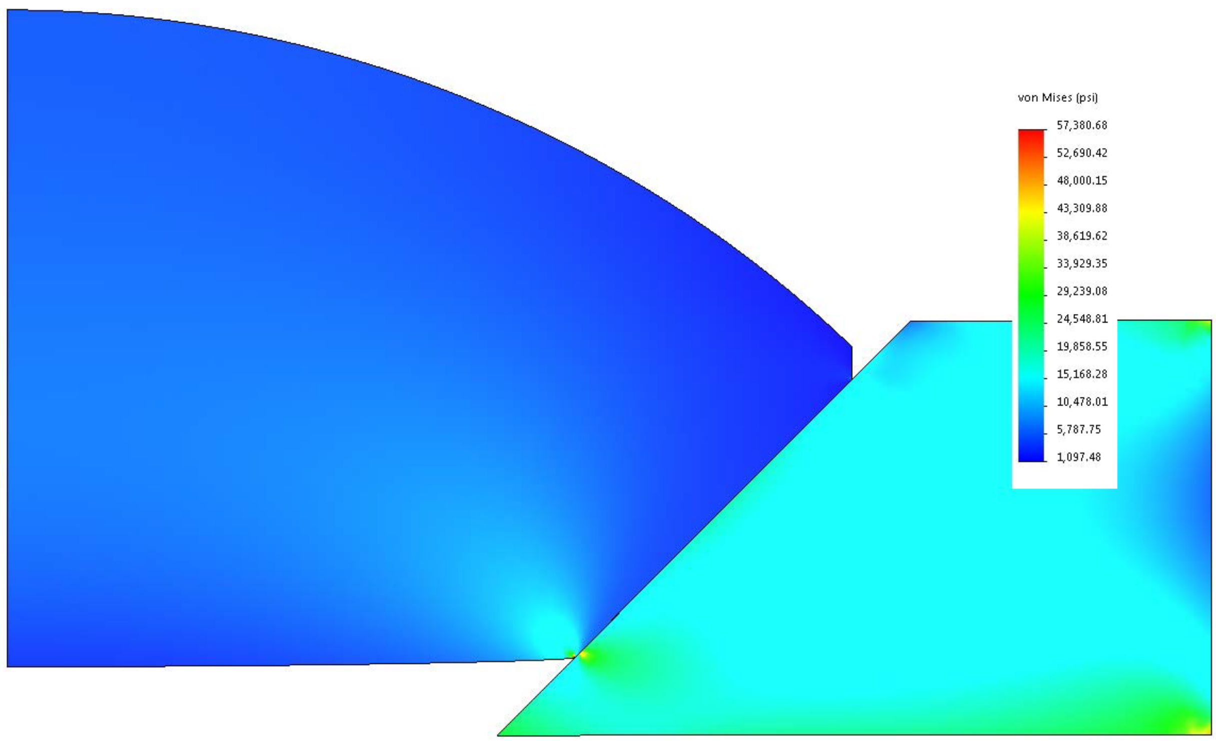

Fig. C4. Linear analysis, 5800 psi. Full range of Von Mises stresses. Peak stresses are in the window seat, which is made of steel and has a much higher yield and ultimate strength. Steel also responds in a linear manner whereas acrylic does not. Future stress plots will be limited to 10,000 psi in order to show stress differential in the viewport. The stresses in the window seat are to be disregarded. The window seat is only to provide a boundary condition for the viewport.

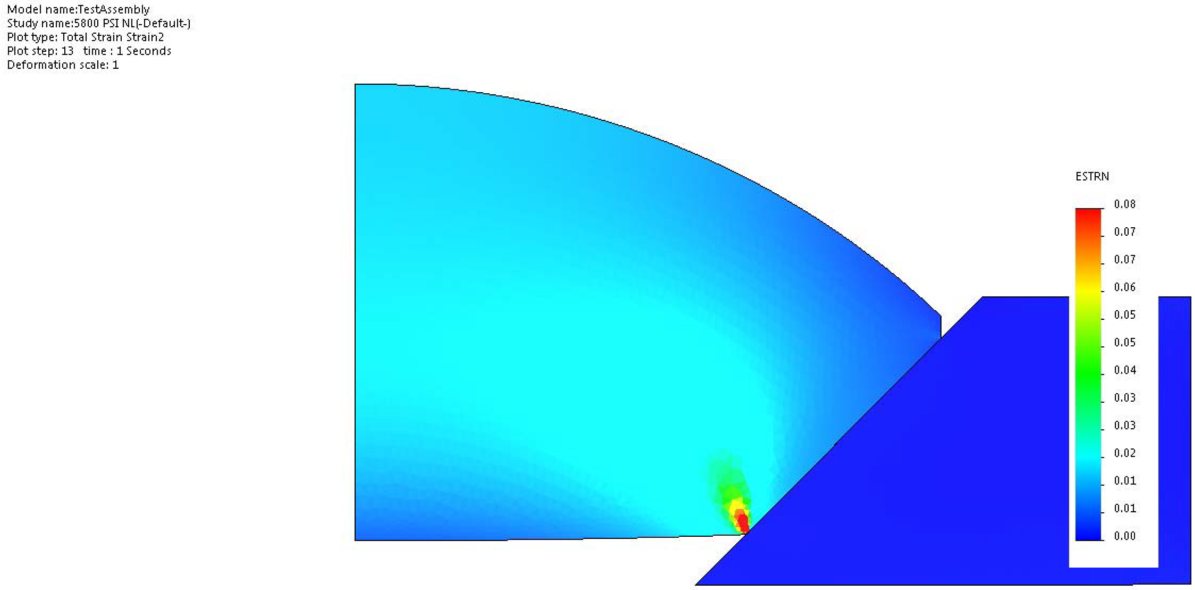

Fig. C5. Nonlinear 5800 psi strain. Strains above 0.06 (red-to-yellow) is of concern. This is consistent with cyclic failure. These results are do not account for heat transfer, dive rates, service life, or creep effects, so any conclusion regarding suitability is preliminary. The intent is to provide a preliminary comparison of the Cyclops design to a flat top design.

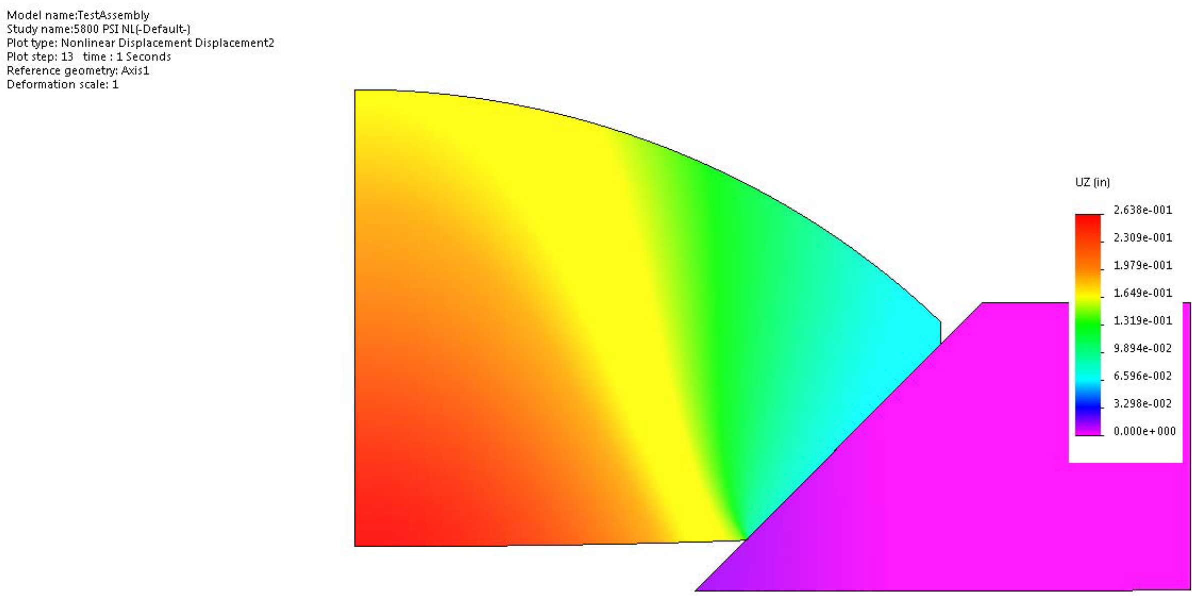

Fig. C6. Nonlinear 5800 psi displacement. Maximum downwards displacement is 0.263 inches.

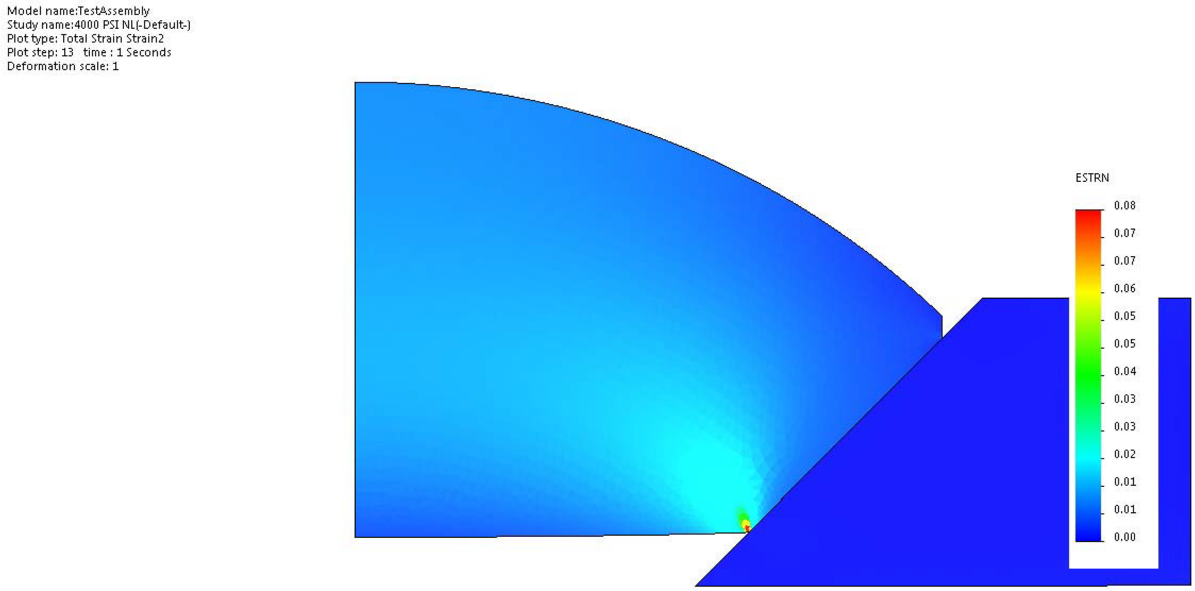

Fig. C7. Nonlinear 4000 psi. Strain constrained to 0.08. The highly localized strain indicates this is more of a case of corner stress instead of a structural concern. A corner fillet would reduce this.

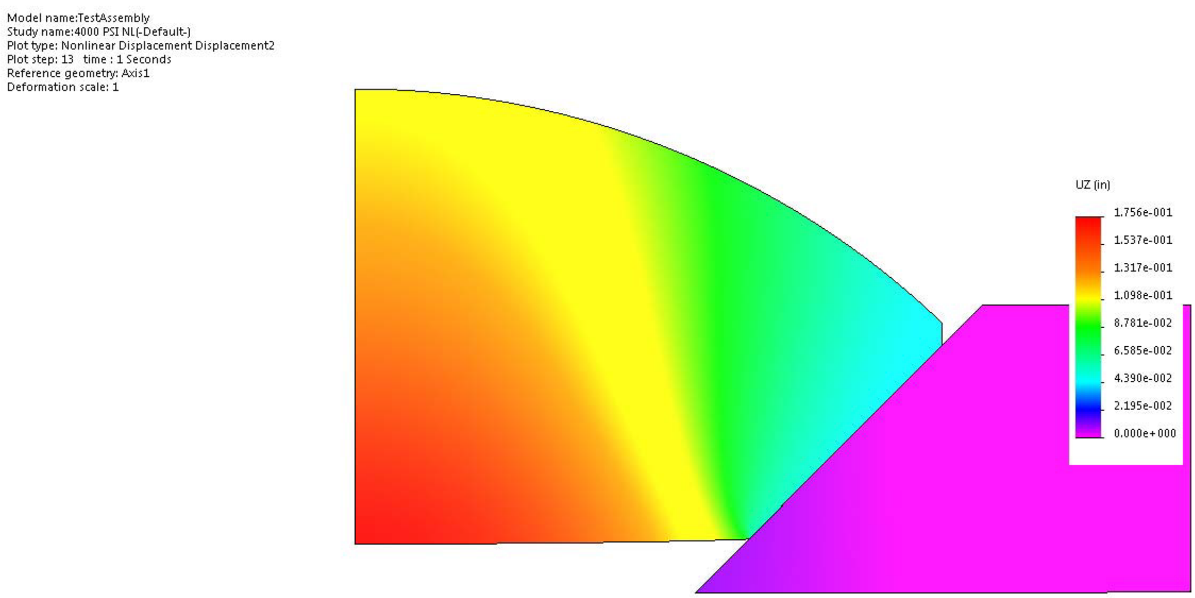

Fig. C8. Nonlinear 4000 psi. Downwards deflection is 0.176 inches

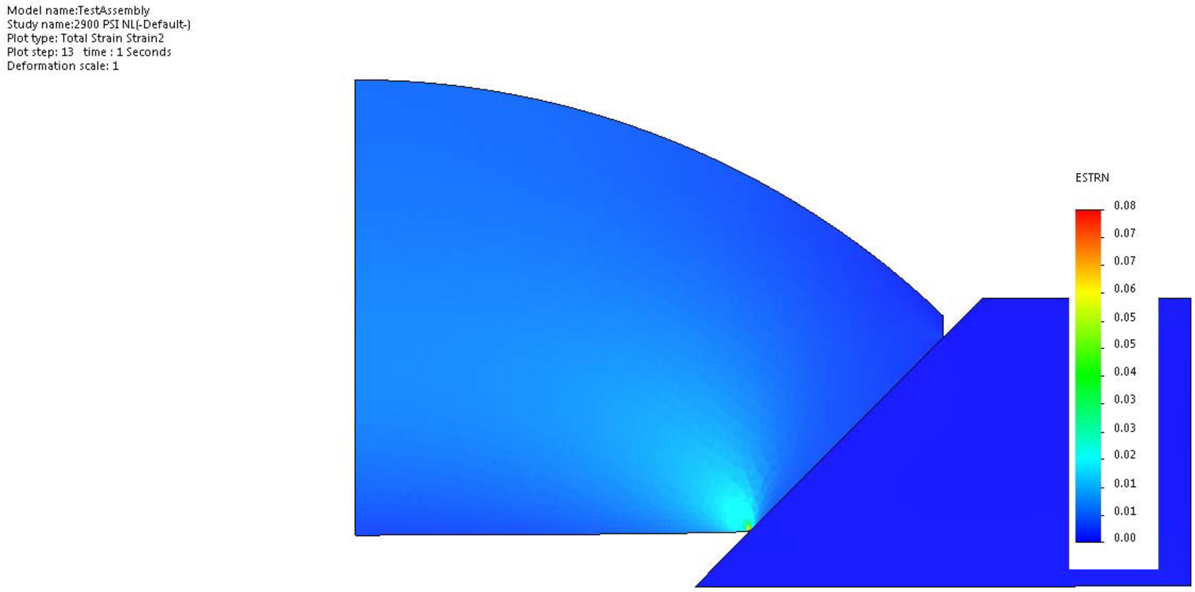

Fig. C9. Nonlinear 2900 psi. The strain is well within normal operational levels.

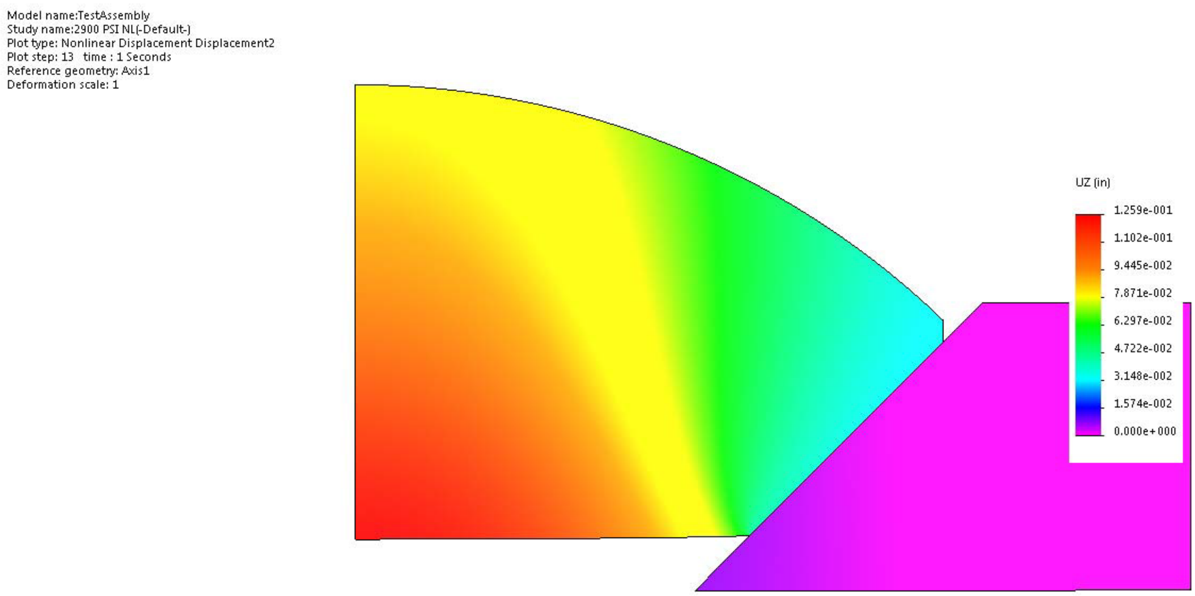

Fig. C10. Nonlinear 2900 psi. Downwards deflection.

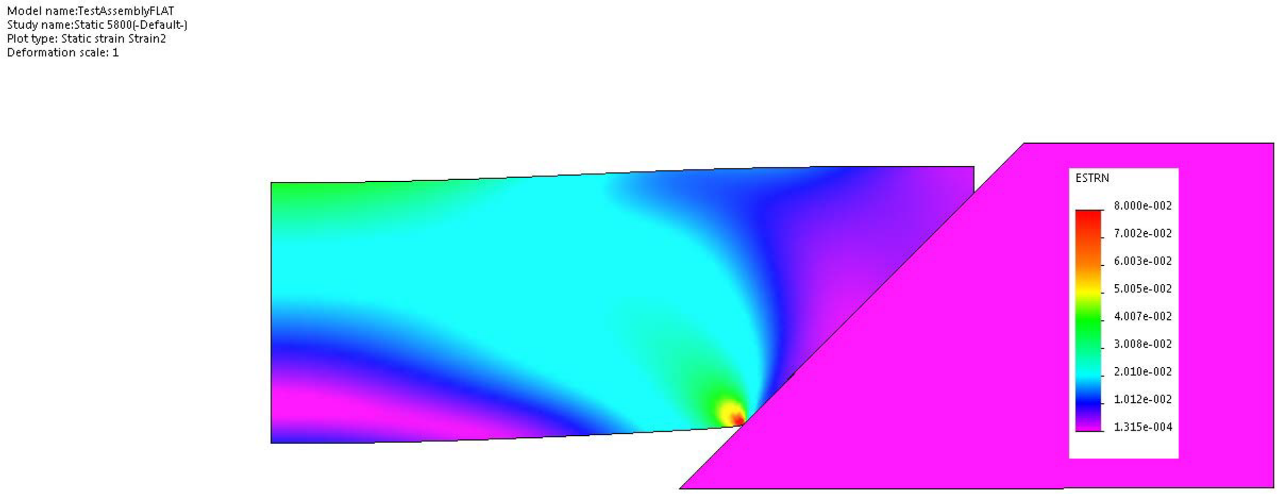

Fig. D1. Flat top, linear at 5800 psi.
The strain level is elevated in comparison to Fig. C2.

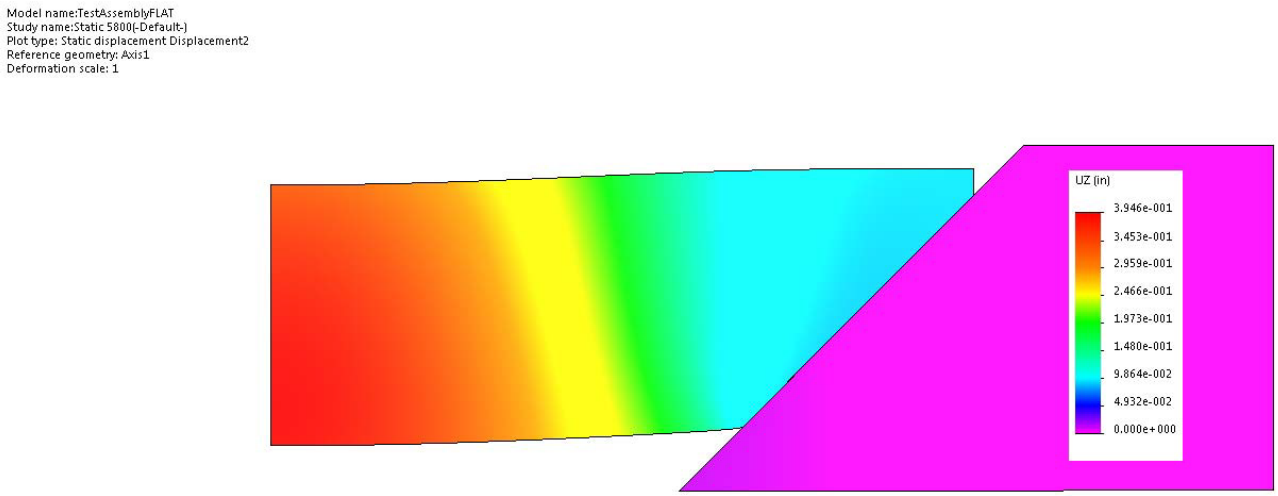

Fig. D2. Flat top, linear at 5800 psi.
The downwards deflection is almost twice the deflection of Fig. C3. The flat top design is significantly more flexible than the Cyclops design, which is consistent with the structure.

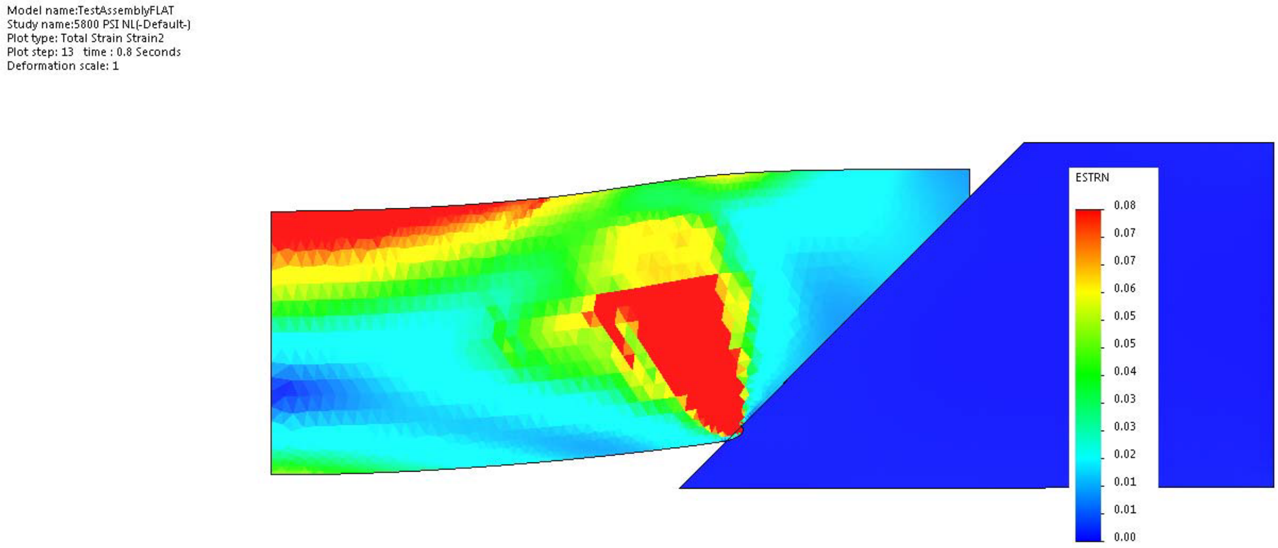

Fig. D3. Flat top window. Nonlinear at 5800 psi pressure. Strain levels and gradients indicate failure.

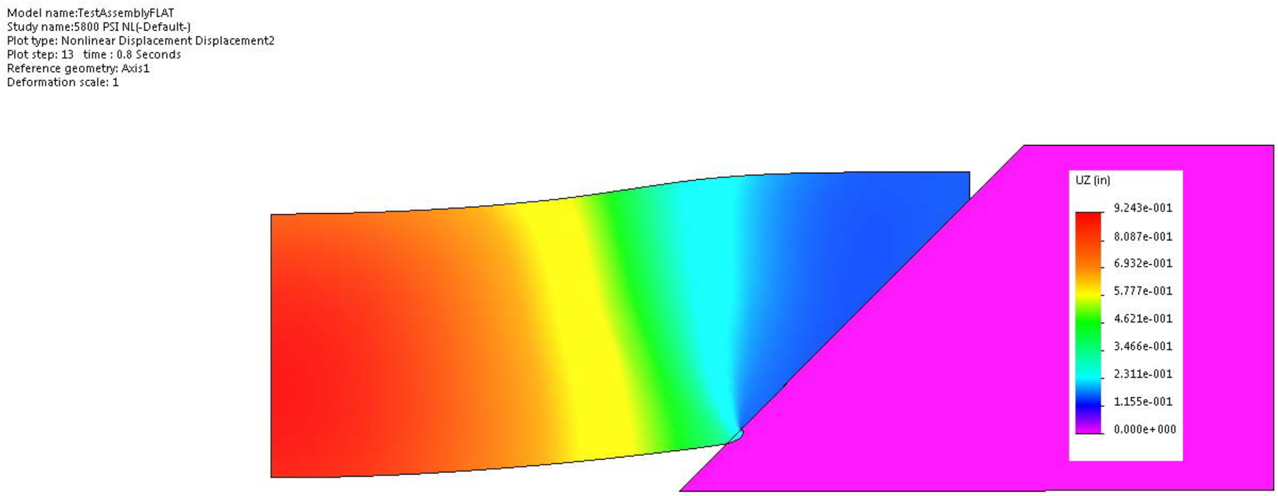

Fig. D4. Flat top window. Nonlinear deflection at 5800 psi pressure. Deflection is over 3 times the Cyclops design and is consistent with failure.

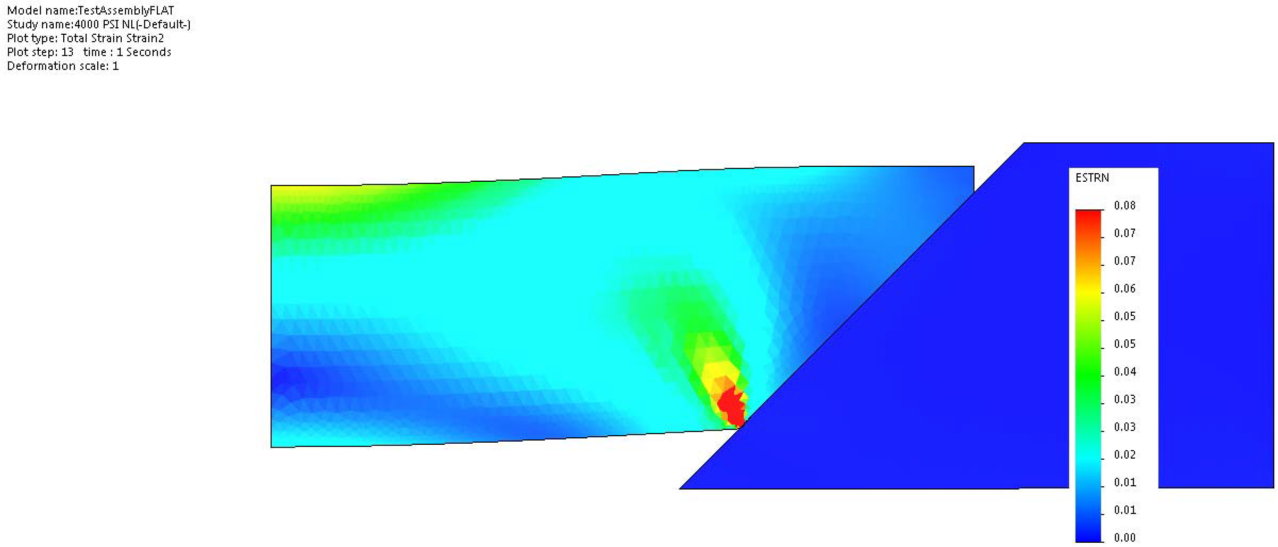

Fig. D5. Nonlinear flat top at 4000 psi. Strain profile is consistent with short cycle failure.

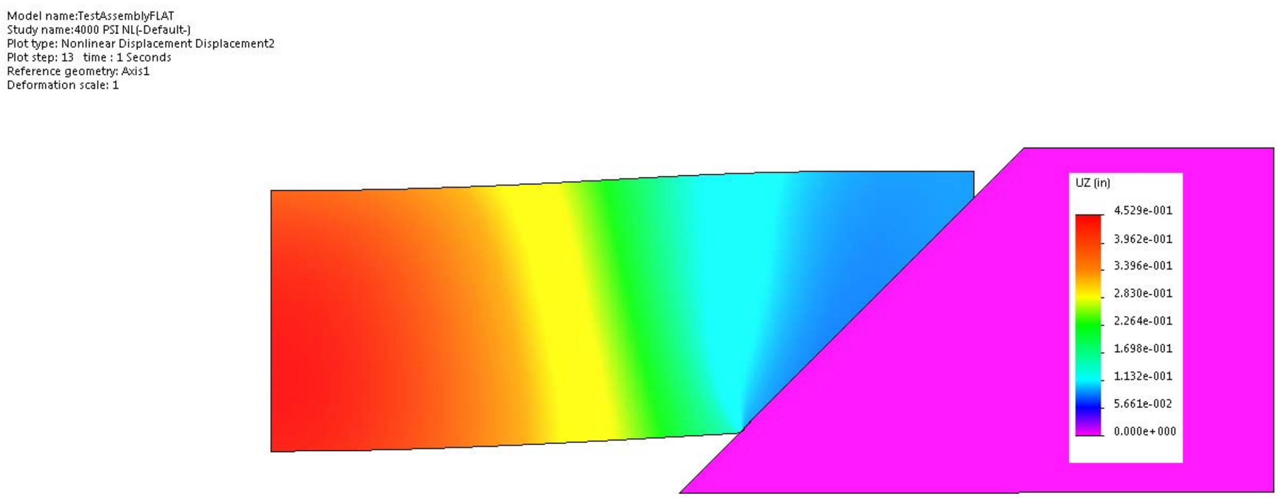

Fig. D6. Nonlinear flattop deflection at 4000 psi. Deflection is over twice the Cyclops design.

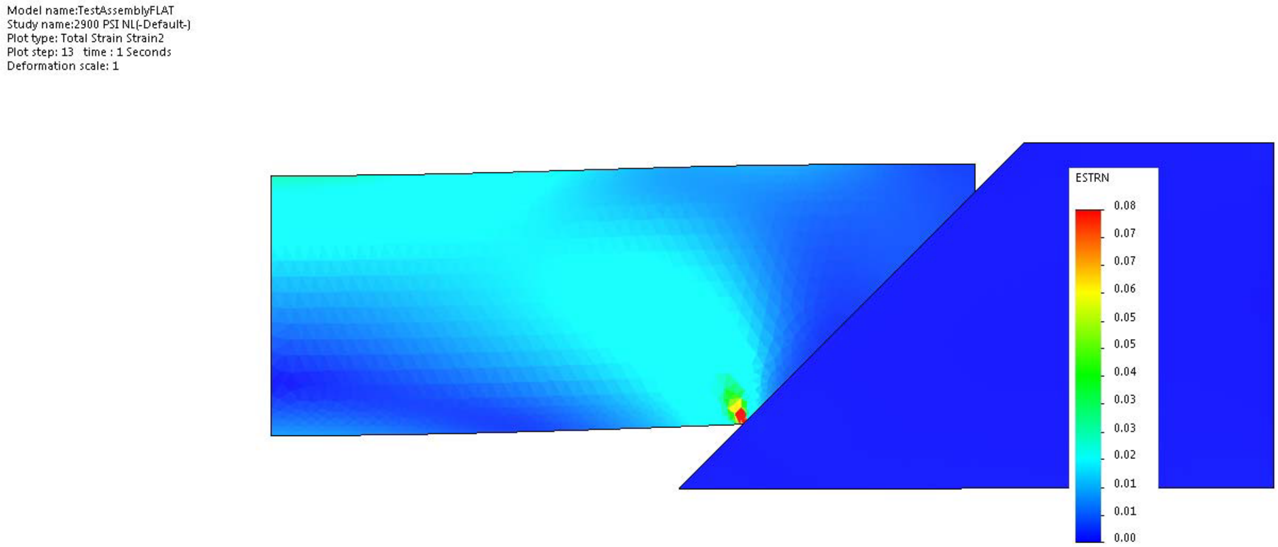

Fig. D7. Flatop strain at 2900 psi. Strain is potentially acceptable, although cyclic failure is possibly indicated.

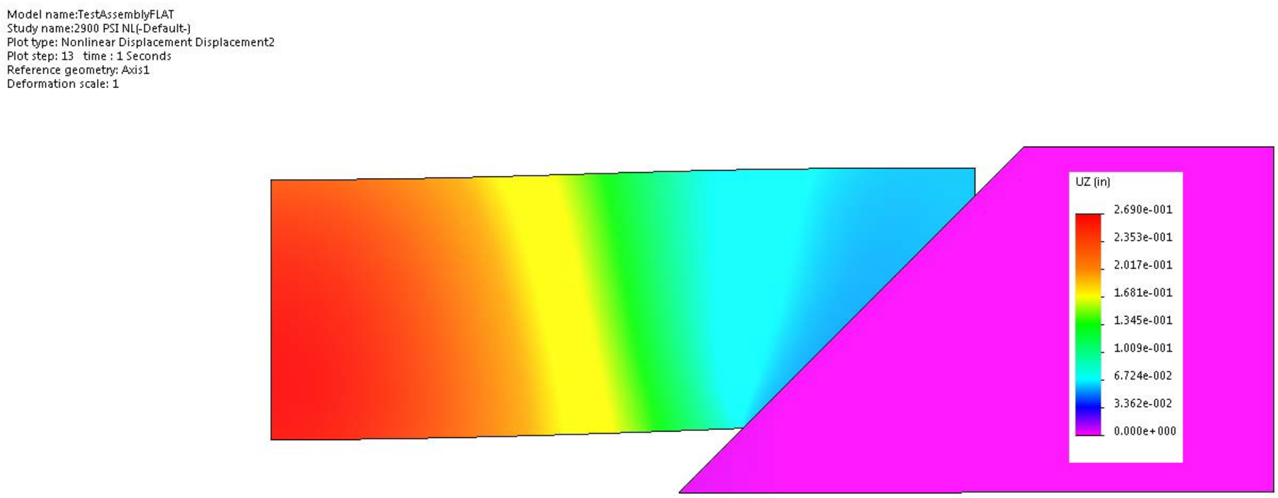

Fig. D8. Flatop deflection at 2900 psi. Downwards deflection is over twice the Cyclops design and is more than the Cyclops design at 5800 psi.

KEMPER
ENGINEERING SERVICES, LLC

INTEGRATED ENGINEERING AND DESIGN

[redacted] President
P.E.| Principal Engineer
P.E.| Senior Consultant

Design Review of TITAN Submersible Window

KES Job: NTS230801

5 September 2023

By
[redacted] P.E.

STATE OF LOUISIANA

[redacted]

[redacted]| President
| Principal Enginee
| Senior Consultan

Abstract

This report summarizes the interactions of Kemper Engineering Services (KES) with Will Kohnen of Hydrospace and several people with OceanGate in 2017 with respect to the window design for the CYCLOPS II submersible, which was later named TITAN. There was no payment for services involved in this. This report then provides additional analysis and commentary regarding the TITAN window and a proposed spherical sector window.

A series of nonlinear Finite Element Analyses were developed based on past work in reviewing testing-to-failure qualification experiments. A solid model of the proposed window design was compared to an ASME Pressure Vessels for Human Occupancy (PVHO) spherical sector window.

Based on a review of Client material and the results of the studies in this report:

- The original strain assessment submitted to OceanGate regarding the likelihood of cyclic failure of the window is reinforced by the work done for this report.
- The load cycle modeled in this report with indications of significant deformation of the window further supports the possibility of cyclic failure of the window.
- The results of the spherical sector are consistent with published results as well as being sufficient for the design load (depth).

In order to develop a forensic analysis of the window respect to its potential contribution to the failure of the TITAN, it is recommended detailed information regarding the manufactured window, the hull and window seat, the window retention structure, and operational history be gathered and incorporated into a comprehensive series of analyses.

[redacted]

Principal Engineer
Kemper Engineering S[redacted]

Contents

Appendices

1. Introduction and Scope

Terminology[1]:

Window: the transparent structure acting as a pressure boundary

Window seat: the structure supporting the window with respect to the pressure load and is connected to the pressure vessel shell

Viewport: the assembly of the window, window seat, and any gaskets, fasteners, retaining rings, and associated hardware

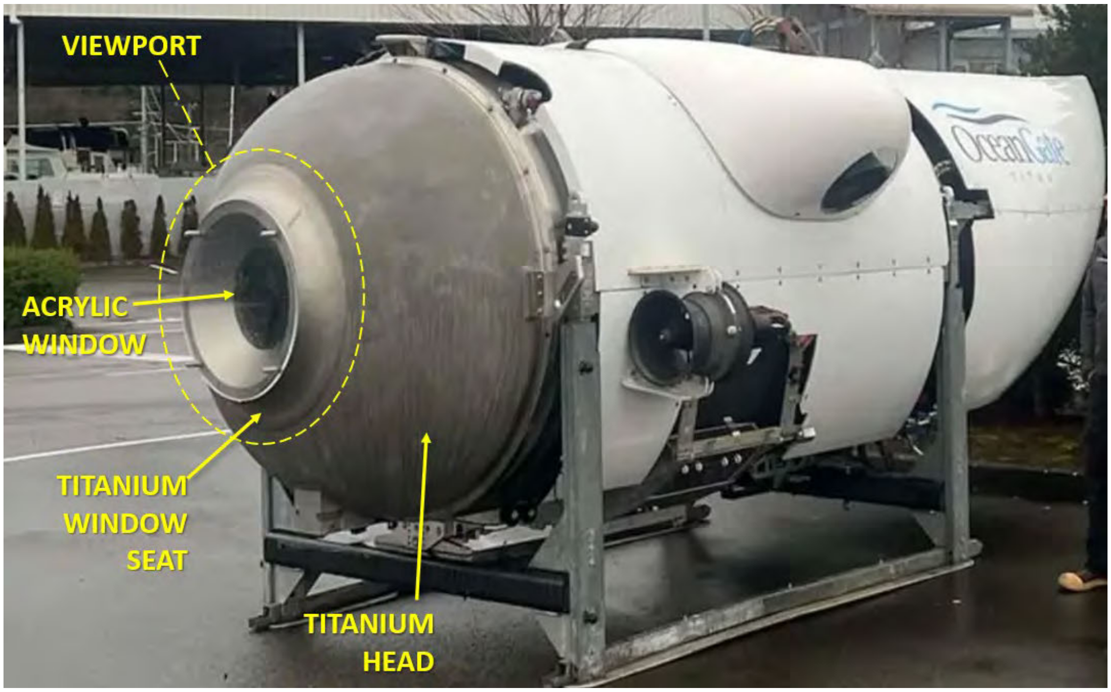

Fig. 1. News photo of the TITAN submersible with key items identified. There is some form of retention or protective feature on the window. It is not addressed in this report due to lack of data.

This report summarizes the interactions of Kemper Engineering Services (KES) with [redacted] of Hydrospace and several people with OceanGate in 2017 with respect to the window design for the CYCLOPS II submersible, which was later named TITAN. There was no payment for services involved in the previous or current report. This report then provides additional analysis and commentary regarding the TITAN window and a proposed spherical sector window. Multiple people at KES are members of the ASME Pressure Vessels for Human Occupancy (PVHO) codes and standards committee and subcommittees. KES has been at the forefront of applying Finite Element Analysis (FEA) to PVHO design, including for windows[2-4]. While work by KES is referenced in this report to establish the basis for opinions, there was early use of FEA[5] and numerous groups currently using FEA in PVHO applications[6-12] as well as in other industries.

The intent of the correspondence and summary report (App. B) was to show the desired shape may be more robust than a conical frustrum of the same height of the CYCLOPS conic section, but it still exhibited the same failure modes. Separately from KES' efforts, Kohnen reportedly used the ASME PVHO-1 (2016)[1] design method to develop a spherical sector which would have been code-compliant and had recommended it as a tried-and-true method for a similar cost. KES was prepared to provide detailed analysis of the CYCLOPS window as well as the ASME spherical sector and had corresponded with OceanGate. There was no interest by OceanGate expressed to KES regarding a 3rd party qualifying the one-off viewport design.

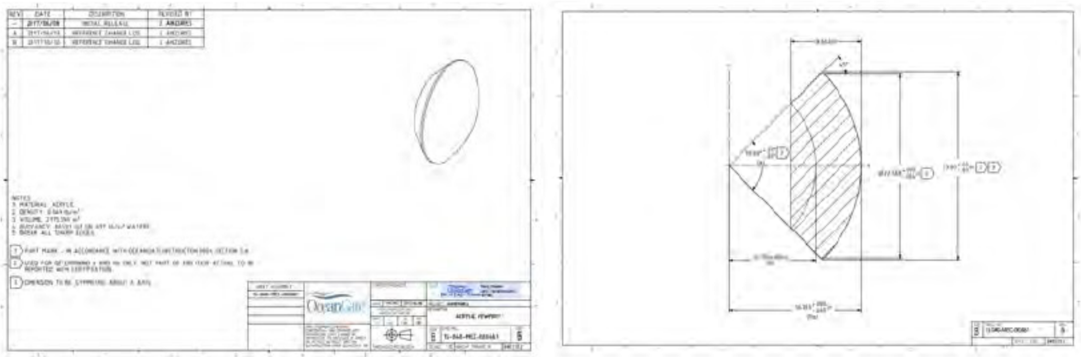

Fig. 2. Design drawings provided by OceanGate

This report represents a "design review" as opposed to a "forensic analysis." The only information provided to KES that directly relates to the TITAN's structure is a drawing of the window and knowing the pressure for the Titanic is 5,800 psig. There is insufficient information available to provide a sufficiently precise analysis to contribute to a root cause analysis of the system or provide a definitive prediction of the Titan viewport. Given the ASME PVHO-1 design methods for pressure vessel components (windows) is highly atypical for pressure vessels or other engineered structures, commentary with citation is provided to help inform readers who are investigation professionals but not familiar with ASME PVHO codes and standards.

2. Qualifications

No other organization has more members of the ASME PVHO codes and standards. We currently have one full time member and three alternate or corresponding members:

- [redacted], *P.E.* Current member of all committees since 2008. Chair, Viewports subcommittee. Chair, Design By Analysis for Glassy Polymers task group. Vice-chair, General Requirements subcommittee.
- [redacted] Former full member since 2009, now a corresponding member and [redacted]
- [redacted] Former full member since 1988, former Chair for Diving Subcommittee, now a KES consultant and a corresponding member
- [redacted] *P.E.* Former full member since 2015, now a KES consultant and a corresponding member on the Design By Analysis task group

Collectively, they have published 12 peer-reviewed papers and 14 conference presentations (with or without formal papers) related to PVHOs. Bart Kemper is the predominant author. Co-authors outside of KES employees include representatives of the US Navy (Deep Submergence), Triton Submarines, Atlantis Submarines, Lockheed-Martin, and Blanson Acrylics.

As the primary author for this review, in addition to various honors and training events as an engineer with licenses in the US and Australia and membership in ASME, Marine Technology Society (MTS), and Society of Naval Architects and Marine Engineers (SNAME), [redacted] has specific qualifications related to forensic investigations:

- Board Certified Forensic Engineer, "Diplomate of Forensic Engineering" (DFE) (Council of Engineering & Scientific Specialty Board, CESB)
- Board Certified Forensic Engineer (International Board of Forensic Engineering Sciences, IBFES)
- Certified Fire & Explosion Investigator (Nat'l Assoc. of Fire Investigators, NAFI)
- Editor-in-Chief, *Journal of the National Academy of Forensic Engineers*
- Peer reviewer, *Journal of the National Academy of Forensic Engineers, Marine Technology Society Journal, Ships and Offshore Structures*
- Senior Member, National Academy of Forensic Engineers (NAFE)
- Member, American Academy of Forensic Scientists (AAFS)

His training includes the Society of Automotive Engineers (SAE) course on Accident Reconstruction; NAFI Fire Investigation Training Program; and multiple seminars through NAFE and AAFS for civil and criminal investigations. He has completed 47 investigations and testified in 12 depositions, 6 civil trials or proceedings, and 2 criminal trials. Forensic work is about 25% of his practice, with the rest of his practice being traditional design, analysis, failure investigations, systems troubleshooting, and project management in a wide range of industries including petrochemical, marine, subsea, aerospace, and defense.

[redacted] is also a retired US Army Corps of Engineers Lt. Colonel (O5), where he served as a member of the Active and Reserve force 1992-2021. He has training, education, and experience related to forensic investigations. The training includes National Ground Intelligence Center (NGIC) Attack Site Forensic Investigation Course; US Army Corps of Engineers (USACE) Security Engineering and Blast Modeling Course which included image analysis, technical analysis, and case review; Counter Explosives Hazard Center (CEHC) Planner's Course which included intelligence processing and targeting; and pre-command courses instructing on the legal roles and responsibilities as a company and battalion commander including rules of evidence and conduct of investigations.

In terms of experience, in Iraq and Afghanistan he conducted or supervised post-attack forensic analysis; "attack the network" forensic analysis regarding associations; targeting analysis for intelligence and kinetic operations; and weapons effect analysis. He has conducted Army Regulation 15-6 investigations and was empaneled on multiple retention boards, which are administrative law review boards at the General Officer command level with the right of legal representation and direct challenge regarding offenses less than General Courts Martial.

In 2016 he was tapped by a 2-star engineering command to establish and command the only permanent federal Explosive Hazards Coordination Cell, an O5 (Lt. Col.) command which includes the explicit requirement of conducting post-attack forensic investigations and conducting intelligence analysis for targeting. He led this unit through validation for world-wide deployment with special focus on the Korean Theater of Operations where he led five training events in two years as well as responded to real-world events. His experience includes the 2014 response to the world-record largest IED captured (60,000 lbs of home-made explosives) in Paktia Province, Afghanistan[13, 14]. His CV is in App. E.

<u>3. Assumptions</u>:

1. This is a design review of the window and not a detailed forensic analysis.
2. The window material meets the requirements of ASME PVHO-1 (2016). The basis for this is the manufacturer is an established PVHO window manufacturer. KES has not reviewed any information regarding the manufacture, testing, or installation of the acrylic window.
3. The window seat is fixed and immovable relative to the acrylic polymer response. The window seat is alloy steel, which is the most common metal used in PVHO window seats. KES does not have information regarding the TITAN head and window seat material specification or geometry.
4. The interface between the window and seat is frictionless. Friction can have significant impact on the mechanical response[15].
5. The conical frustrum window and spherical sector window designs are based on meeting the same conic dimensions of the OceanGate window and assumes the same inner window diameter, or *Di*. This is to provide an apples-to-apples comparison of windows that all fit the same window seat.
6. The acrylic window material is equivalent to the acrylic MIL-P 8184 at 80 degrees F (27 degrees C)[16]. This is a material used to develop what became the ASME PVHO-1 process. Further, past experiments have been analyzed and validated using the nonlinear stress-strain curve used in this design review. It is noted these older forms of acrylic have less strength than modern formulations.
7. Analysis excludes elements that are excluded from the ASME PVHO-1 window design process, shown in App. C. Items a-f can significantly contribute to failure. Specifically, this neglects:
    a. Creep[2]
    b. Thermal retention as an insulator (vs temperature of hull materials being a conductor in response to water temperature)[17]
    c. Progressive deflection (ratcheting) due to plastic loading creating residual strain with each pressure event (dive)[18]
    d. Tolerance stack and angular misalignment[15]
    e. Impulse (shock) and/or impact loading from implodable volumes
    f. Friction between the window and window seat[15]
    g. Mechanical properties of the acrylic polymer, which is not directly used in the design process as shown in App. C[19, 20]
    h. Deflection of the window seat or hull/seat joint, which in turn goes to window deformation and potential for leak or slip
    i. Load rate (diving rate)
    j. Any data from installation or in-service inspection reports
8. Axisymmetric modeling for FEA is sufficient. This neglects examining the issue of improper window/seat fit up or alignment since it is assumed in design the window will be properly aligned and installed[15].
9. Implicit nonlinear modeling is sufficient for design review[2]. This is per ASME "design by analysis" practice that uses implicit FEA for thin-wall and thick-wall pressure vessels as well as in API 579/ASME FFS1 for "fitness for service". It is possible a full forensic analysis would require explicit nonlinear modeling.

10. The window is reported to "squeeze inwards" about ¾ of an inch. It is not clear if this is a translational movement inwards, an inwards bending of the acrylic window, or a combination of the two. The basis is video footage of Stockton Rush reporting the window performance and being documented as such in the media[21].

4. Analysis Method

The design of the spherical sector window was done using the methods specified in Section 2, ASME PVHO-1. This is a fairly simple process in which a shape is assumed, the design depth and temperature is selected to determine the Correction Factor (CF) to calculate the Short Term Critical Pressure (STCP).

Table 2-2.3.1-3 Conversion Factors for Acrylic Spherical Sector Windows With Conical Edge, Hyperhemispherical Windows With Conical Edge, and NEMO-Type Windows With Conical Edge

Operational Pressure Ranges	Temperature, °F (°C) 50 (10)	75 (24)	100 (38)	125 (52)	150 (66)
N = 1 2,500 psi (17.2 MPa)	CF = 4	CF = 6	CF = 8	CF = 10	CF = 16 1,500 psi (10.3 MPa)
N = 2 5,000 psi (34.5 MPa)	CF = 4	CF = 6	CF = 8	CF = 10 3,500 psi (24.1 MPa)	3,000 psi (20.7 MPa)
N = 3 7,500 psi (51.7 MPa)	CF = 4				

GENERAL NOTES:
(a) The CFs in this Table apply only to STCPs plotted in Figures 2-2.5.1-6 and Figures 2-2.5.1-7 for spherical sector windows with conical edge and Figures 2-2.5.1-14 and 2-2.5.1-15 for hyperhemispherical windows with conical edge and NEMO-type windows with conical penetrations.
(b) Dotted lines refer to intermediate pressure ranges as indicated by the adjacent pressure figures.
(c) Interpolation between CFs is allowed.

Fig. 3. Table for acrylic spherical sector windows from ASME PVHO-1 (2016). Note it does not consider temperatures above 50°F (10°C) at pressures beyond 5000 psi (34.5 MPa). This is a flaw in the design method as it neglects the fact acrylic is a thermal insulator and many times thicker than the metallic hull, which is a thermal conductor. Traditional heat transfer calculations demonstrate deep-diving windows will retain elevated temperatures for hours. This is moot with respect to OceanGate as it is not an ASME PVHO-1 window.

The CF is not a design margin because it does not return consistent results when evaluating mechanical response across the range of PVHO-approved shapes[22]. The STCP is then applied to a chart for a given geometry, and an adjusted pressure value provides a relationship of t (window thickness) divided by Di (interior diameter of the window seat.)

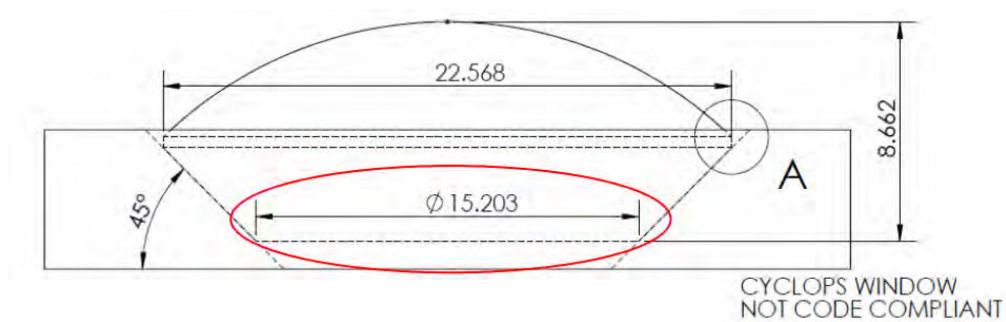

Fig. 4. The value for Di is 15.2 inches by using the dimensions CYCLOPS II window as a design constraint to ensure compatibility with the window seat.

Given the assumed seat dimension is the same as the OceanGate window, this returns the value of the window thickness. At no point are the material propreties used in the process other than to check they meet minimum requirements. This is detailed in App. C. Conversely, the conical frustrum was developed using the base portion of the OceanGate window in order to examine how the domed addition impacts the design. This is shown in the report sent to OceanGate in 2018 in App. B

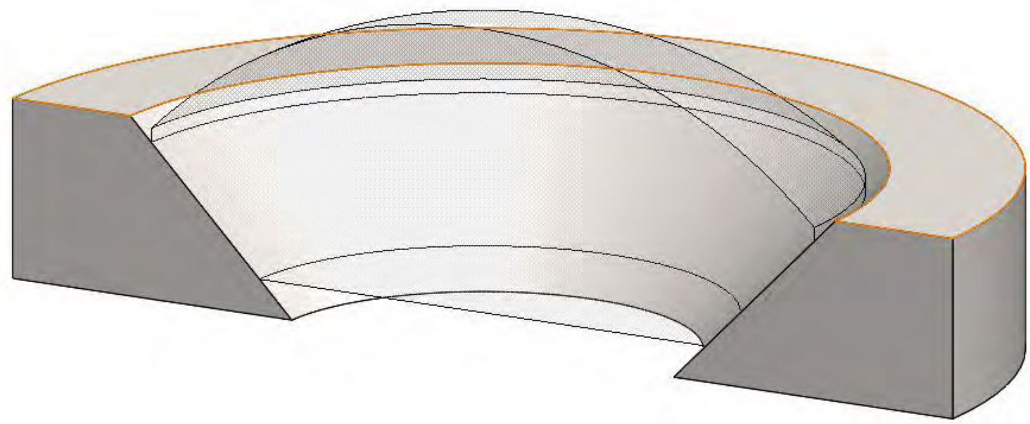

Fig. 5. Cross section view of the solid model of the OceanGate window and the assumed window seat. There is no retaining device because no information on it is available, but also when operational the outer pressure is the primary retention force.

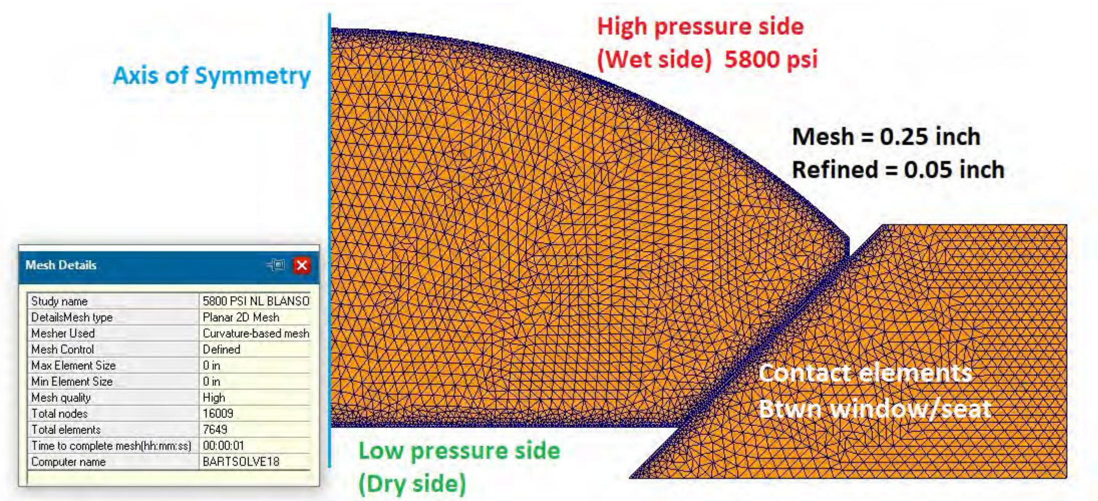

Fig. 6. Mesh of the OceanGate window and window seat. Contact element allows the window to move relative to the seat as well as pull away from it. This allows gaps between the window and seat as local regions may rotate or deform.

Solid models were developed for the analysis, such as the OceanGate viewport model shown in Figure 5. These models were then assigned axisymmetric parameters in the FEA package with the same mesh size as shown in Figure 6. In past examination of PVHO windows and their performance, contact elements have proven to be a key modeling technique in developing accurate response by PVHO windows, whether they are in a conical seat as they are with the TITAN submersible[15] or in gasketed arrangements such as those typical in decompression or medical chambers[23].

Only the conic window seats are designed for metal-to-acrylic contact. Other PVHO viewports, such as flat disc windows, require bearing gaskets. In those designs, acrylic-to-metal contact is often a crack initiator leading to failure[18, 23]. An improper retaining system can also be a crack initiator. Friction is neglected. Friction can change the mechanical response[15].

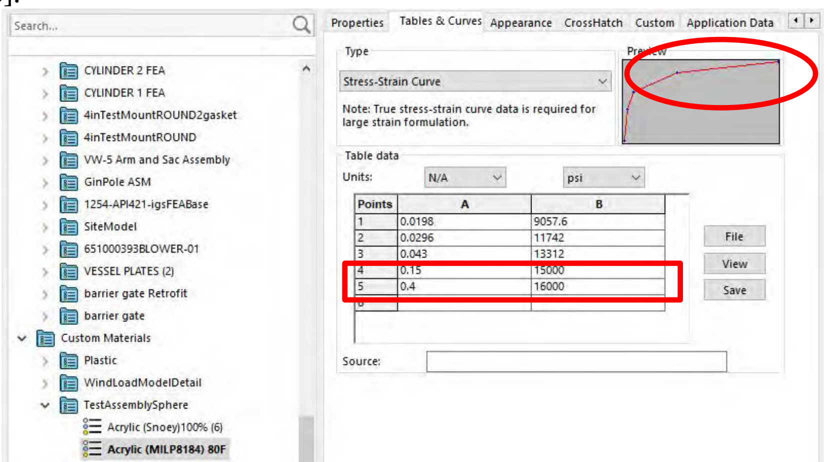

Fig. 7. Stress-strain curve used for MIL-P 8184 acrylic.

Figure 7 shows the true stress-strain curve used for all analyses. The material is only reliably modeled up to 4.3% strain in tension at 80 degrees F. The temperature is based on summertime temperatures in the North Atlantic. A more rigorous approach is needed for non-PVHO window shapes[2].

Previous investigation in the behavior of acrylics under load indicates being loaded in compression has a higher yield strength than in tension as well as having a higher strain rate. Submarines and diving bells generally have compression as the primary load. A maximum of 15% strain localized strain in compression is possible with conical frustrums. The higher strain rate for the last segment of 15% to 40% is a modeling technique to allow the material to “fail” locally with increased displacement without causing the model to fail.

This technique was developed to analyze the test-to-failure data from the original work commissioned by the US Navy[24-26]. This is intended to indicate failure but not provide an accurate prediction regarding displacement. For this material at this temperature, strains above 3% are consistent with low-cycle failure mechanisms.

The FEA of the spherical sector as well as the original evaluation of the conical frustrum and OceanGate window used a straight line loading curve using “pseudo time.” While transient analyses use actual time, steady state models apply the designated load in a stepwise manner in order to allow the model to computationally respond in an incremental manner. The most common loading scheme is the desired load is the maximum load at pseudo-time = 1.0, such that at pseudo-time = 0.5 only half the load has been applied. This is shown in the left hand curve in Figure 8.

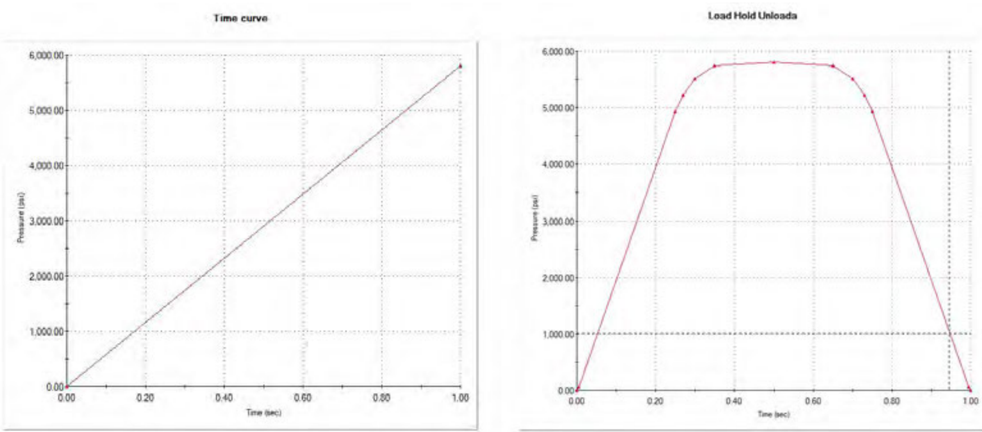

Fig. 8. The left shows a traditional linear load curve using "pseudo time" to increment the load in a linear manner. The right curve show the load incremented to its maximum at time = 0.5 and completes unloading at time = 1.0. At time equals 0.05 (loading) and 0.95 (unloading), the load is 1000 psi of pressure, which is the dashed line on the right figure.

The right image in Figure 8 is a cyclic loading/unloading curve. Previous work in examining the US Navy tests by Dr. Jerry Stachiw has shown that short cycle failure (less than a 100 cycles, often less than 10 cycles) correlates with around FEA results of 3% residual strain in cyclic load modeling[18, 19, 23]. The steady-state nonlinear analysis of the OceanGate window in 2018 concluded it was likely to fail in repeated cycles. This report further examines that conclusion by applying a loading/hold/unloading cycle to approximate the effects of a single dive to 5800 psi pressure.

In the course of the analysis the run stopped around t = 0.95 due to geometric discontinuities. In essence, after the last 5% of the time curve (1000 psi) the elastic energy in the window "popped" the window completely out contact with the frame, violating the requirements for implicit nonlinear FEA. Ideally, the computer solves the full run so the deflections and strains remaining when the applied load reaches zero are clearly "residual." Instead, to have an "apples-to-apples" comparison, we will compare the first 5% (t = 0.049) and the last 5% (t = 0.945). Because these were not programed points in the curve, there is about a 10% difference in the applied pressures. Accordingly, because this is in the elastic portion of the material, the amount of strain and deflection should be within 10% of each other unless the window was designed in such a way to allow for significant residual strain to occur.

5. Verification, Validation, and Uncertainty Qunatification

Verification, Validation, and Uncertainty Quantification (VVUQ) is addressed as an aggregate effort. Typical pressure vessel "design by analysis" can be considered to be within a proven codes & standard such that the VVUQ efforts are implicitly included in the code requirements[27]. All work is done using Solidworks Advanced Professional for the solid modeling, drawings, and analysis. As a verification of the program, the linear and implicit structural nonlinear package meets the required benchmarks of solving known problems within acceptable precision and accuracy.

Validation of the PVHO-1 analyses (conical frustrum submitted to OceanGate, spherical sector shown herein) is based on previous work reviewing the work of Dr. Jerry Stachiw and others with respect to the PVHO-1 design process and the experiments used to develop those methods. This design system has been in service for over 40 years with considerable examination by industry[24]. The design system is highly conservative to address the uncertainty inherent in a new design system with a developing technology. While there have been shortcoming identified with the code, it must be noted there is not a single known failure of a window designed and manufactured to ASME PVHO-1 unless it has been abused in some manner[28]. Examples of such abuse include a submarine travelling too close to subsea thermal vents or having an incandescent light placed adjacent to a decompression chamber window for a long period of time.

The validation of the OceanGate model is less strong. Given the shape is not one that has been proven experimentally, vetted by years of use by multiple parties, and codified in a published standard, the FEA is a reasonable approximation but would require some form of physical testing to have sufficient reliability for this service. It is noted the Design By Analysis method being developed by at ASME task group requires experimentation in conjunction with simulation and literature review[2, 3, 22].

Adding to the uncertainty for the OceanGate window is the use of two different loading curves, which can produce a variance in the convergence values. In reviewing the solutions, there is a significant difference in the peak values; however, these are isolated nodes and are considered to be low precision. The peak strain in the 2018 model was 44%, well above the 15% of the curve used at that time. Since this is design review, peak values are for relative assessment and screening rather than a precise prediction of crack onset.

6. Results

All work is done using Solidworks Advanced Professional for the solid modeling, drawings, and analysis. Model details are shown in App. C and results details are shown in App. D. The summary of the 2018 report (in App B) is shown below:

TABLE 1: Summary of 2018 Report

	Cyclops Viewport		Flat top Viewport	
Model	*Max Strain (in/in)*	*Deflection (in)*	*Max Strain (in/in)*	*Deflection (in)*
5800 psi Linear	0.12	0.203	0.16	0.394
5800 psi Nonlinear	0.44 (possible cyclic fail)	0.264	0.73 (catastrophic failure)	0.924
4000 psi Nonlinear	0.27 (no failure)	0.174	0.54 (failure)	0.453
2900 psi Nonlinear	0.16 (no failure)	0.123	0.33 (cyclic failure)	0.269

The reason for presenting linear results was past observations of various parties asserting a linear analysis is sufficient for assessing the window design. This has been proven false due to the inability to correlate linear stresses and strains to test-to-failure data, particularly with conical frustums due to the localize compression on the low pressure corner. A different material curve was used for that analysis, which also accounts for some of the variances between that study and this one. This was intended as an initial design review. The results indicated there was strong similarities to observed strain patterns associated with test-to-failure data and the end-user (OceanGate) was informed.

Polymers in compression often exhibit a “shape factor” response, although to a lesser degree than hyper-elastic or viscoelastic materials. This means how the item is constrained, whether it has a tall or short aspect ratio, how it is loaded, and other factors can result in a different response than a classic elastic solid mechanics approach. Given the OceanGate window is a polymer shape that has not been studied, tested to failure, and put through peer review, there is no literature to make a direct comparison with.

The ASME spherical sector, on the other hand, has been studied, tested to failure through a range of thickness aspect ratios, and has decades of service history. Mechanically, the OceanGate shape is closer to a conical frustrum, to include its primary fracture failure mode coming from the corner of smaller (dry side) face. App. A includes an excerpt from one of Dr. Stachiw's studies depicting failures of a conical frustrum[29]. A spherical sector with a conic ends acts as an arch (2D) or sphere (3D), with a uniform distribution of stress and strain relative to the radius. Comparing the two shapes is not quite an "apples to apples" comparison, but important distinctions can be observed.

TABLE 2: Summary of Results

LD	LD/UN	PEAK	OceanGate-Cycle	OceanGate-2018	ASME Spherical
	0.05	*Stress (psi)*	2700		
		Strain (%)	0.97%		
		Defl (inch)	0.032		
1.0 (Max)	0.5 (Max)	*Stress (psi)*	17300	18100	11500
		Strain (%)	18.7%	44%	2.54%
		Defl (inch)	0.205	0.26	0.19
	0.95	*Stress (psi)*	3800		
		Strain (%)	16.9%		
		Defl (inch)	0.022		

In Table 2, "LD" is the linear load curve with max values at t=1.0. "LD/UN" is load/unload curve with the max value at t=0.50. This is the only point of direct comparison. All units are in US customary to be consistent with the OceanGate units. The 2018 values are provided as a reference, which in part illustrates the potential impact of using different material curves and the value of using one that matches the specific window.

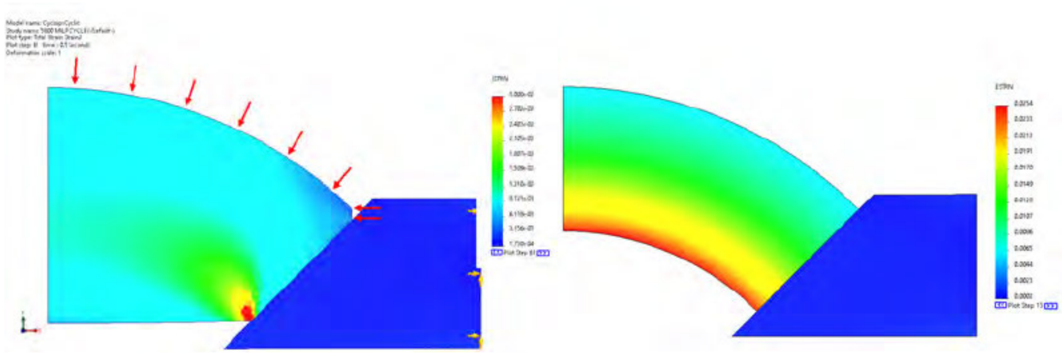

Fig. 9. Strain comparison. Left shows the OceanGate window with strain truncated at 3%, with a peak strain value of 18.7%. The right image shows a spherical sector window designed per ASME PVHO-1 with a peak strain of 2.54% with a smooth transition of strain levels. Based on experience, the sharp difference between a 3% peak strain and the yellow region (2.4%) is consistent with cyclic failure in less than 100 cycles, potentially as few as 10. This indicates additional analysis is needed as well as some form of physical testing.

The ASME spherical sector has lower peak stress and strain but comparable deflection. This is due to the design being more efficient in distributing the load through its volume. The strains below 3% and the lack of "hot spots" that could correlate to crack initiation points[18] illustrates why a spherical sector is the shape used by hadal depth submersibles such as Woods Hole Oceanographic Institute's DSV ALVIN[2] and the DSV LIMITING FACTOR developed by Triton Submarines[3, 4].

A key observation of the cyclic results is the significant increase in strain. There is about 1% strain at 1000 psig loading, but 16.9% strain at 1000 psig unloading. Even accounting for these are peak strains at specific nodes and not well conditioned results such as the spherical sector results, it is over an order of magnitude difference. The other observation regarding the results is in regards to the deflection, shown below.

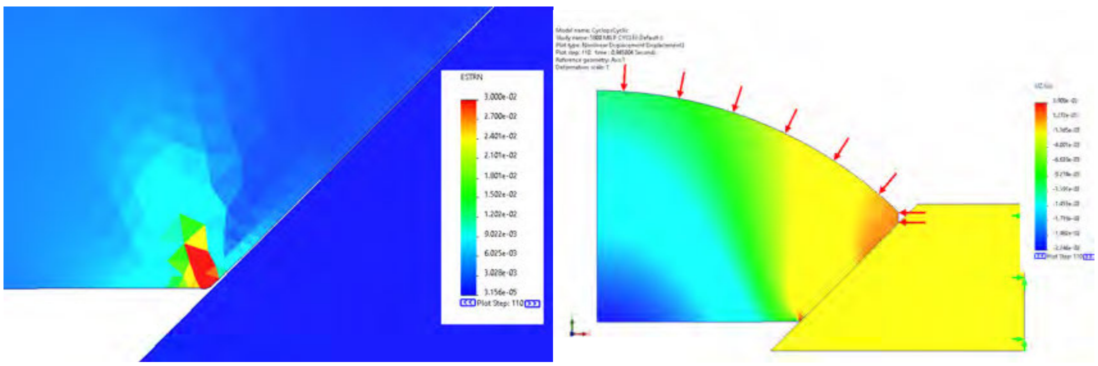

Fig. 10. Response at t=0.95 (1000 psi, unloading.) Left image is a detailed view of the stress limited to 3%. There is a noticeable gap between the window and seat. The right image shows the axial (vertical) displacement of the system, with yellow being "zero displacement." The upper corner of the window has marginally risen above its original position.

The left image shows the strain with displacement at true scale. There is a visible gap between the window and seat despite the 1000 psi pressure. There is also a noticeable rise in the lower window corner corresponding to the strain, indicating an inwards displacement consistent with the strain. There is also the region of about 1/1000th of an inch rise in the upper corner of the window. This is consistent with the flow of materials under sufficient pressure such that when the pressure is reduced, the elastic energy pushes the item back up the conic face of the window seat.

The net effect is each successive pressure cycle will deform the window further. As the water pressure pushes the window into the seat, the seat acts as an extrusion die at high enough pressures. The round dome on top, which is not part of the established body of shapes, appears to act as a reservoir of elastic energy for the upper section as well as creating more total force on the window than a flat top would. While the projected axial area is the same with respect to the pure axial force down into the seat, the radial component of the pressure is further compressing the plastic shape. When the pressure is removed, the result is the upper section expands due to being almost exclusively elastic while the lower portion remains deformed. In the next iteration, only the upper portion of the window in direct contact with the seat, requiring less force for the window to travel axially inwards until the lower edge is engaged and the full surface resumes resistance. At that point, the "extrusion die" continues to push inwards, causing material to flow. Given there was sufficient force to create permanent deformation in the first cycle, it is likely to continue with each cycle.

This is consistent with the material mechanism observed in a number of cyclic loading failures during the development of the PVHO standard. Conical frustums that are designed to ASME PVHO-1 may have some residual strain in the lower corner, but they do not exhibit a gap along their contact face after a single cycle. Some polymers exhibit a form of work hardening in compression, which would resist successive cyclic deformation. All thermoset polymers such as acrylic exhibit creep under load over time, which would contribute to successive cyclic deformation.

This phenomena of a gap formation is made more significant by the assessment by Stockton Rush that his fielded window “squeezed in” about 3 times the modeled displacement. This supports that some form of deformation had occurred. Given the outmost section would still be elastic and water tight, it would not be obvious there was a progressive change to the window dimensions. If there was about a ¾ inch “squeeze”, it’s also possible for the window to become misaligned. It is also possible that small debris could get into that gap and create sealing issues or stress concentrators.

This is also made more significant by the temperature sensitivity of acrylic in terms of stiffness (moduli of elasticity and flexure), yield strength, ultimate strength, and elongation [17, 19, 20]. A change of as little as 25 degrees F (14 degrees C) will have a significant impact on the design, as shown in Figure 3 as well as material data shown in App. A[16, 24, 29]. The design method shown here assumes a surface air temperature of 80 degrees F to be the window temperature instead of the more common practice of using the “at depth” water temperature. Given the material stiffens and increases yield strength as temperatures decrease, the FEA displacement results for 80 degrees F of 0.20-0.25 inches should be less than the reported value in cold Atlantic waters, let alone be three times the warmer prediction. It is also unknown if the forces on the window will cause deformation of the window seat and hull.

6. Conclusions and Recommendations

Based on a review of Client material and the results of the studies in this report:

- The original strain assessment submitted to OceanGate regarding the likelihood of cyclic failure of the window is reinforced by the work done for this report.
- The load cycle modeled in this report with indications of significant deformation of the window further supports the possibility of cyclic failure of the window.
- The results of the spherical sector are consistent with published results as well as being sufficient for the design load (depth).

In order to develop a forensic analysis of the window respect to its potential contribution to the failure of the TITAN, the following is recommended:

- Obtain the detailed “as fabricated” design notes of the installed window, to include material testing, in order to have a more precise model.
- Develop a detailed model of the head and window seat, including the window retention structure.

- Review the full operational history to estimate air temperature prior to dive, water temperatures during the dive, and the dive profile for time vs. pressure in order to develop analysis parameters.
- Incorporate creep effects into the analysis.
- Analyze the window for at least two temperatures to bracket potential response.

7. References

[1] ASME, *PVHO-1 Safety Standard for Pressure Vessels for Human Occupancy* ( ). New York: American Society of Mechanical Engineers, 2016.

[2] [redacted] "Developing 'Design by Analysis' Methodology for Windows for Pressure Vessels for Human Occupancy," *ASCE-ASME J Risk and Uncert in Engrg Sys Part B Mech Engrg,* vol. 6, no. 3, 2020, doi: 10.1115/1.4046742.

[3] [redacted] "Advancing Towards Design By Analysis for Glassy Polymers," presented at the MTS Submarine Symposium, New Orleans, Louisiana, December 2022, 2022. [Online]. Available: https://www.researchgate.net/publication/366820945_Advancing_Towards_Design_By_Analysis_for_Glassy_Polymers.

[4] [redacted] "Evolving Methods for Design by Analysis for Glassy Polymers in Marine Applications," in *Offshore Technology Conference*, 2023: OnePetro, doi: 10.4043/32369-MS. [Online]. Available: https://onepetro.org/OTCONF/proceedings-abstract/23OTC/3-23OTC/D011S011R007/519182

[5] [redacted] "Stress Analysis of a Conical Acrylic Viewport R675," US Naval Civil Engineering Laboratory, Port Hueneme, California, Technical Report 675, 1970. [Online]. Available: https://apps.dtic.mil/sti/pdfs/AD0708009.pdf

[6] P. S. Das, "Redesign of NEMO-type spherical acrylic submersible for manned operation to 3000 ft (914 m) ocean depth," *J. Pressure Vessel Technol.,* vol. 124, no. 1, pp. 97-107, 2002, doi: 10.1115/1.1428746.

[7] [redacted] "The Use of Acrylic as a Structural Material in the Design of Translucent Elements of Deep-Submergence Vehicles," in *Materials Science Forum*, 2021, vol. 1031: Trans Tech Publ, pp. 196-200.

[8] [redacted] in a deep sea manned submersible," *Ships and Offshore Structures,* vol. 15, no. 7, pp. 769-779, 2020.

[9] [redacted] "Prediction of the service life of deep-sea conical acrylic portholes at designing," *Eastern-European Journal of Enterprise Technologies,* vol. 1, no. 1 (103), 02/29/ 2020, doi: 10.15587/1729-4061.2020.194584.

[10] [redacted] "Safety assessment of the acrylic conical frustum viewport structure for a deep-sea manned submersible," *Ships and Offshore Structures,* vol. 12, no. sup1, pp. S221-S229, 2017, doi: 10.1080/17445302.2016.1261390.

[11] [redacted] *al.*, "Strain Rate Sensitivity of Yield Response of PMMA: Experimental Characterization and Material Modeling," *Journal of Testing and Evaluation,* vol. 48, no. 5, pp. 3752-3767, 12/05 2018, doi: 10.1520/JTE20180019.

[12] [redacted] "Failure process analysis of frustum windows for deep-sea manned cabin," *Ships and Offshore Structures,* pp. 1-11, 01/04 2021, doi: 10.1080/17445302.2020.1861709.

[13] [redacted] "Blast Modeling for Facility Security Management," in *45th Annual Conference on Explosives and Blasting Techniques*, Nashville, Tennessee, 2019: International Society of Explosives Engineers, 2019.

[14] [redacted] "Truck Bombs and Standoff," *Engineer, the Professional Bulletin of Army Engineers,* vol. 47, no. Sept-Dec, 2017 2017.

[15] [redacted] "Validation of Modern Finite Methods for Glassy Polymers Using Historical Studies," in *ASME 2021 Pressure Vessel & Piping Conference*, Virtual, Online, July 2021 2021: ASME, doi: 10.1115/PVP2021-62146

[16] (1973). *MIL-HDBK-17A, PART II Plastics for Aerospace Vehicles, Transparent Glazing Materials*.

[17] [redacted] "Heat Retention and Structural Integrity of Glassy Polymer Windows," in *15th Manned Underwater Vehicle Symposium*, New Orleans, Louisiana, USA, 2018: Marine Technology Society, doi: 10.13140/RG.2.2.14435.91685.

[18] [redacted] "Failure modes for acrylic polymers in Section VIII pressure vessels," in *ASME 2021 Pressure Vessel & Piping Conference*, Virtual, Online, July 2021 2021: ASME, doi: 10.1115/PVP2021-62148. [Online]. Available: https://doi.org/10.1115/PVP2021-62148

[19] [redacted] "NEMO joint design in ASME PVHO Code," in *16th Manned Underwater Vehicles Symposium*, New Orleans, Lousiana, USA, February 2019 [redacted]

[redacted] [redacted] "Shortfalls in polymer specifications for PVHOs," in *Underwater Intervention 2019*, New Orleans, Louisiana, USA, February 2019 2019, doi: 10.13140/RG.2.2.32884.60807/1.

[21] [redacted] "OceanGate CEO Stockton Rush said in 2021 he'd "broken some rules" in design of Titan sub that imploded." CBS News. https://www.cbsnews.com/news/titanic-submarine-implosion-oceangate-ceo-stockton-rush-2021-hes-broken-some-rules-in-design/ (accessed 3 July 2023, 2023).

[22] [redacted] "Attempting To Establish Design Margins for Glassy Polymers In Critical Structural Service," in *ASME 2021 International Mechanical Engineering Congress and Exposition*, 2021, vol. Volume 13: Safety Engineering, Risk, and Reliability Analysis; Research Posters, doi: 10.1115/imece2021-71836. [Online]. Available: https://doi.org/10.1115/IMECE2021-71836

[23] [redacted] "Criteria For Eliminating Cyclic Limit For PVHO Flat Disc Windows," in *2013 Joint ASME/USCG Workshop on Marine Technology & Standards*, Arlington, Virginia USA, July 2013 2013, vol. Proceedings of the ASME/USCG 2013 3rd Workshop on Marine Technology and Standards.: ASME, pp. pp. 214-223., doi: 10.13140/2.1.3242.1447. [Online]. Available: https://doi.org/10.1115/MTS2013-0323

[24] [redacted] *Handbook of Acrylics for Submersibles, Hyperbaric Chambers, and Aquaria*. Best Publishing Company, 2003, p. 1080.

[25] [redacted] "Recommended Practices for the Design, Fabrication, Prooftesting and Inspection of Windows in Man-Rated Hyperbaric Chambers," US Navy, San Diego, California, AD-773 737, 1973 1973. [Online]. Available: https://apps.dtic.mil/dtic/tr/fulltext/u2/773737.pdf

[26] J. D. Stachiw and K. O. Gray, "Procurement of Safe Viewports for Hyperbaric Chambers," *Journal of Engineering for Industry,* vol. 93, no. 4, pp. 943-952, 1971, doi: 10.1115/1.3428088.

[27] [redacted] "Application of VVUQ Concepts to ASME Codes and Standards for Pressure Vessels," presented at the ASME 2023 Verification, Validation, and Uncertainty Quantification Symposium, May 2023, 2023, VVUQ2023-108506. [Online]. Available: https://asmedigitalcollection.asme.org/VVS/proceedings/VVUQ2023/86748/V001T02A001/1164362.

[28] [redacted] "Hyperbaric and hypobaric chamber fires: a 73-year analysis," *Undersea & Hyperbaric Medicine: Journal of the Undersea and Hyperbaric Medical Society, Inc,* vol. 24, no. 3, pp. 153-164, 1997. [Online]. Available: https://europepmc.org/article/med/9308138.

[29] (1967). *Technical Report No. R-512, Windows for External or Internal Hydrostatic Pressure Vessels: Part 1—Conical Acrylic Windows Under Short-Term Pressure Application*. [Online] Available: https://apps.dtic.mil/dtic/tr/fulltext/u2/748583.pdf

APPENDIX A

Material Information

Material Data
Job: NTS230801
Material: MIL-P 8184 Acrylic
By: [redacted] P.E.

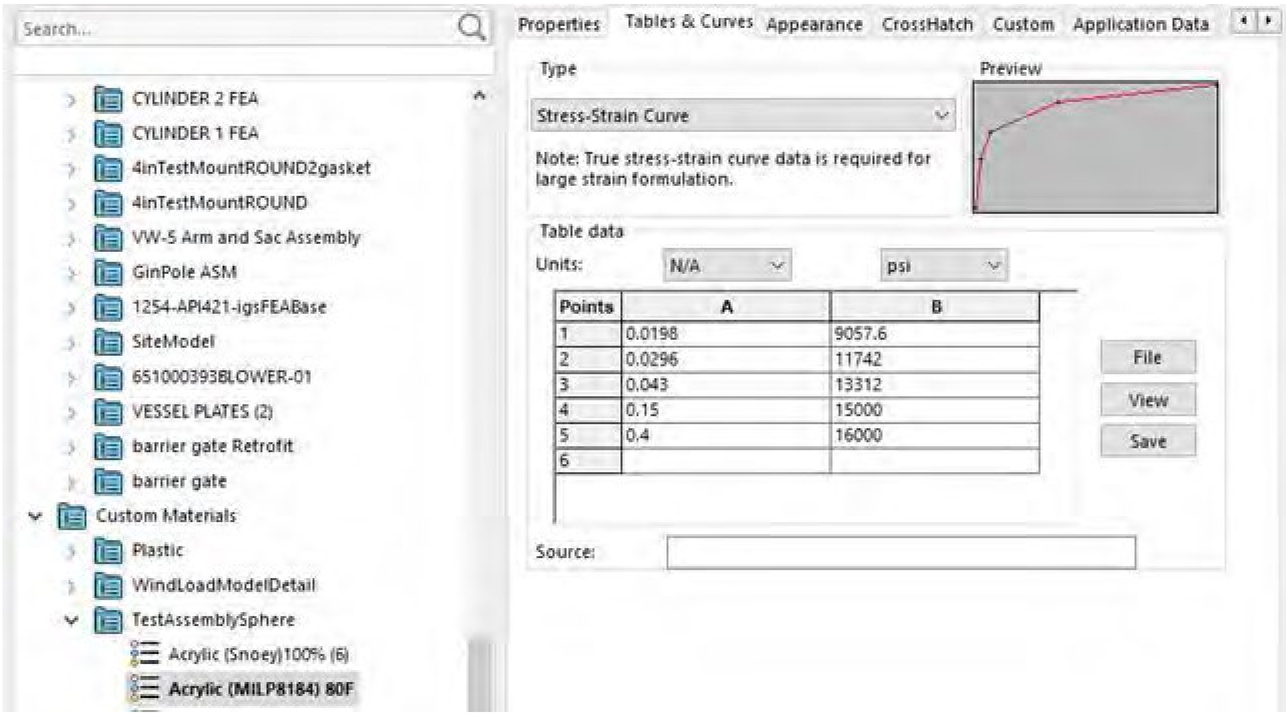

The figure above shows the true stress-strain curve used for all analyses performed for this study. A slightly different curve was used in 2018. The material is only reliably modeled up to 4.3% strain in tension at 80 degrees F based on the information provided in *MIL HDBK 17A*, *Aerospace Plastics*. The excerpt containing the data for MIL-P 8184 follows. The temperature is based on summertime temperatures in the North Atlantic. A more rigorous approach is needed for non-PVHO window shapes

Previous investigation in the behavior of acrylics under load indicates being loaded in compression has a higher yield strength than in tension as well as having a higher strain rate. Submarines and diving bells generally have compression as the primary load. A maximum of 15% strain localized strain in compression is possible with conical frustrums. The higher strain rate for the last segment of 15% to 40% is a modeling technique to allow the material to “fail” locally with increased displacement without causing the model to fail.

This technique was developed to analyze the test-to-failure data from the original work commissioned by the US Navy. This is intended to indicate failure but not provide an accurate prediction regarding displacement. For this material at this temperature, strains above 3% are consistent with low-cycle failure mechanisms.

MILITARY HANDBOOK

MIL-HDBK-17A, PART II
(Proposed Revision)

Superseding
MIL-HDBK-17, PART II
14 August 1961

PLASTICS FOR AEROSPACE VEHICLES

PART II TRANSPARENT GLAZING MATERIALS

Richard S. Hassard

Goodyear Aerospace Corporation
Litchfield Park, Arizona

GERA-1863

CONTRACT F33615-71-C-1465

PROJECT 7381

JANUARY 1973

AIR FORCE MATERIALS LABORATORY
AIR FORCE SYSTEMS COMMAND
WRIGHT-PATTERSON AIR FORCE BASE, OHIO

TABLE 4.3-II - EFFECT OF ANNEALING ON THE K-VALUE OF STRETCHED MIL-P-5425 MATERIAL

Stretching temperature (deg F)	Degree of stretch (percent)	K-value	
		Unannealed (10^3 lb/in.$^{3/2}$)	Annealed (10^3 lb/in.$^{3/2}$)
260	73	3.44	2.58
270	73	3.38	2.85
290	73	3.58	2.68
390	100	3.23	3.50
310	100	3.39	3.22

4.3.3 MIL-P-8184

4.3.3.1 GENERAL

The MIL-P-8184 material was developed to support the higher temperatures required by aircraft designs at the time as well as to have the capability of a greater resistance to crazing than the MIL-P-5425 material.

4.3.3.2 PROPERTIES

Tensile stress-strain, ultimate strengths versus temperature, and creep-rupture curves are found in section 4.2, Figures 4.2-1 through 4.2-6. Flexural fatigue and coefficients of thermal expansion versus temperature are found in Figures 4.2-8 and 4.2-9 of the same section (4.2) with the information of Table 4.2-I, which concerns light transmittance and haze before and after controlled Taber abrasion.

4.3.3.2.1 TEMPERATURE EFFECTS ON TENSILE PROPERTIES

The stress-strain curves at various temperatures above room temperature are shown in Figure 4.3-26. Figure 4.3-27 is a cross plot which shows the effect of temperature on tensile strength, modulus of elasticity, and strain at failure. Tensile-creep data follow at three temperatures in Figures 4.3-28 through 4.3-32. Cyclic tensile creep-strain curves are in Figure 4.3-33.

4.3.3.2.2 FLEXURAL DATA

Both notched and unnotched specimens were tested. The notch was of the ARTC standard needle scratch 5 mils deep by 60 deg. Failure curves are shown for both. A third curve represents the crazing level of stress versus time in Figure 4.3-34. Figure 4.3-35 demonstrates the effect of craze depth on the flexural strength. Figure 4.3-36 contains the remaining flexural data and shows the loss in strength caused by notching.

4.3.3.2.3 THE EFFECT OF ANNEALING

As with the MIL-P-5425 material, annealing improves the resistance to crazing as shown in Table 4.3-III. The level at which crazing occurs is at a higher stress and percentage of strain than the unannealed material for both stress and stress-solvent crazing.

4.3.3.2.4 LUMINOUS TRANSMITTANCE

The luminous transmittance of MIL-P-8184 material is shown in Figure 4.3-37 over a wide frequency range which includes ultraviolet and part of the infrared spectra.

4.3.4 MIL-P-25690

4.3.4.1 GENERAL

With the discovery of the crack propagation resistance property associated with stretched acrylic, MIL-P-8184 material was found to also be stretchable but to a lesser degree than MIL-P-5425. Because the MIL-P-8184 acrylic is partially cross-linked in its molecular structure, it cannot consistently attain the high percentages of stretch associated with the MIL-P-5425 material. Stretching within a 65- to 75-percent range, however, provided

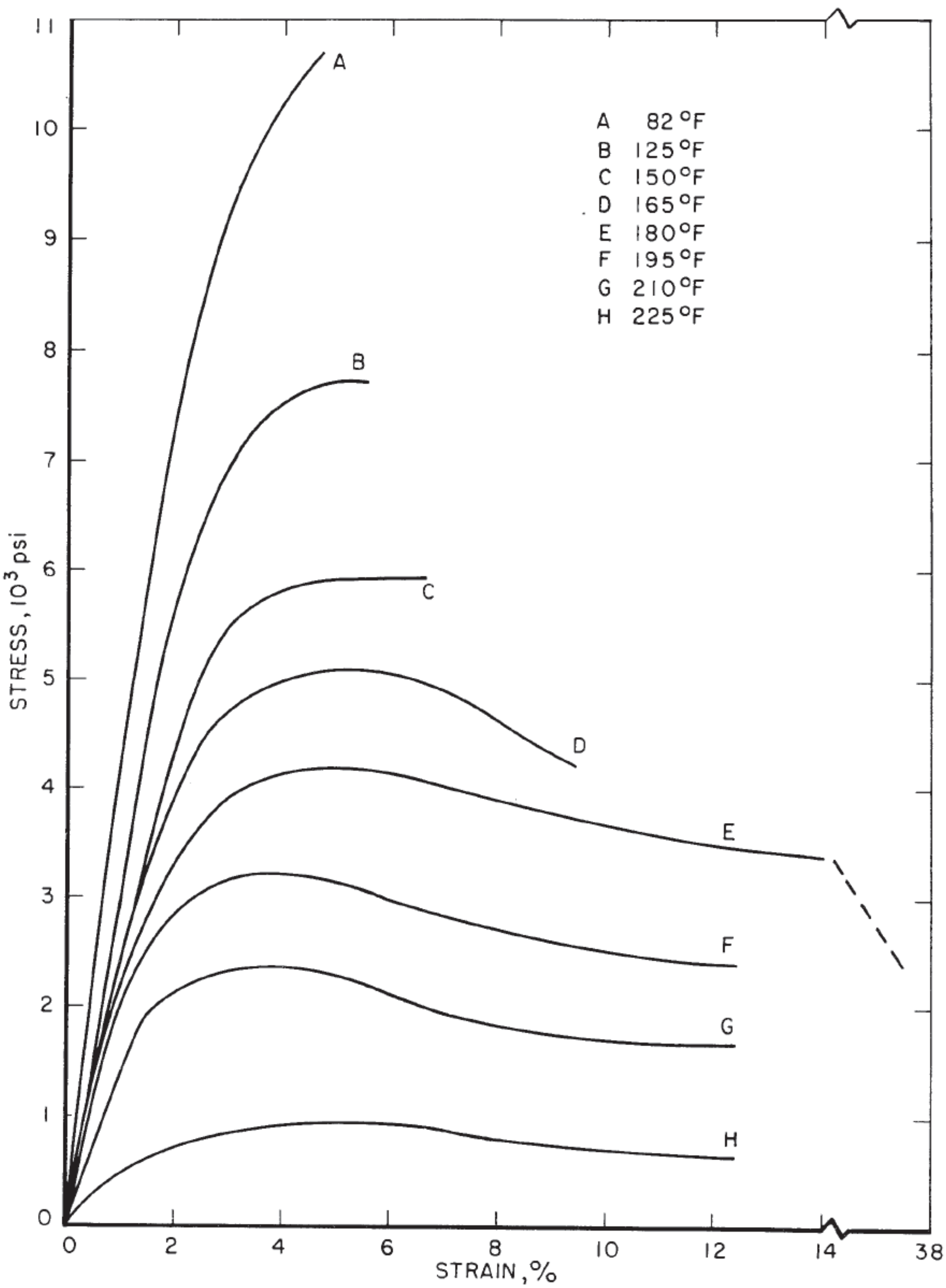

Figure 4.3-26 - Tensile Stress-Strain Curves for MIL-P-8184 Material at Various Temperatures

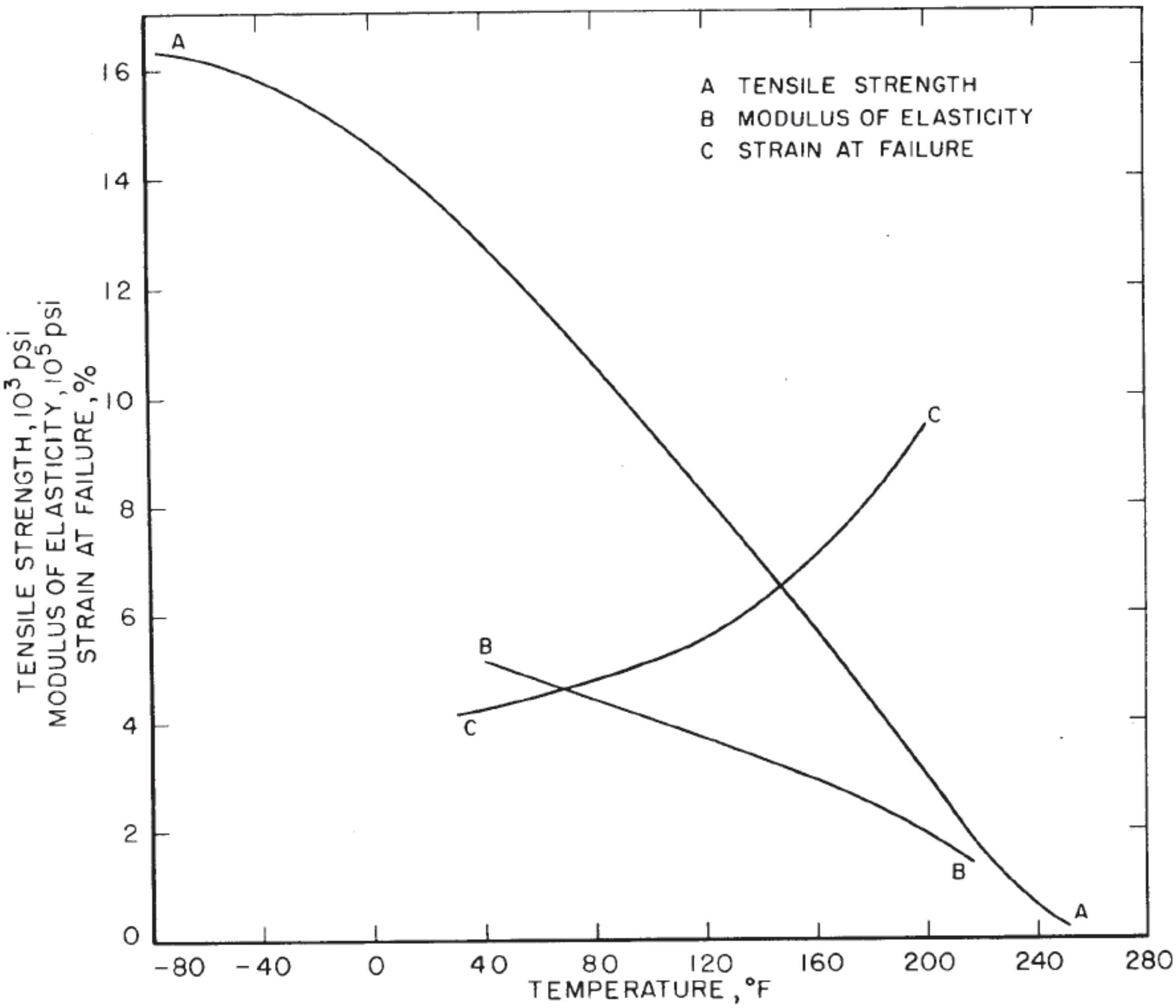

Figure 4.3-27 - Effect of Temperature on Tensile Properties (Short-Time Test) of MIL-P-8184 Material

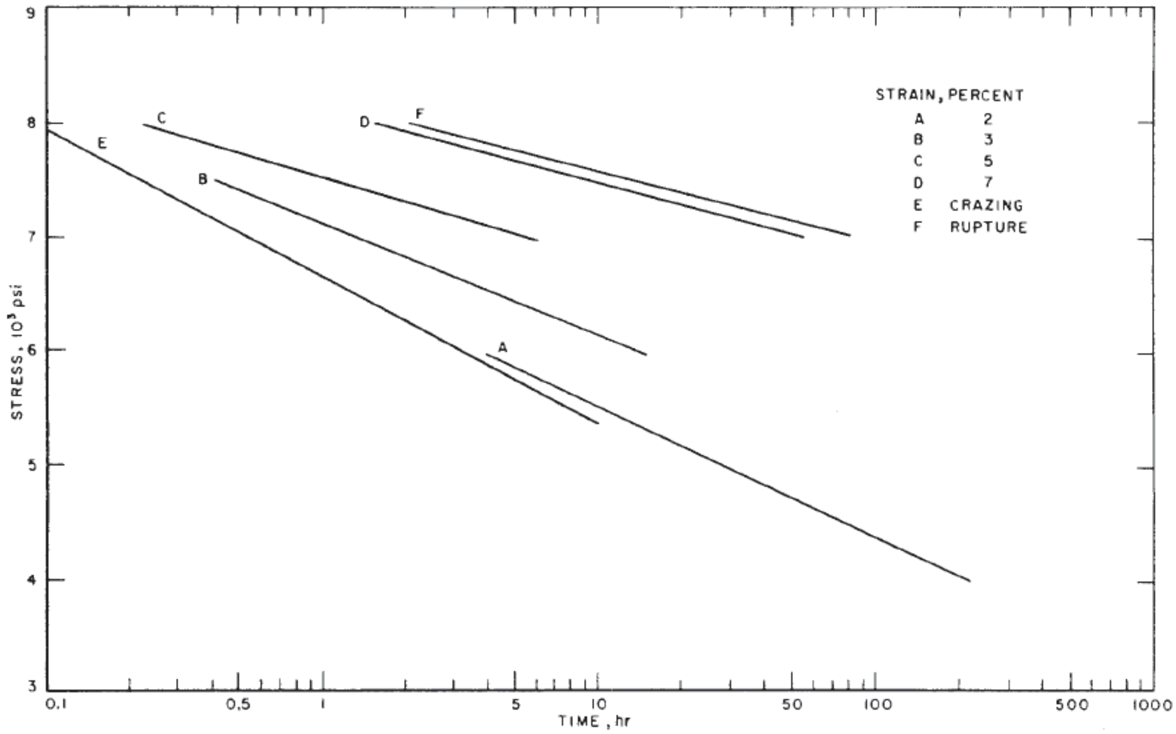

Figure 4.3-28 - Tensile Creep Data for MIL-P-8184 Material at 80 Deg F

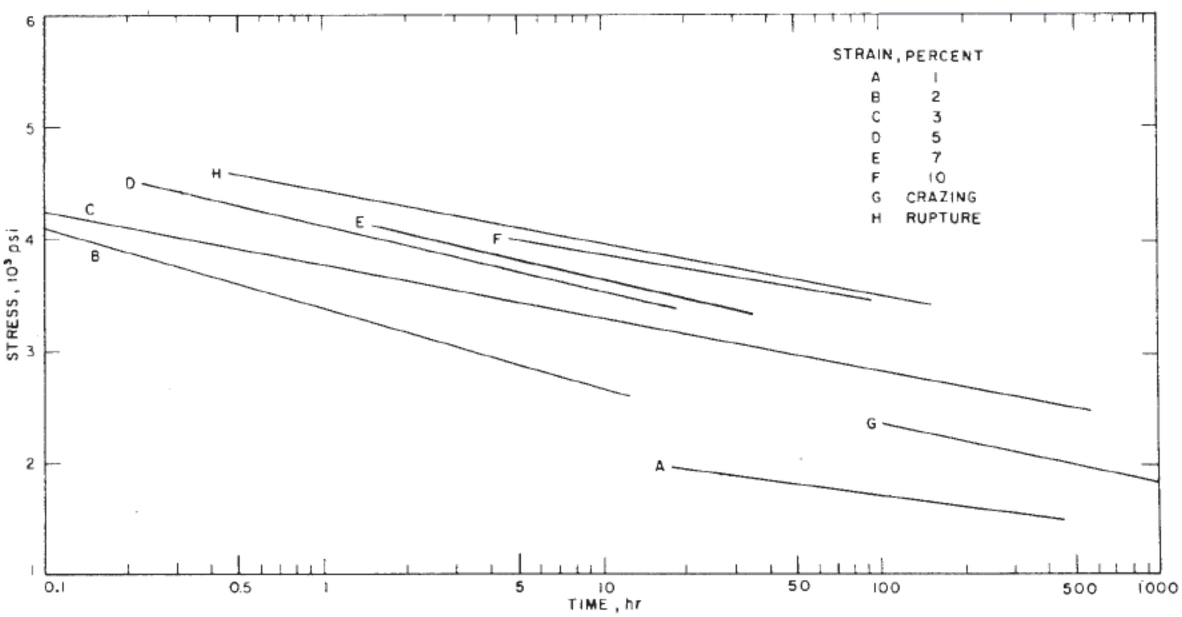

Figure 4.3-29 - Tensile Creep Data for MIL-P-8184 Material at 160 Deg F

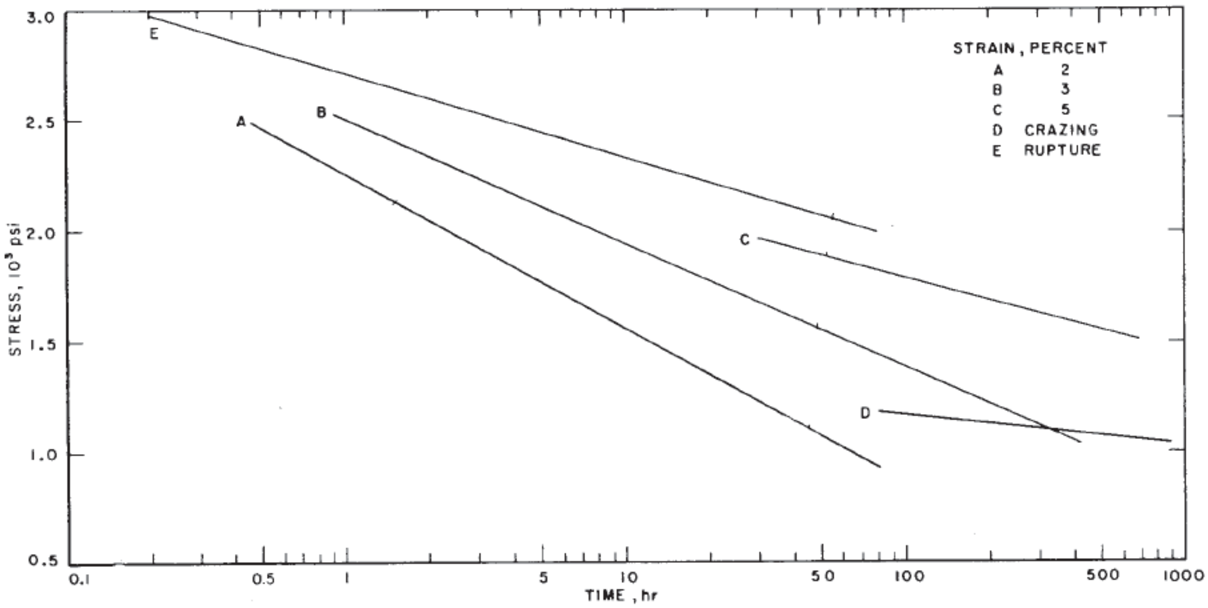

Figure 4. 3-30 - Tensile Creep Data for MIL-P-8184 Material at 200 Deg F

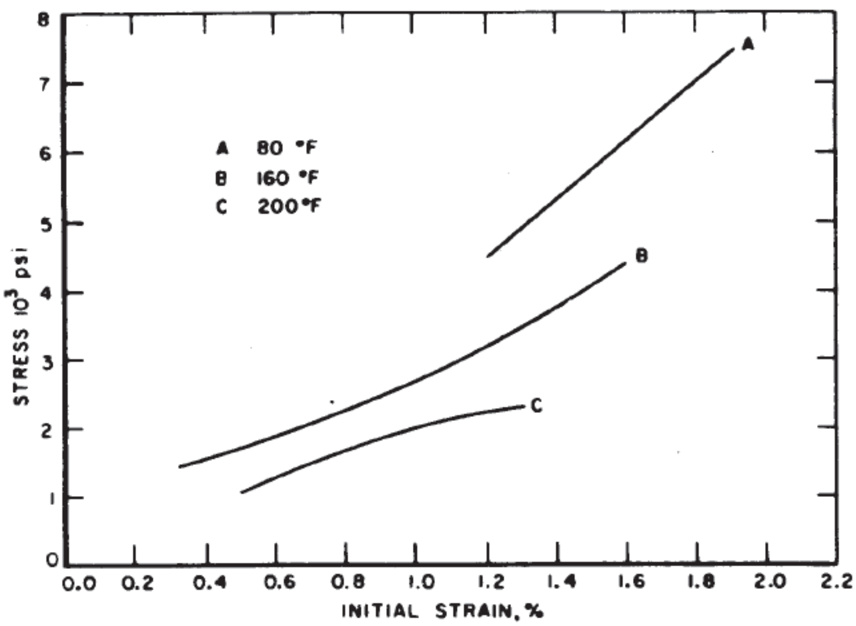

Figure 4. 3-31 - Effect of Stress on Initial Strain in Tensile Creep of MIL-P-8184 Material at Various Temperatures

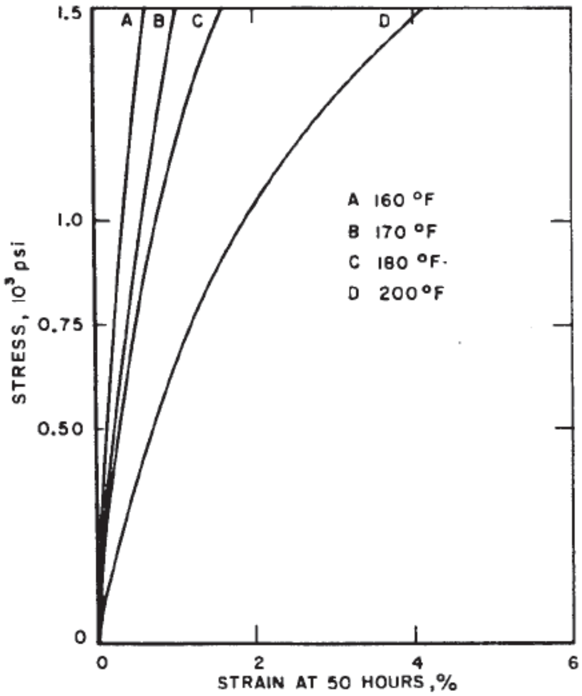

Figure 4.3-32 - Creep Strain of MIL-P-8184 Material at Various Temperatures at 50 Hours after Stress Was Applied

superior crack propagation and craze resistance to that of the stretched MIL-P-5425 material. As a consequence, stretched MIL-P-5425 never held military specification status, and the stretched MIL-P-8184 became the specified MIL-P-25690 material.

Material which has been stretched gains the crack propagation resistant property, but loses laminar shear strength. This change is attributed to an internal realignment during stretching which tends to straighten out the molecular chains into a semiparallel orientation. In this process, the strengths in the chains also become oriented to be nearly parallel with the surface of the material, and the 90-deg components of the chain structures, which represent shear strength, become weakened. As a result, edge attachment designs for stretched material depend upon a bolt-through construction rather than a construction which depends upon adhered reinforcements to the surfaces.

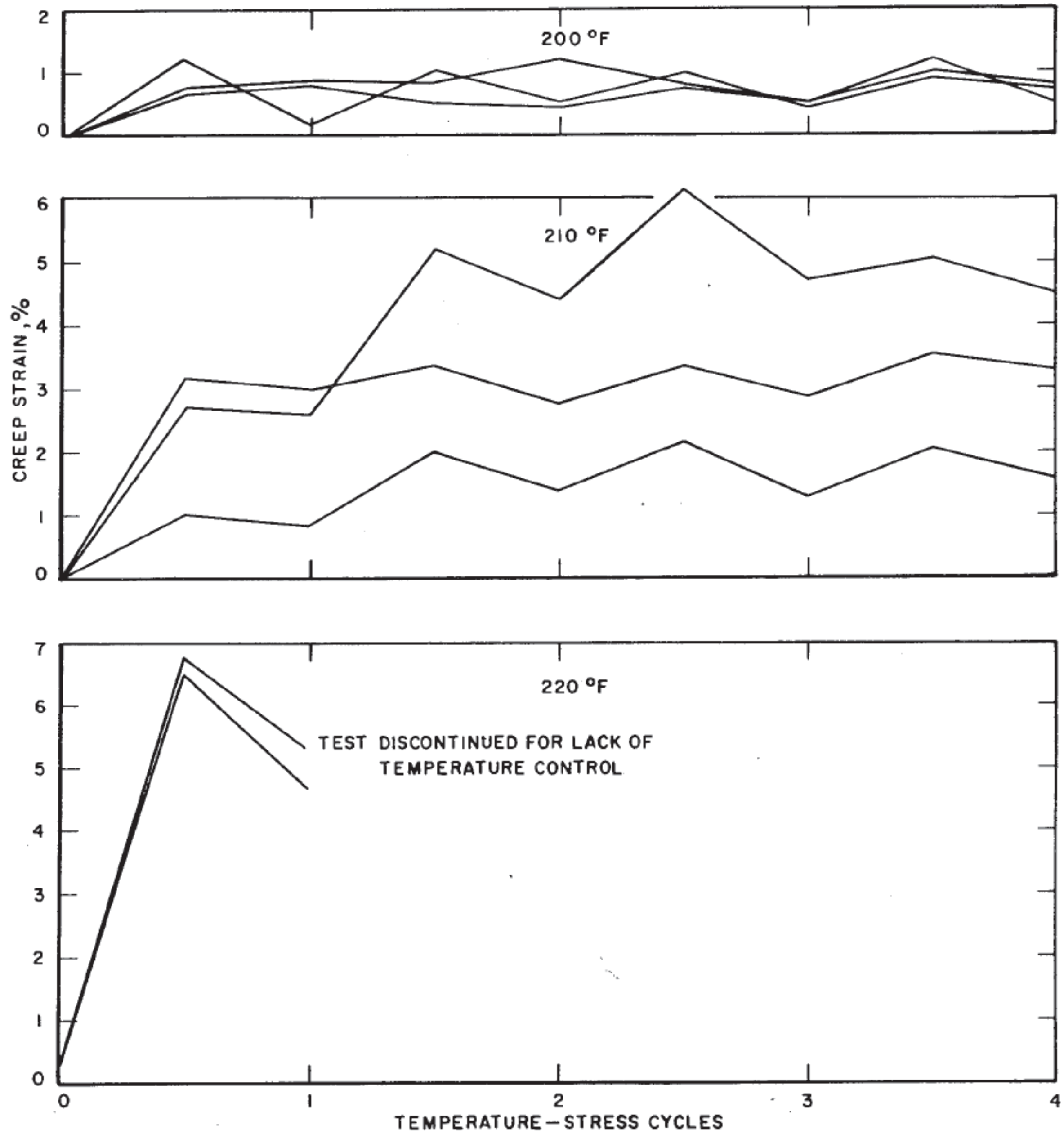

NOTES:
EACH CYCLE CONSISTED OF—
1. ONE HOUR AT TEST TEMPERATURE WITH NO LOAD.
2. ONE HOUR AT TEST TEMPERATURE WITH A STRESS OF 600 POUNDS PER SQUARE INCH.
3. ONE HOUR AT TEST TEMPERATURE WITH NO LOAD.
4. STEPS 2 AND 3 WERE REPEATED TWICE.
5. THE LOAD WAS REAPPLIED AND AFTER ONE HOUR THE MAXIMUM EXTENSION WAS DETERMINED.
6. THE SPECIMENS WERE UNLOADED AND COOLED TO ROOM TEMPERATURE. AFTER 16 HOURS THE PERMANENT EXTENSION WAS MEASURED.

Figure 4.3-33 - Creep Strain of MIL-P-8184 Material Under Cyclic Stress-Temperature Conditions

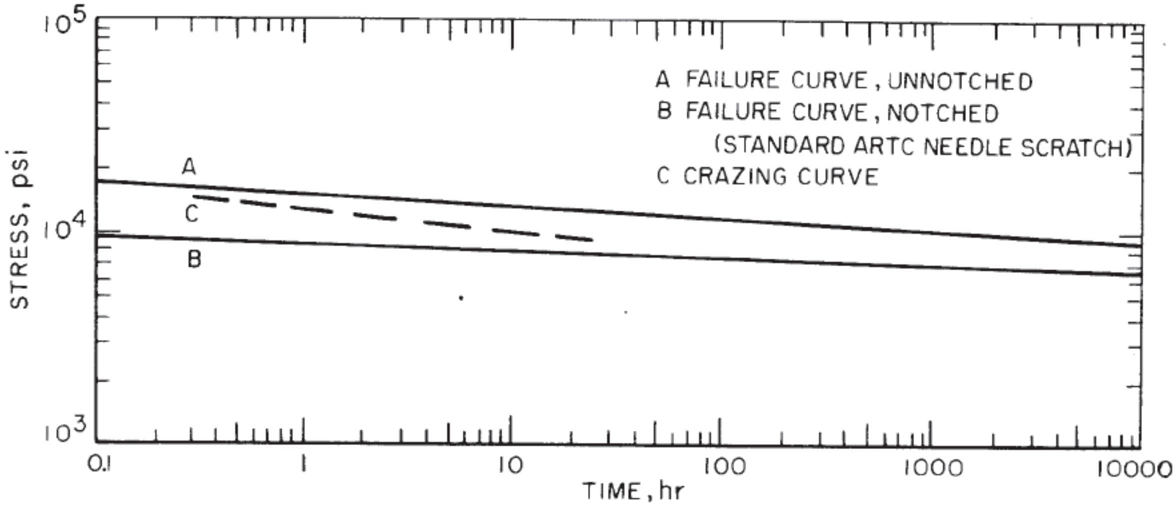

Figure 4.3-34 – Effect of Duration of Loading on Flexural Properties of 0.250-Inch-Thick MIL-P-8184 Material at Room Temperature

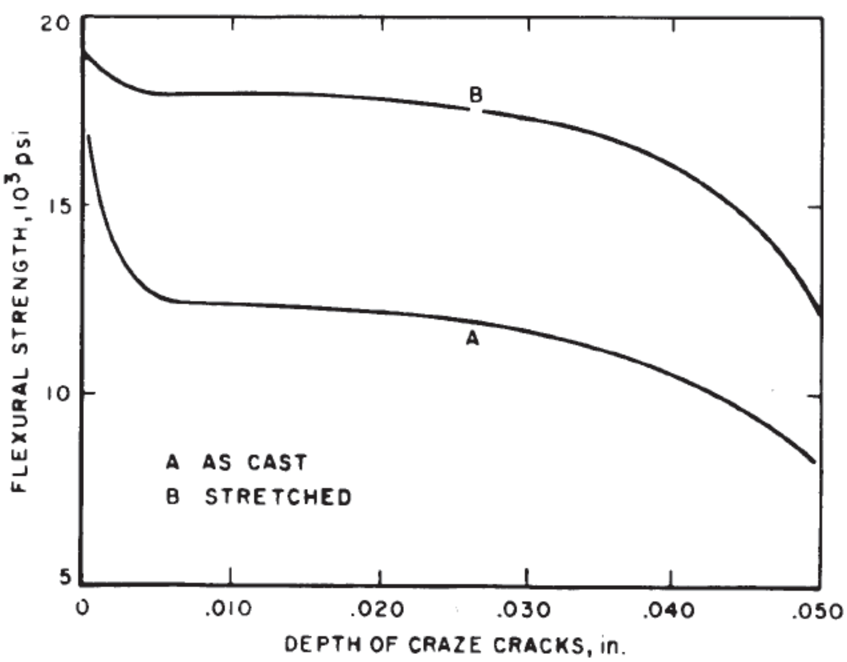

Figure 4.3-35 – Effect on Depth of Craze Cracks on the Flexural Strength of Crazed MIL-P-8184 Material

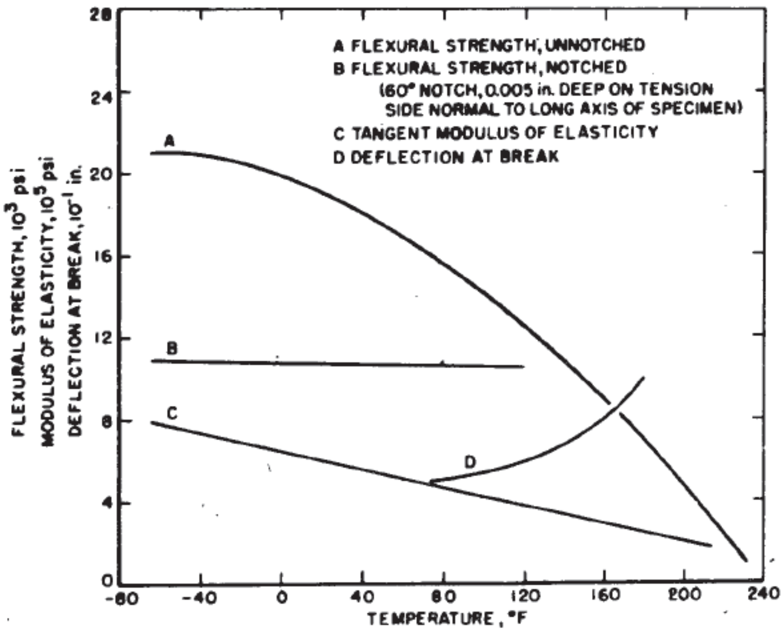

4601-47

Figure 4.3-36 - Effect of Temperature on Flexural Properties (Short-Time Test) of MIL-P-8184 Material

4.3.4.2 PROPERTIES

Among the comparative properties of other materials, tensile-rupture cures at three temperatures are in Figures 4.2-3, 4.2-4, and 4.2-5 on pages 4-6, 4-6, and 4-7. K-value versus temperature is found in Figure 4.2-7 on page 4-9; and luminous transmittance after Tabor abrasion in Table 4.2-I on page 4-13.

4.3.4.2.1 TENSILE DATA

Stress-strain, tensile strength versus temperature, stress versus secant modulus curves, tensile creep data, and acrylic creep data are found in Figures 4.3-38 through 4.3-52. The modulus of rupture curve (Figure 4.3-42) indicates +160 F to be the optimum operational temperature.

TABLE 4.3-III - EFFECT OF HEAT TREATMENT ON THE CRAZING PROPERTIES OF MIL-P-8184 MATERIAL UNDER TENSILE LOAD AT 73.5 DEG F

	Stress (PSI × 10^3)	Strain (percent)	Threshold stress for stress solvent crazing (PSI × 10^3)
MIL-P-8184			
Unannealed	9.6	3.4	2.4
Annealed*	10.2	4.0	3.1
Heated**	9.8	4.0	2.7
Heated and annealed	10.0	4.0	3.2

Notes:

1. Test method 1011 of Federal Specification L-P-406, type 1 specimens. Testing speed was 0.05 inch per minute up to 10 percent strain at which point the speed was increased to 0.25 inch per minute. The relative humidity was 50 percent. Data are based on 3 to 8 specimens.
2. Threshold stress for stress-solvent crazing is the minimum stress required to cause crazing upon application of solvent. The solvent used in these tests was ethylene dichloride.

*Annealing: heated to 212 F for 6 hours, followed by slow cooling.
**Heating: heated to 365 F for 39 minutes, followed by rapid cooling in air.

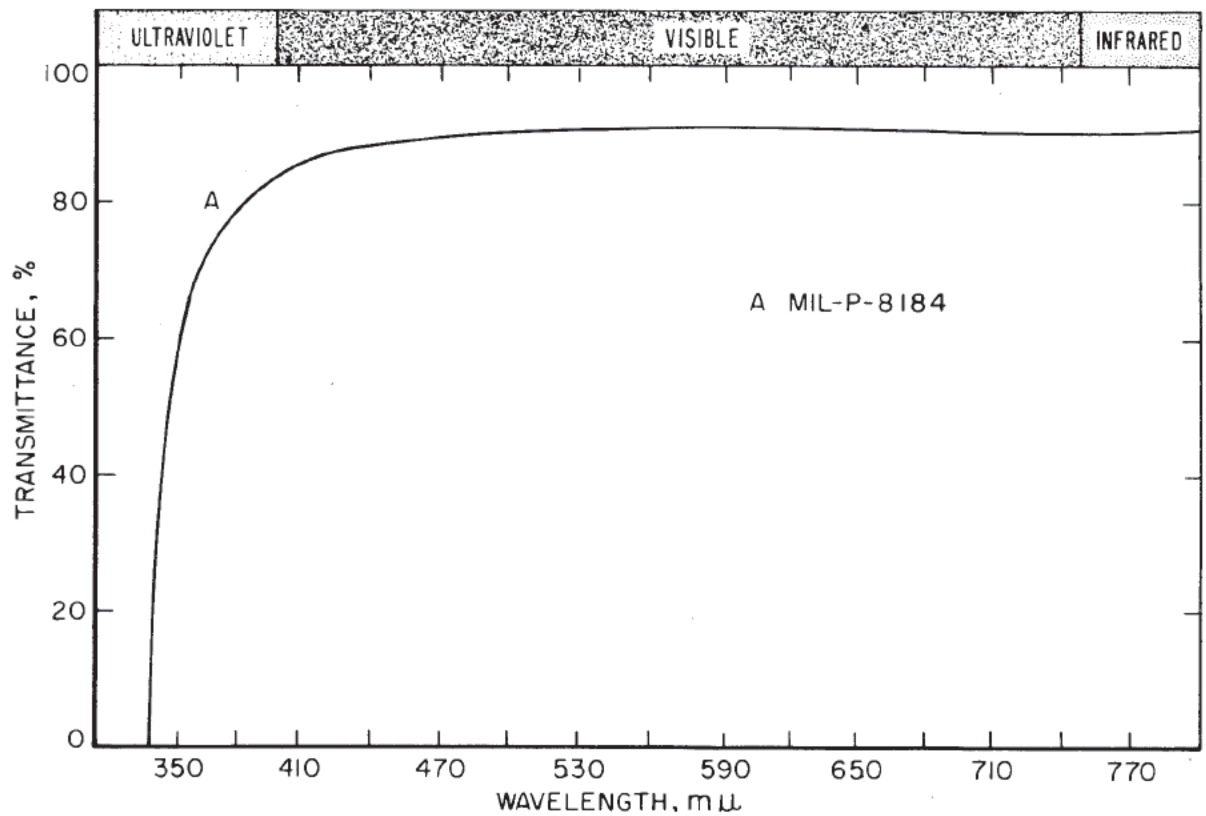

Figure 4.3-37 - Luminous Transmittance of MIL-P-8184 Material

N

See also Report # 10020

R 512

Technical Report

WINDOWS FOR EXTERNAL OR INTERNAL HYDROSTATIC PRESSURE VESSELS

Part I — Conical Acrylic Windows Under Short-Term Pressure Application

January 1967

NAVAL FACILITIES ENGINEERING COMMAND

U. S. NAVAL CIVIL ENGINEERING LABORATORY

Port Hueneme, California

Distribution of this document is unlimited.

Appendix B

MODES OF FAILURE OF CONICAL ACRYLIC WINDOWS

In the following descriptions of failure modes for conical acrylic windows, certain terms have special definitions. Cold flow is the plastic deformation of the acrylic window material at room temperature resulting from application of high hydrostatic pressure to the window high-pressure face while the low-pressure face remains at atmospheric pressure. Cratering denotes the formation of a roughly circular depression in the center of the window high-pressure face as a result of cold flow. A fracture cone is a cone-shaped fracture surface inside the body of a window observed at the termination of the test.

In the photographs supplementing the descriptions of the failure modes, the grid pattern seen on many of the high-pressure window faces is the reflection of a grid cast there at the time the photographs were made. This reflection is a device intended to reveal any cratering or other irregularity on the high-pressure face, as a result of cold flow or partial mechanical failure. Any irregularity in the mirrorlike window surface is made apparent by a distorted reflection of the regular square pattern of the grid.

One-Inch-Diameter, 30° Conical Windows

All the 1-inch-diameter, 30° conical windows failed explosively, with all fragments ejected from the pressure vessel. An interesting feature was the lack of deformation on the high-pressure faces of these windows. Examination of a test specimen removed from the flange after being pressurized to approximately 85% of its critical pressure revealed almost no cold-flow cratering on the high-pressure face (Figure B-1) but a considerable amount on the low-pressure face, as evidenced by the moderately long, cylindrical extrusion (Figure B-2). The low-pressure face also exhibited the circumferential cracks typical of low-pressure faces of all conical acrylic windows regardless of their included angle size. Since the deformation was noted at a pressure very close to the critical pressure of the window, it is reasonable to assume that the failure of the 30° window does not result from any deep cratering of the high-pressure face, but propagation of cracks from the bearing surfaces to the interior of the window. When these cracks, already apparent in the specimen examined, penetrate to the window center, fracturing of the window occurs followed by ejection of the fragments from the mounting flange.

One-Inch-Diameter, 60° Conical Windows

The mode of failure of the 1-inch-diameter, 60° conical windows was not as uniform as that of the 30° windows, but varied with the t/D ratio. Windows with low t/D ratios, 0.125 and 0.25, failed by fracturing in such a manner that only the center portion was ejected, with the rest of the window staying in the mounting flange in the form of a continuous ring. The low-pressure face of these windows (Figure B-3) exhibited a conical fracture surface, while the high-pressure face remained flat without trace of cold flow, showing only a round hole with ragged edges in the center (Figure B-4).

The 60° windows with an intermediate t/D ratio (0.375 to 0.625) also fractured in the center, so that only the center portion of the window was ejected, while the other fragments remained in the flange in most cases. The windows with the intermediate t/D ratios had very severe cold-flow symptoms on the high-pressure face (Figures B-5 and B-6). This extensive cold flow was a bona fide indication that the proportions of the window were such that the failure of the material had to occur in the plastic range of its properties. The low-pressure face of the windows with intermediate t/D ratios had the same type of conical fracture cavity as the low t/D ratio, 60° windows (Figure B-7). The cold flow on the high-pressure face, when considered together with the conical fracture cavity on the low-pressure face, indicated that, although the amount of cold flow increased with the increase of t/D ratio, the actual mechanism of fracture was the same.

The third phase of deformation of the high t/D ratio, 60° windows took place at the point of critical pressure. At that time, the cold-flow crater in the high-pressure face had progressed to such a depth of the window body that the small cracks at the bottom of the crater united with the cracks progressing from the window bearing surface at the cone-to-cylinder transition zone, and a conical fracture surface was created. When the conical fracture surface was generated, the center portion of the window was ejected first, followed immediately by the remainder propelled by the high-velocity stream of water.

One-Inch-Diameter, 90° Conical Windows

The 1-inch-diameter, 90° conical windows failed in a manner similar to the 60° windows. The low t/D ratio windows failed by ejection of the center portion of the window with the rest remaining in the flange. The intermediate and high t/D ratio windows in most cases failed by complete fragmentation. The low t/D ratio windows failed without cold flow (Figures B-12 and B-13), while those with intermediate and high t/D ratios exhibited cold flow. The phases of window deformation were the same as in the 60° windows, except that the magnitudes of deformation were different for the same t/D ratios. Again, as in the 60° windows, one could see the minute cold flow on the high- and low-pressure faces in Phase 1 (Figures B-14 and B-15) and the fair amount of cold flow in Phase 2 (Figures B-16 and B-17). The basic difference in Phases 1 and 2 of the 90° windows from the corresponding phases of the 60° windows lay in the amount of cold flow at the same pressure. While the cold flow was extensive for the 60° windows, for the 90° windows only slight indication of it was evident. Thus, when a comparison was made between a 60° and a 90° window from interrupted failure tests, one could see that although both windows had the same t/D ratio (0.625) and both had been pressurized to 26,600 psi prior to removal from the vessel, only the 60° window exhibited cold flow extensively on both the high-pressure and low-pressure faces (Figures B-6 and B-18).

One-Inch-Diameter, 120° Conical Windows

In the $0.125 \le t/D \le 0.625$ range of ratios, conical windows failed consistently by fracturing in the middle, so that the center portion was ejected (Figures B-19 through B-24) while the remainder of the window was retained by the mounting flange. This was quite different from the failure of 60° and 90° windows, where the center portion of the window was ejected only in the low and intermediate $0.125 \le t/D \le 0.375$ range of ratios, while at the high t/D ratios the whole window was invariably ejected.

During some of the testing (arrested failures) it was possible to retrieve the center portion. Close inspection of this portion revealed that the mechanism of failure of the 120° windows was quite complex, as the center portion exhibited, in addition to the cold-flow crater on the high-pressure face, a conical fracture cavity on the low-pressure face which also showed signs of cold-flow displacement into the cylindrical opening in the mounting flange.

Thus, a typical 120° window, as exemplified by the 0.5 t/D ratio window in Figures B-25 and B-26, had two fracture cones, an inner one and an outer one. The latter surrounded the whole center portion of the window generally ejected from the flange in small fragments. In the example shown of a typical 120° window failure, the center portion, including the inner fracture cone, was not ejected from the flange, but retrieved from a basket hung immediately below it on the high-pressure side of the window. The reason in this case for the center portion of the window not being ejected was probably the fact that the apex of the inner fracture cone on the low-pressure face met the apex of the cold-flow crater on the high-pressure face, creating a passage for the fluid and thus permitting the pressure in the vessel to be relieved a split second before the center portion of the specimen was extruded sufficiently to be ejected through the cylindrical opening in the flange.

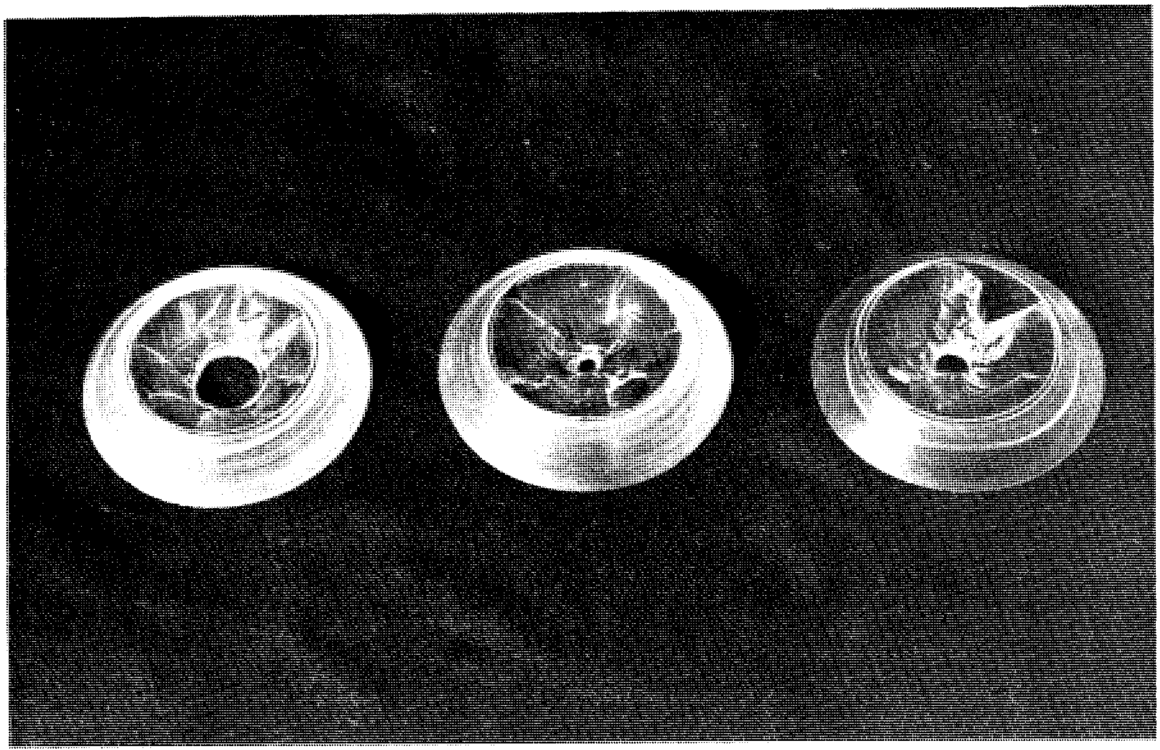

Figure B-12. Failed 1-inch-diameter, 90°, 0.25 t/D ratio windows, low-pressure faces.

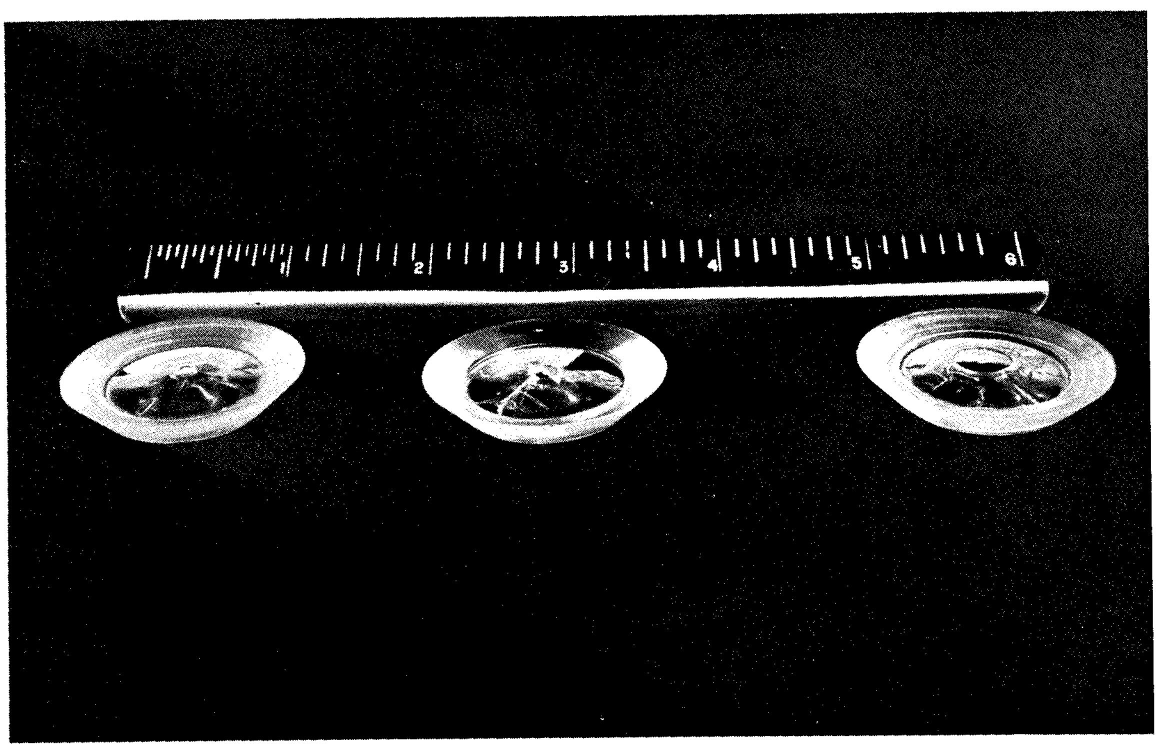

Figure B-13. Failed 1-inch-diameter, 90°, 0.25 t/D ratio windows, high-pressure faces.

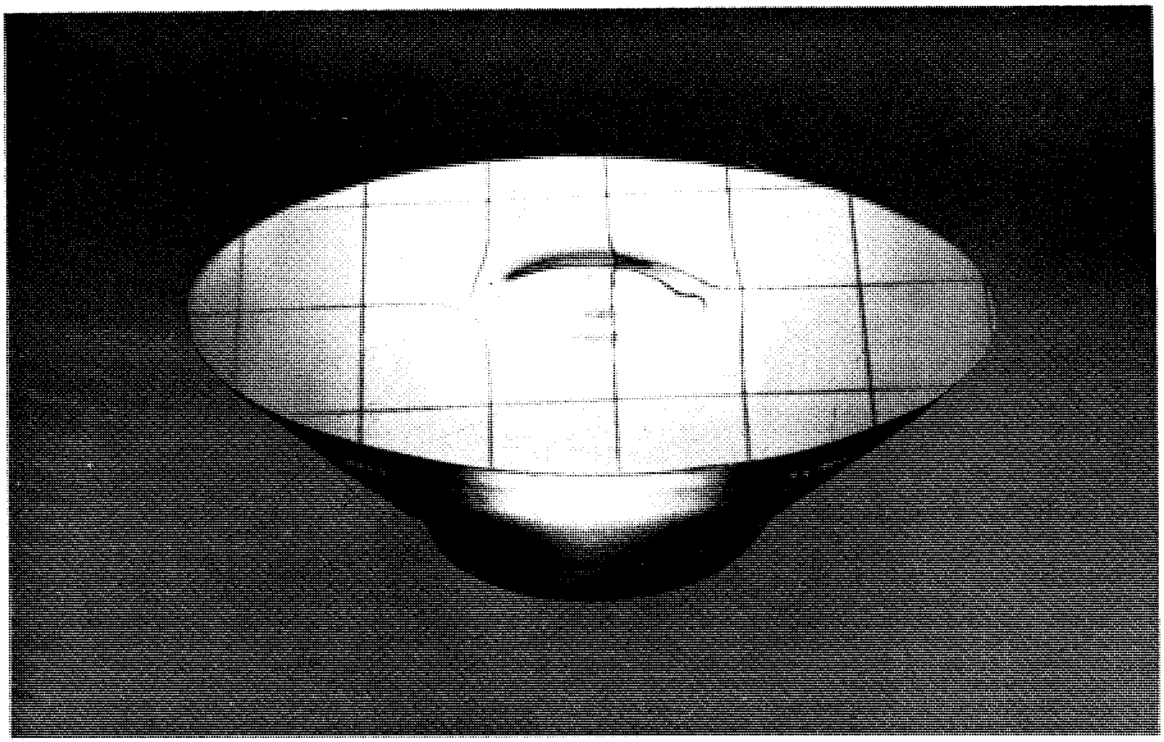

Figure B-14. Arrested failure of 1-inch-diameter, 90°, 0.625 t/D ratio window at 26, 500 psi, high-pressure face. (Phase 1 of deformation.)

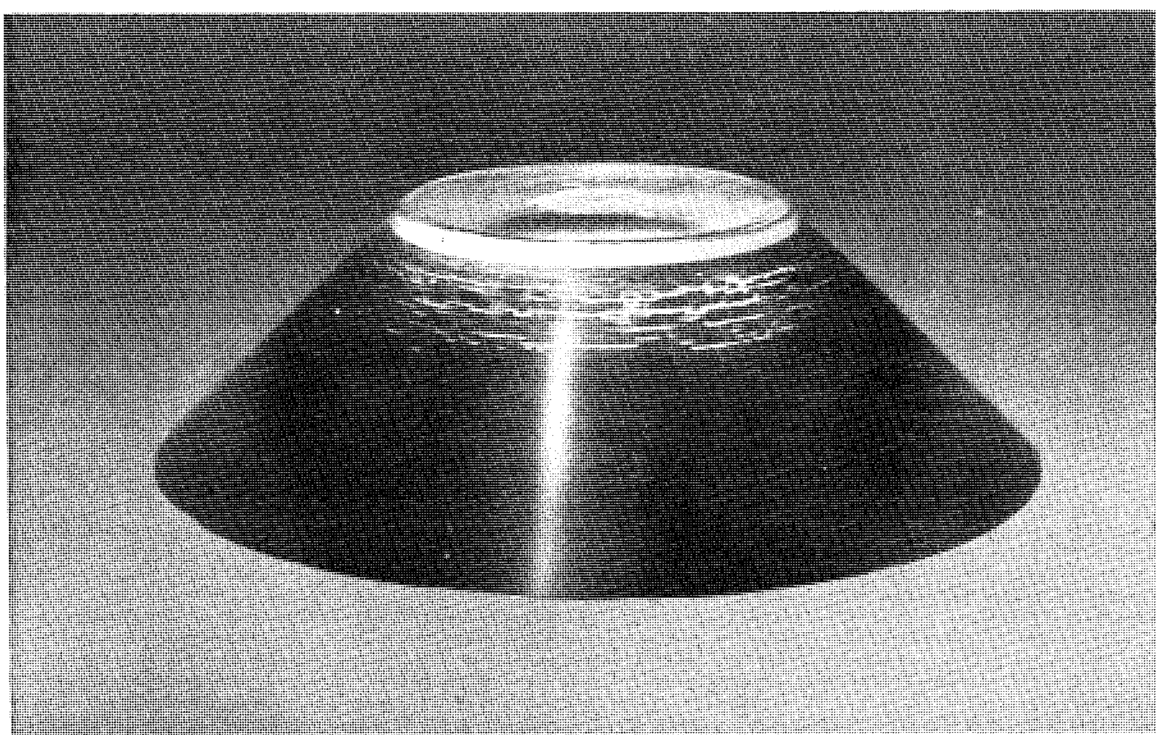

Figure B-15. Arrested failure of 1-inch-diameter, 90°, 0.625 t/D ratio window at 26, 500 psi, low-pressure face. (Phase 1 of deformation.)

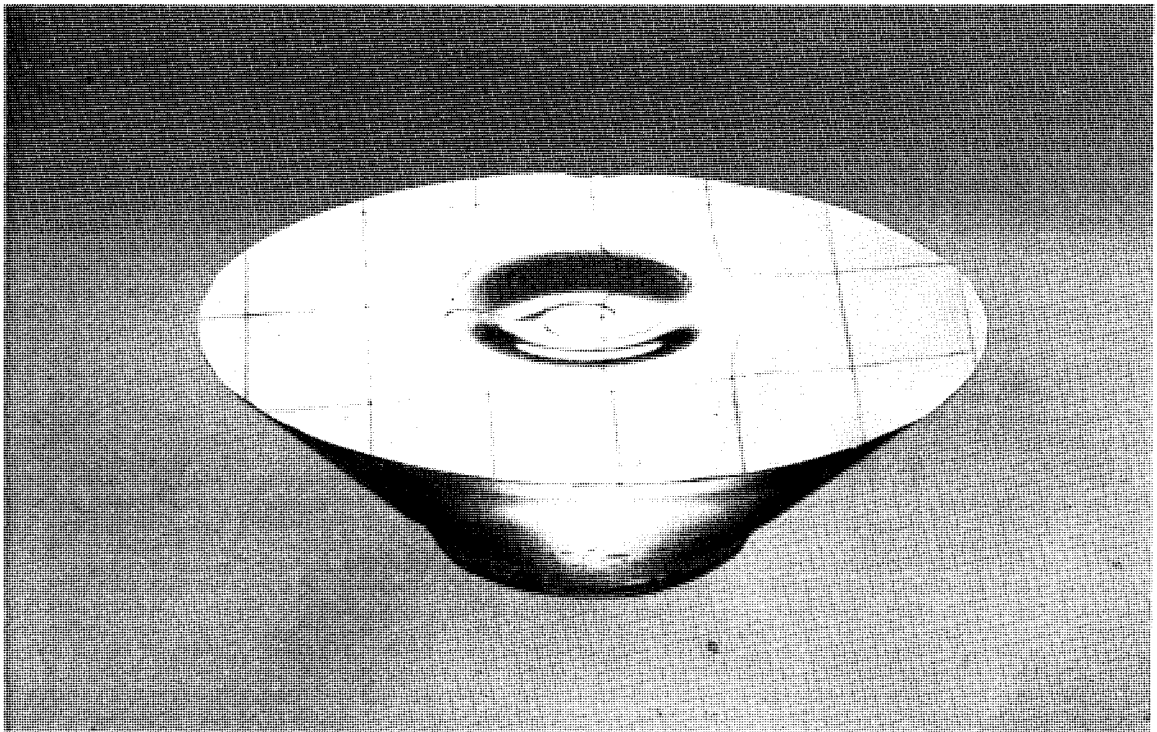

Figure B-16. Arrested failure of 1-inch-diameter, 90°, 0.625 t/D ratio window at 28,600 psi, high-pressure face. (Phase 2 of deformation.)

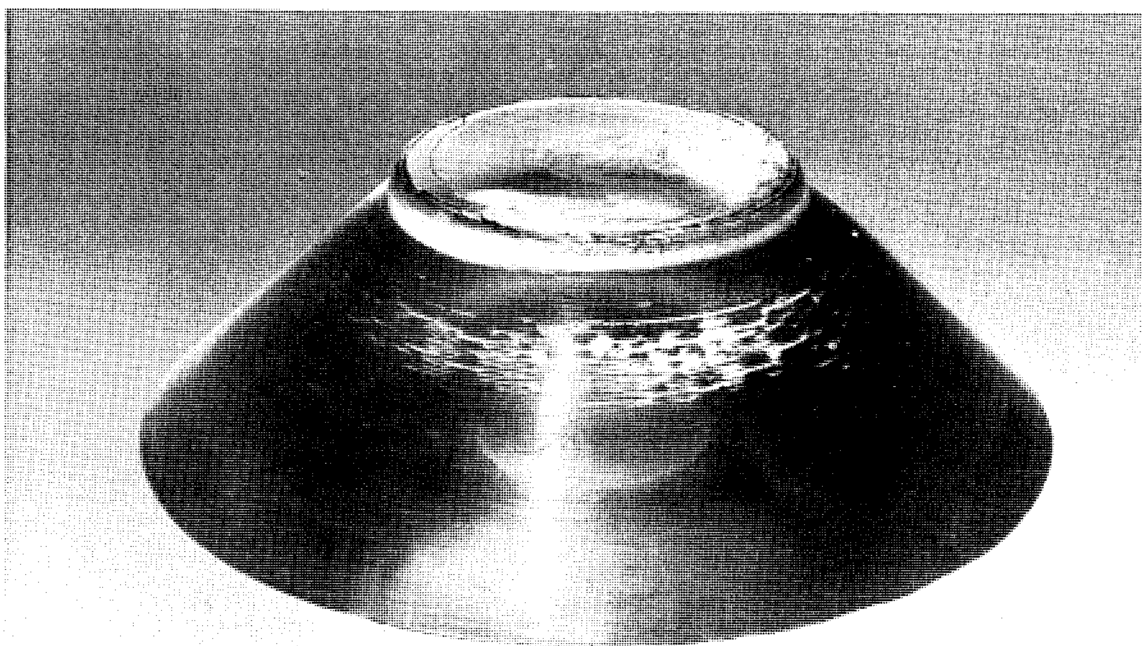

Figure B-17. Arrested failure of 1-inch-diameter, 90°, 0.625 t/D ratio window at 28,600 psi, low-pressure face. (Phase 2 of deformation.)

APPENDIX B

OceanGate Correspondence
2018 Window Review

From: [redacted]
Sent: Thursday, December 14, 2017 1:49 PM
To: [redacted] P.E.
Subject: 1124 - Window Performance review
Attachments: DWG 1124-100-010 4000m SphericalDome 90 Deg.pdf; 1124 - Conical Frustum window model (10-31-17).pdf; Dwg 1S-040-MEC-000461 REV-B.pdf

Dear [redacted],
Thank you very much for your time this morning. It was most useful to share some ideas and concerns. Thank you.

Please find attached two acrylic window designs.
The first (DWG 1124-100-010) is a standard PVHO 90 deg spherical sector window rated to 4000m, with a CF 4, at 50F and a Di of 15.203 inch (Ri = 10.75")
This is what I have recommended to the user to install in their vehicle.

The window they have ordered (DWG 1S-040-MEC-000461 Rev B), is a similar design but with the inside LPS as a flat surface. We have run some very basic FEA and it is quite clear that the stress distribution of this type of geometry follows the performance behavior of a conical frustum window, not a spherical sector.
I have shared some of this information with the company and urged them to carefully run a full FEA analysis on their design and perform actual testing on scale model windows to verify the actual limits of performance.

The client wishes to push beyond the limits (considered overly safe) of ASME PVHO. There is no basis presented as to the basis on which they will establish the "safe operating range" of the window. Their only proposed plan is to measure the axial displacement of the window during the dive and assess the window performance based on the requirement that the window does not go past the window seat (or hopefully some safe distance before the end of the seat). It is likely that there is no concern or awareness of the creep factor and even less of the cyclic fatigue the window.

It appears that the window will exceed the material strength well before 5800 psi.
Can you have a look and provide your assessment of the limits of performance of the Flat dome geometry compared to the Spherical sector.

Thank you in advance for your help in this matter.
Let me know if you have any questions.

Best regards

[redacted]

[redacted]
HYDROSPACE Group Inc
[redacted]

9559 Center Avenue, Suite P
Rancho Cucamonga, CA 91730
USA

From: [redacted]
To: [redacted]
Cc: Stockton Rush; [redacted] P.E.
Subject: Re: Preliminary performance behavior of Flat internal spherical sector windows
Date: Tuesday, January 30, 2018 1:35:56 PM

Thanks, [redacted].

I will consider and discuss with my team.

All the best,

[redacted]
Director of Engineering
OceanGate, Inc.
1205 Craftsman Way Suite 112
Everett, WA 98201
[redacted]
(office) 425.595.5017
www.oceangate.com

From: [redacted]om>
Sent: Tuesday, January 30, 2018 11:08:23 AM
To: [redacted]
Cc: Stockton Rush; [redacted] P.E.
Subject: Preliminary performance behavior of Flat internal spherical sector windows

[redacted] Stockton,
Please find attached a prelim study of the behavior of a spherical sector window with the flat inside, low pressure, surface.
As we discussed, there is interest among other MUV manufacturers for this same type of geometry.
The optical benefits are a strong motivating factor for all involved.

[redacted] is one of the leading FEA analysts in the US today, an expert in pressure vessels and a specialist in PVHO acrylics.
[redacted] is also the chairman of the PVHO viewports committee and the subject at hand is of interest to many.
I asked Bart to have a look at the interesting behavior exhibited by this geometry. I have done some analysis and others have as well on their own windows.
The results were not what was expected, which I shared with you earlier. In addition, most of the early analysis was performed with simple linear analysis. This is usually an approximation since acrylic is fundamentally non-linear. Bart agreed to have a precise look into this and do comparative study with linear and non-linear models.

I consider this a very generous service from Kemper Engineering to perform such a “knowledge acquisition” exercise to see the difference in behavior between a Flat Conical frustum window against that of a flat conical window with an added spherical dome, both using linear and non-linear analysis.

The Flat conical Frustum model provides a guideline of the behavior and performance of a PVHO certified design. This can then serve as a comparative baseline to evaluate the new geometry.

This was all pro-bono work based on the general interest from the PVHO community and the growing interest in this new type of geometry in the submersible industry. I would invite and encourage you to contact Kemper Engineering for their expertise and services.
Bart is copied herein and I am sure would be more than happy to support a study of the performance envelope of this new geometry of windows.
Please feel free to contact him directly.

Likewise, if you have any questions, please feel free to contact me.

Best regards

[redacted]

[redacted]
President/CEO

HYDROSPACE Group Inc
9559-P Center Avenue
Rancho Cucamonga, CA 91730, USA
Tel. +01 (909) 989-7773
[redacted]
www.HydrospaceGroup.com

"Quality and Performance through Precision Engineering"

KEMPER
ENGINEERING SERVICES, LLC

INTEGRATED ENGINEERING AND DESIGN

[redacted]| President
[redacted]al Engineer
[redacted] Consultant

14 Jan 2018

[redacted]
President/CEO
Hydrospace Group
9559 Center Ave., Suite P
Rancho Cucamonga, CA 91730
Email: [redacted]

Ref: Preliminary evaluation of Cyclops viewport design at 5800 psi

Dear [redacted]

Based on the provided materials and our conversation, Kemper Engineering Services (KES) proposes the following estimate for services:

BACKGROUND: The Client (Hydrospace) has a hypothetical design for a submersible window. It uses PVHO-1 grade acrylic (PMMA) but does not use PVHO-1 geometry. The question posed by the Client is what benefit the domed "Cyclops" design has to a traditional conical frustum PVHO-1 design with the same seat profile. The pressure designated was 5800 psi. The window is shown below.

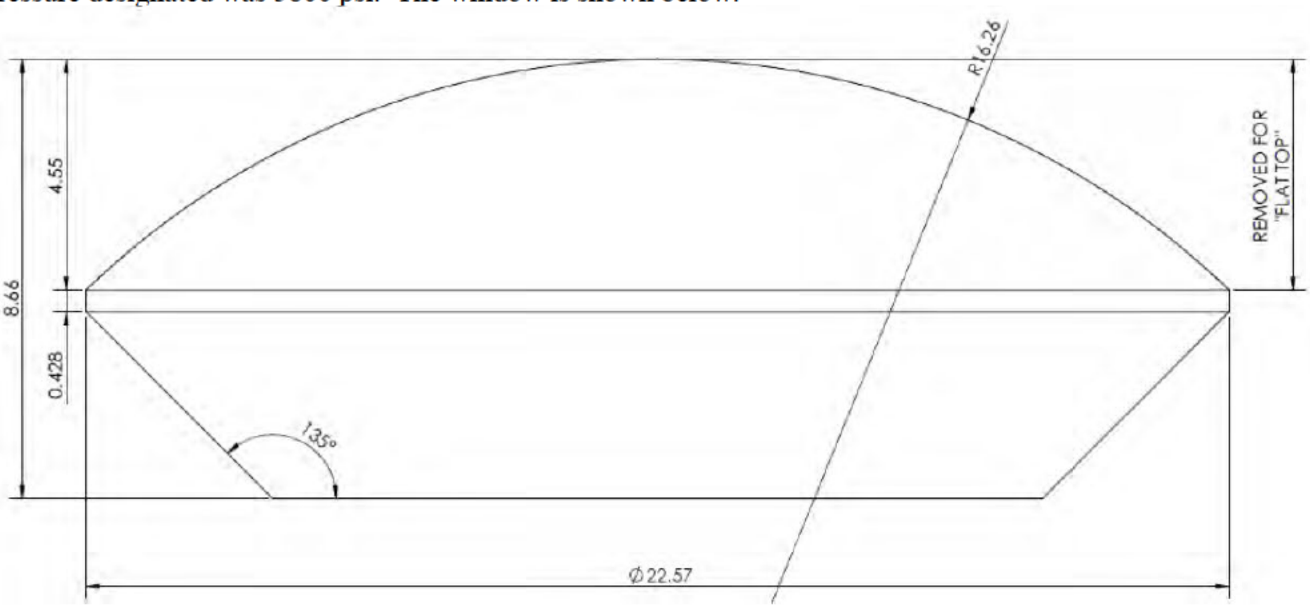

Fig. 1. Cyclops window design. Dimension are in inches. The "flat top" design is the same dimensions with the dome section removed.

METHOD: KES performed linear and nonlinear analysis. The material properties. included the stress-strain curve, is for 80F of MIL Grade 8184P acrylic. No material information was provided by the Client as this is a geometry comparison and not a design review of an actual submersible viewport. The effects of heat transfer, creep, and cyclic load are neglected in this preliminary assessment. The window seat is assumed and is only provided to develop the boundary conditions for the viewport. Axi-symmetric modeling is used, with contact elements allowing the viewport to slide along the window seat. Nonlinear analysis is the primary focus since acrylic window is a polymer that does not behave in a purely linear manner under significant load. Linear analysis is conducted as part of a normal modeling process and is presented for reference purposes. More information is in the attached pages.

RESULTS: Given the results are above the nominal yield of 7500 psi, the strain is used to evaluate potential for failure. Axial (inwards) deflection is provided as another measure.

	Cyclops Viewport		**Flat top Viewport**	
Model	*Max Strain (in/in)*	*Deflection (in)*	*Max Strain (in/in)*	*Deflection (in)*
5800 psi Linear	0.12	0.203	0.16	0.394
5800 psi Nonlinear	0.44 (possible cyclic fail)	0.264	0.73 (catastrophic failure)	0.924
4000 psi Nonlinear	0.27 (no failure)	0.174	0.54 (failure)	0.453
2900 psi Nonlinear	0.16 (no failure)	0.123	0.33 (cyclic failure)	0.269

CONCLUSIONS: The preliminary conclusions based on the assumptions specified are as follows:

1. The Cyclops design provides more axial stiffness and generates less strain than the same seat dimensions without the domed portion.
2. The specified Cyclops design at 5800 psi indicates significant strain that is consistent with potential short cycle failure modes.
3. The specified Cyclops design at lower pressures indicate acceptable strain levels, with the 2900 psi load being most consistent with traditional PVHO windows operating within normal design conditions.
4. The “flat top” viewport design would be likely to fail at 2900 psi pressure and will fail at higher pressures.
5. Actual material data, the window seat design, and operational information would be needed to conduct a design review and performance prediction.

KES offers a full range of engineering services, including solid modeling, CAD, stress analysis, transient and dynamic analysis, fluid flow with heat transfer simulations, kinematic modeling, animations, and presentation support. While some of the services are not part of the current estimate, they are available if needed to better assist the Client in their needs.

Thank you for giving KES the opportunity to support this project.

Sincerely,

[redacted] ***P.E.***
Principal Engineer

CONFIDENTIAL NTSB/USCG

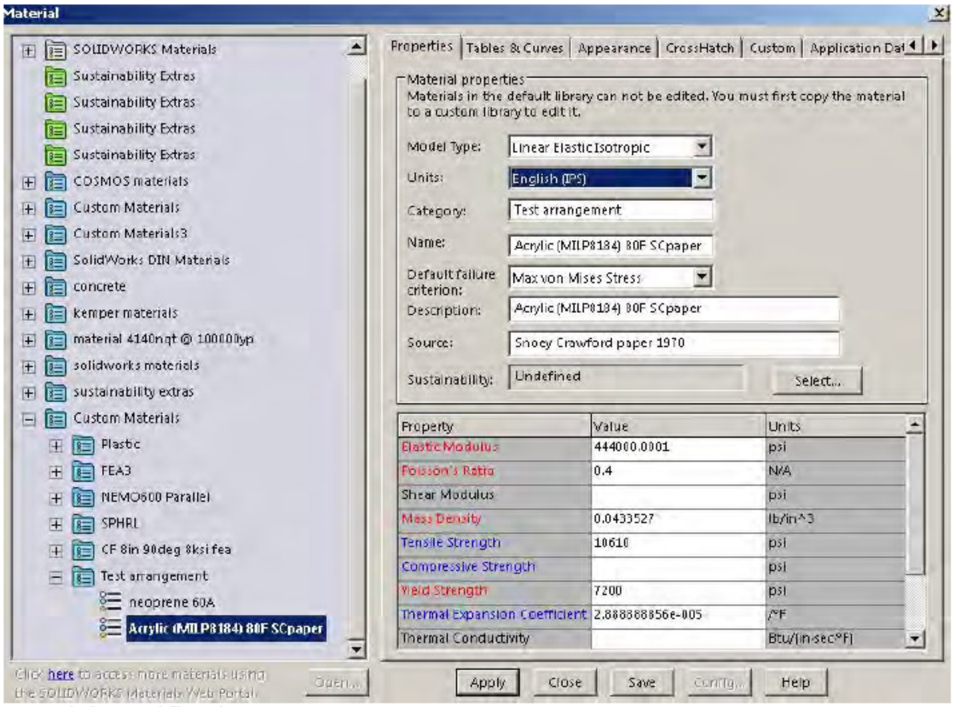

Fig. A1. Linear material specifications

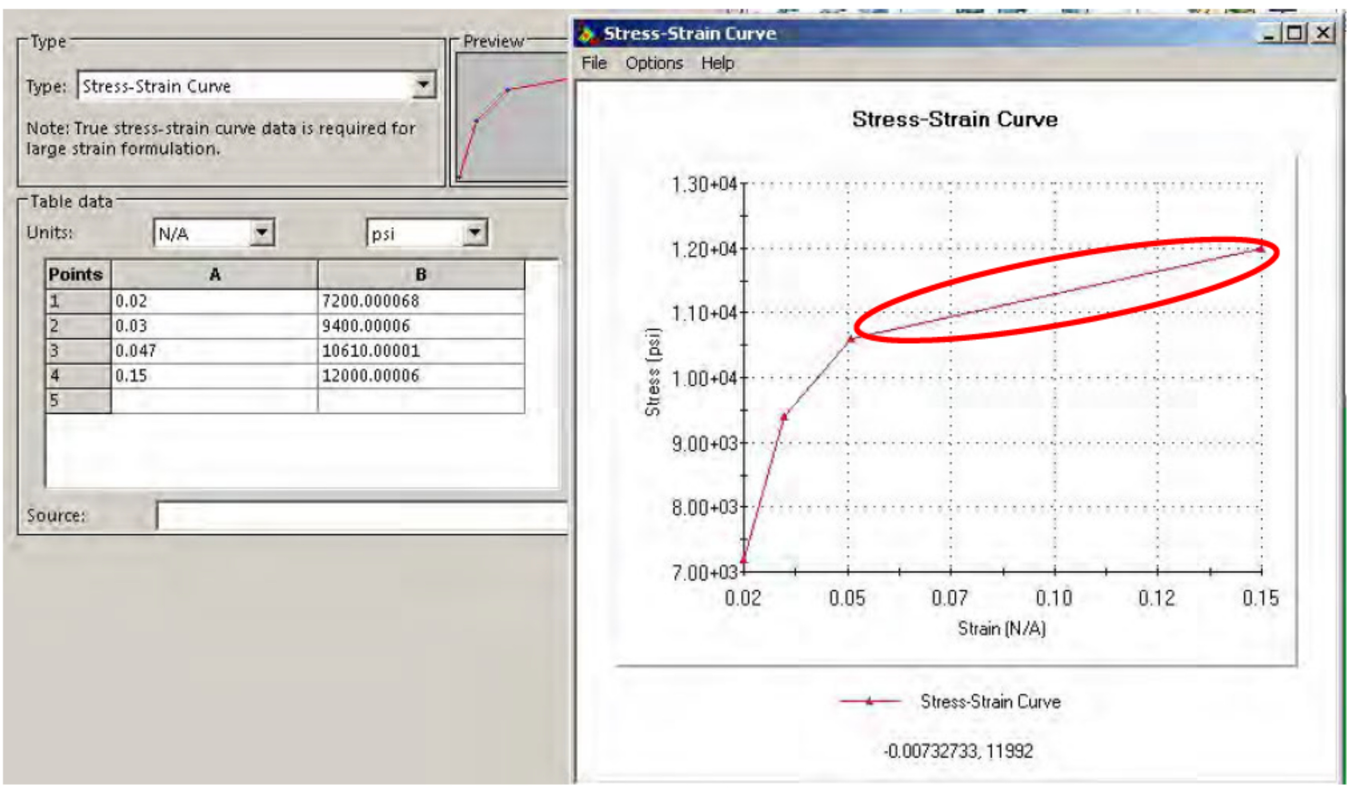

Fig. A2. Nonlinear curve used. This is for 80 degrees F, which is a mid-temperature from maximum surface ambient conditions and temperature at depth. The maximum strain is 0.05. The last segment (circled in red) is above ultimate strength to allow greater strain rate for an implicit nonlinear analysis to approximate a localized failure mode and allowing it to propagate.

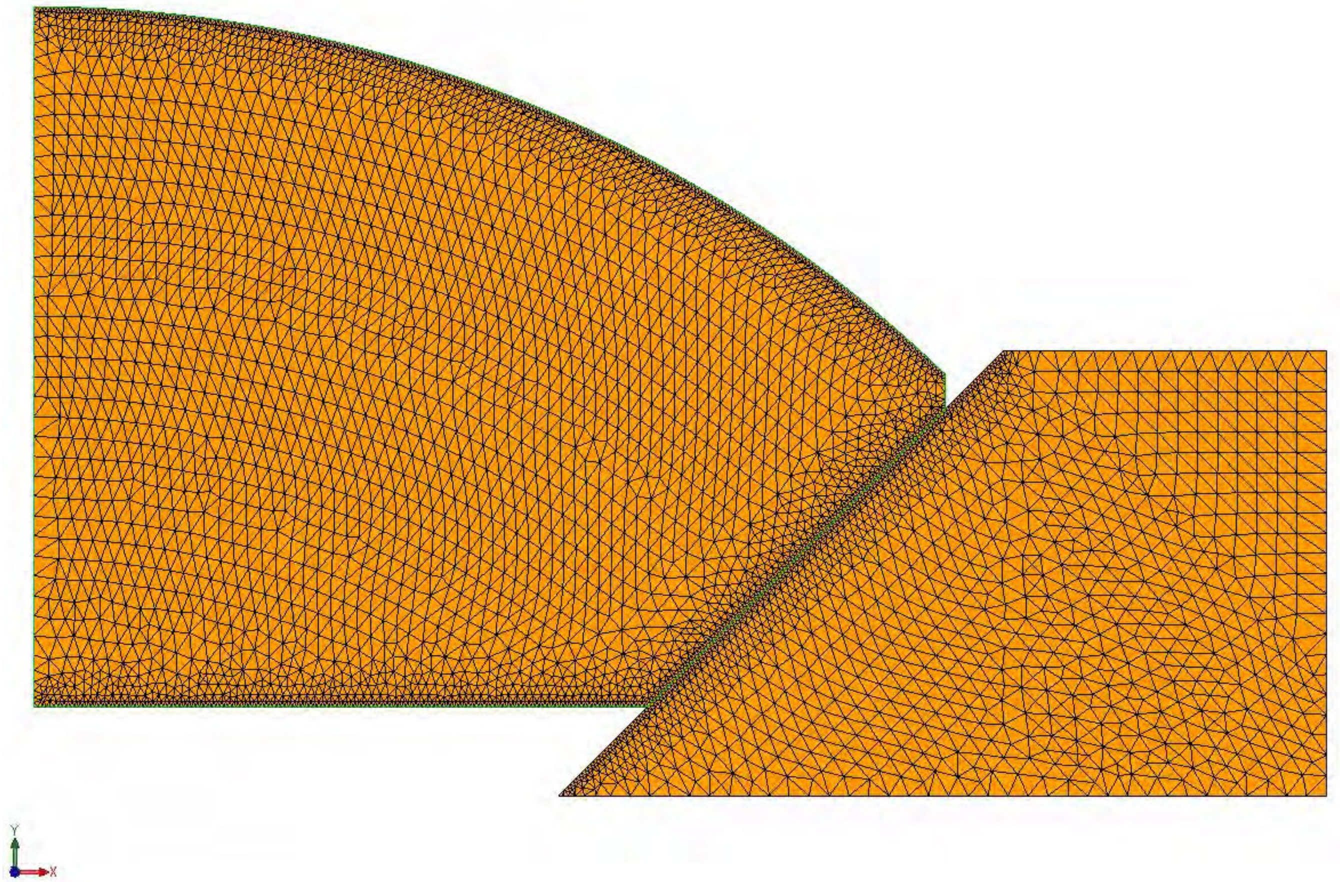

Fig. B1. Mesh for the cyclops geometry. Contact elements allow the window to slide against the fixed window seat.

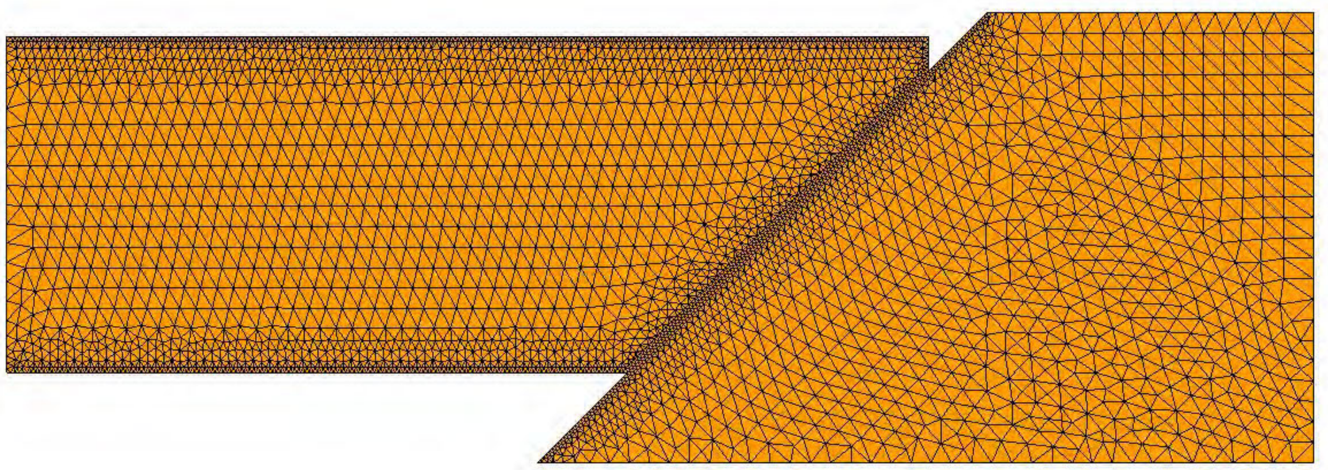

Fig. B2. Mesh for the truncated window geometry. It removes all of the material at the curved upper portion. All other dimensions are the same.

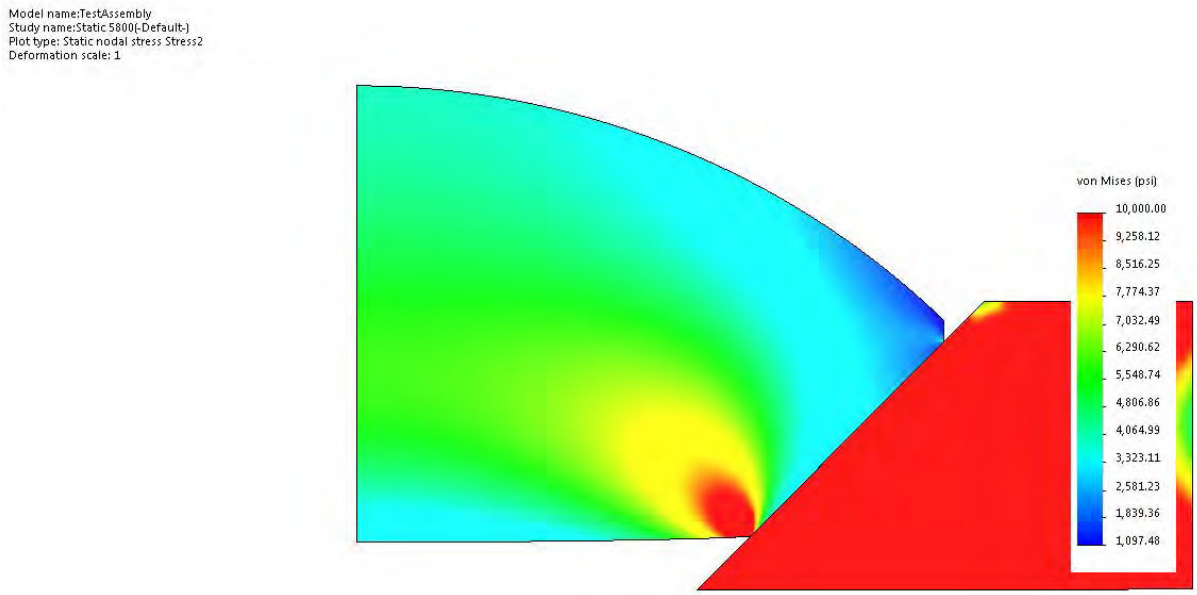

Fig. C1. Linear analysis, 5800 psi. Von mises is proportional to strain.

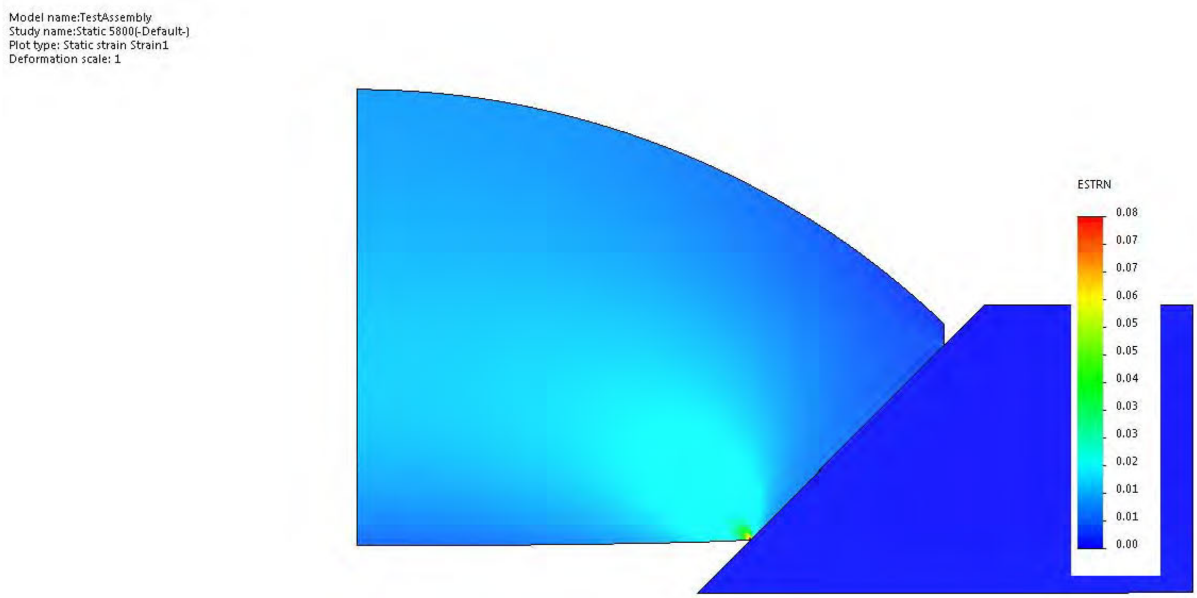

Fig. C2. Linear analysis, 5800 psi. Strain limited to 0.08 for consistency for comparison to other results. Maximum strain is 0.12.

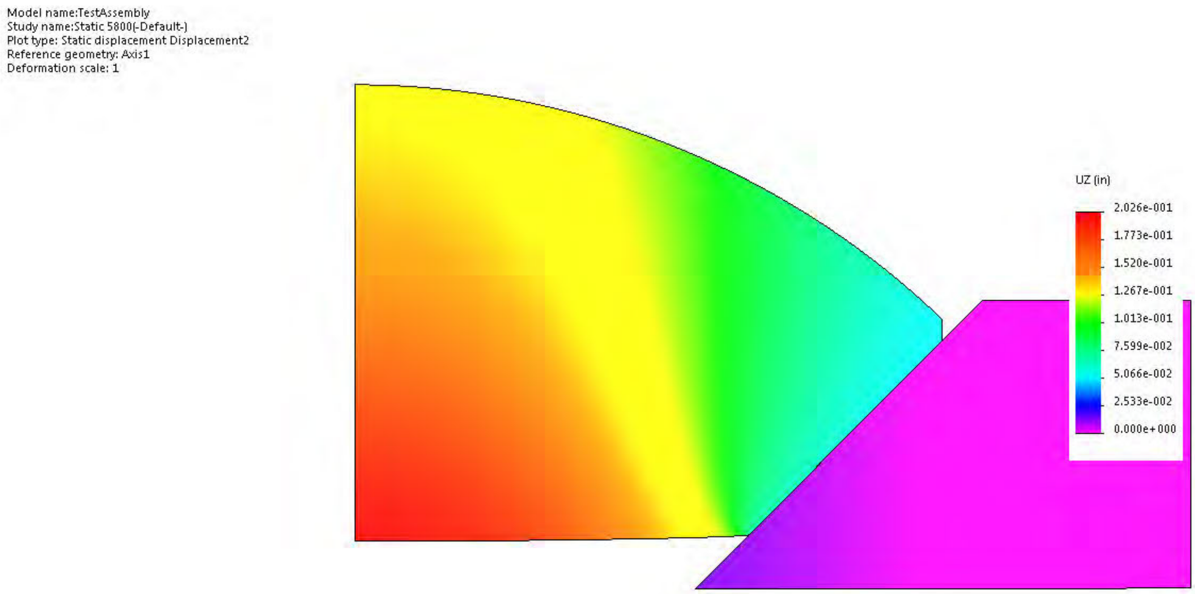

Fig. C3. Linear analysis, 5800 psi. Downwards displacement. Linear analysis is unsuitable for analyzing acrylic windows, but is being used for a purpose of comparison to the work by others.

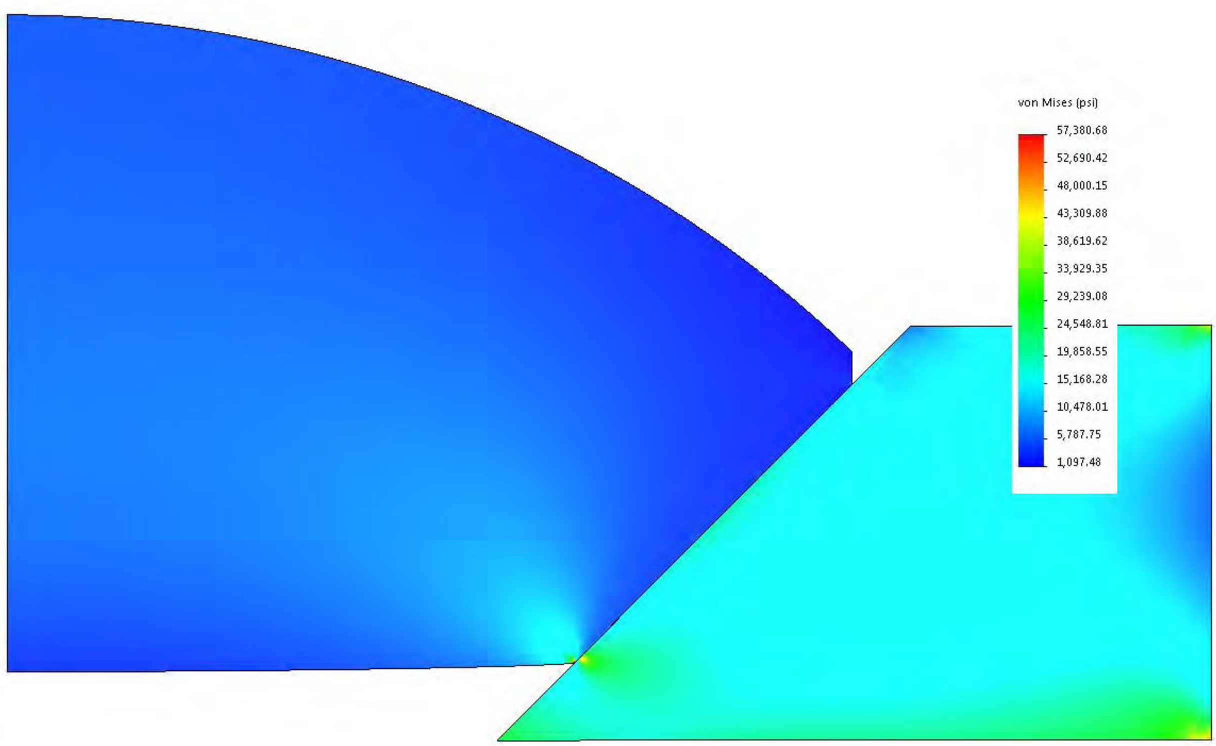

Fig. C4. Linear analysis, 5800 psi. Full range of Von Mises stresses. Peak stresses are in the window seat, which is made of steel and has a much higher yield and ultimate strength. Steel also responds in a linear manner whereas acrylic does not. Future stress plots will be limited to 10,000 psi in order to show stress differential in the viewport. The stresses in the window seat are to be disregarded. The window seat is only to provide a boundary condition for the viewport.

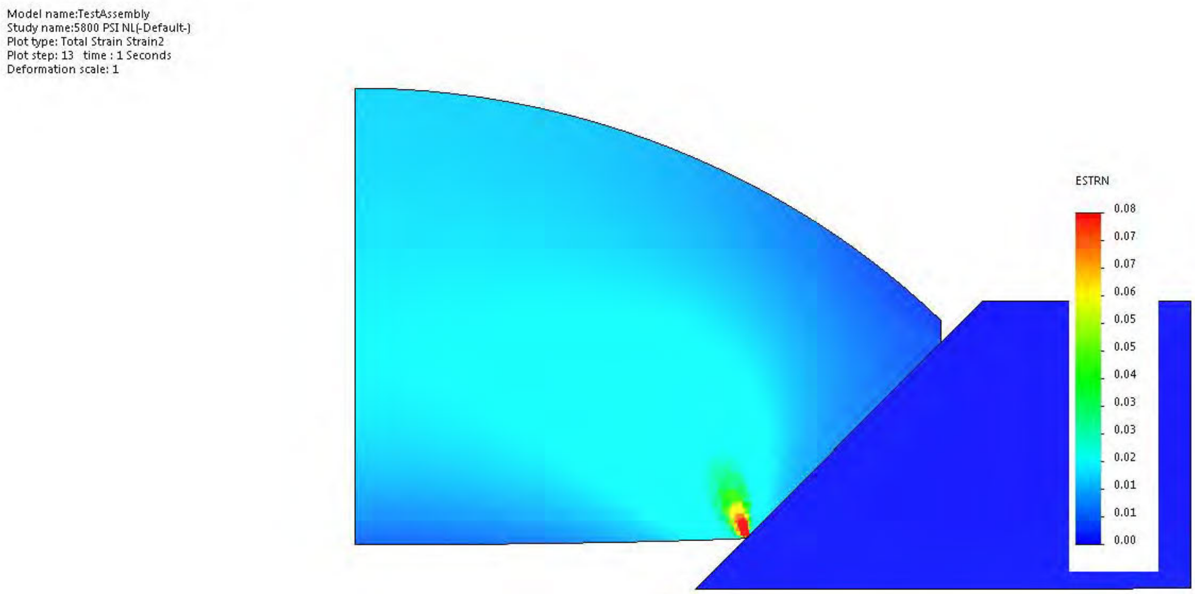

Fig. C5. Nonlinear 5800 psi strain. Strains above 0.06 (red-to-yellow) is of concern. This is consistent with cyclic failure. These results are do not account for heat transfer, dive rates, service life, or creep effects, so any conclusion regarding suitability is preliminary. The intent is to provide a preliminary comparison of the Cyclops design to a flat top design.

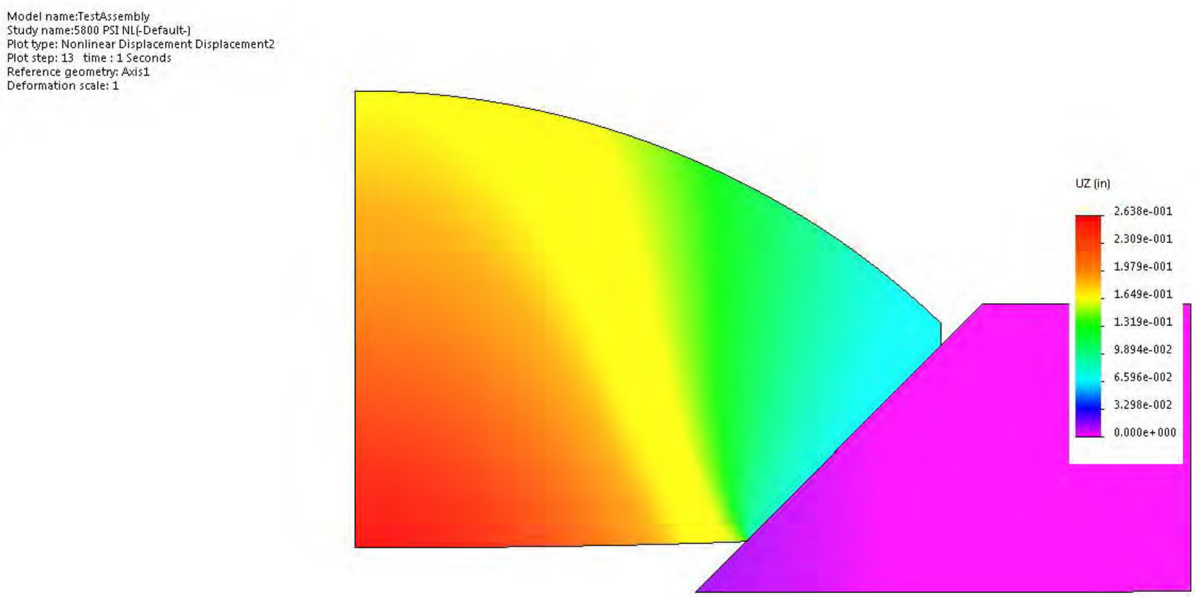

Fig. C6. Nonlinear 5800 psi displacement. Maximum downwards displacement is 0.263 inches.

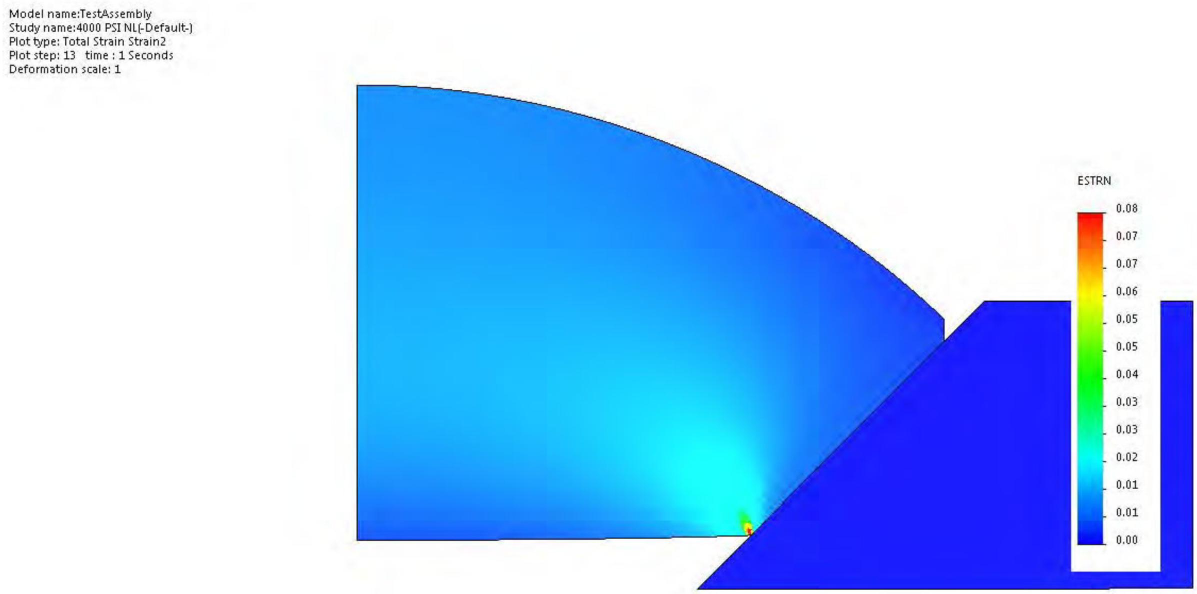

Fig. C7. Nonlinear 4000 psi. Strain constrained to 0.08. The highly localized strain indicates this is more of a case of corner stress instead of a structural concern. A corner fillet would reduce this.

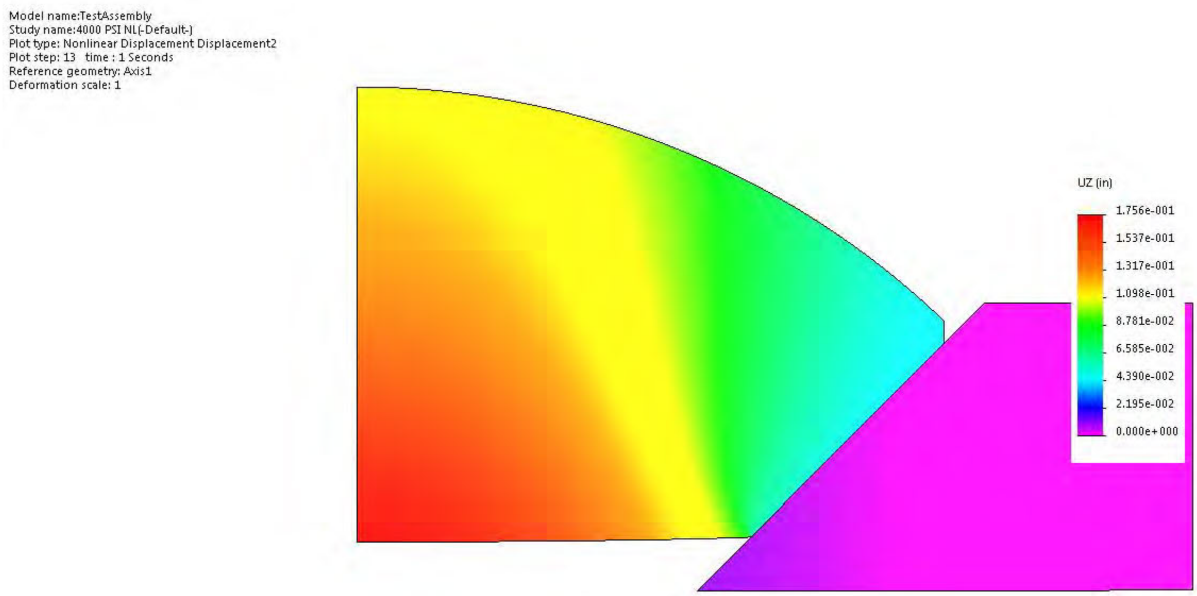

Fig. C8. Nonlinear 4000 psi. Downwards deflection is 0.176 inches

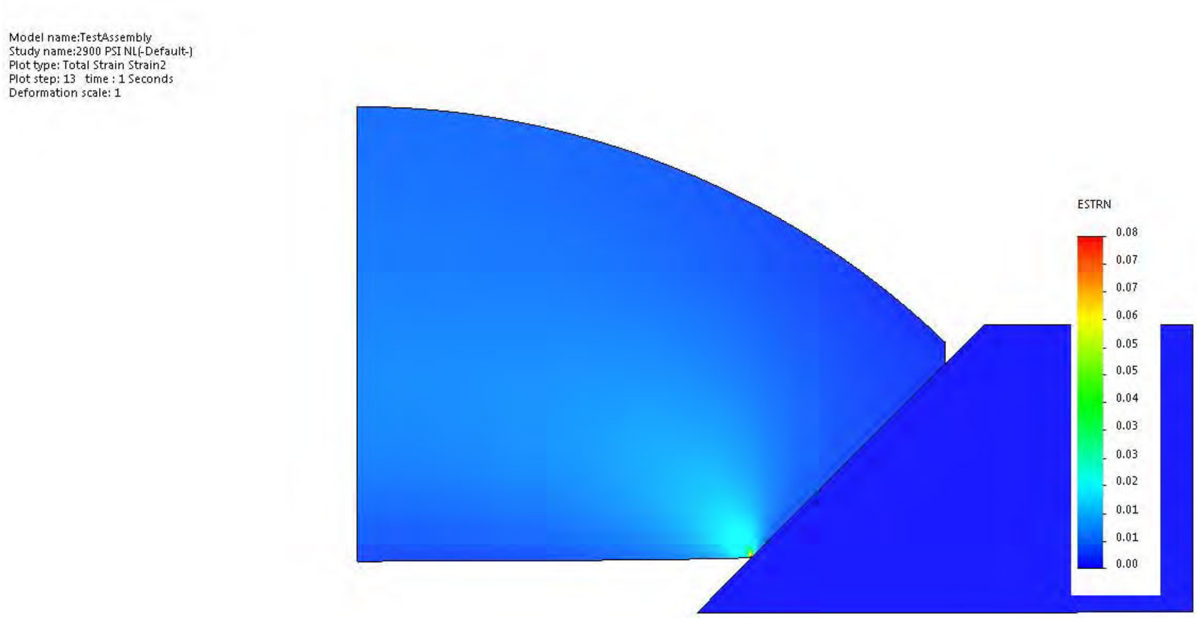

Fig. C9. Nonlinear 2900 psi. The strain is well within normal operational levels.

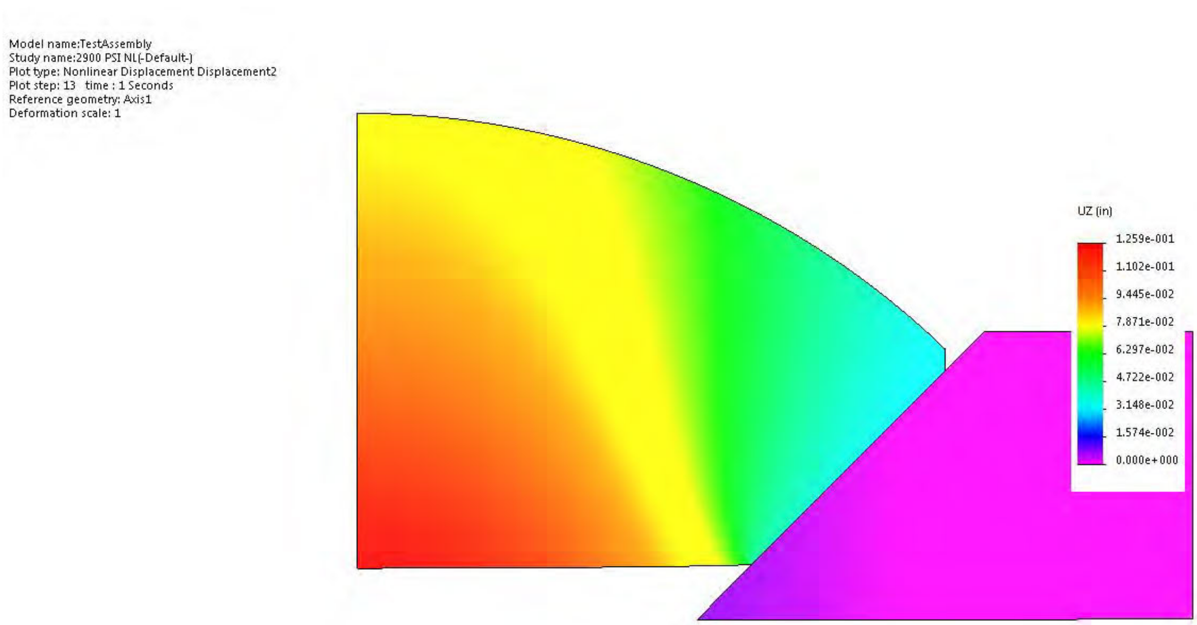

Fig. C10. Nonlinear 2900 psi. Downwards deflection.

CONFIDENTIAL NTSB/USCG

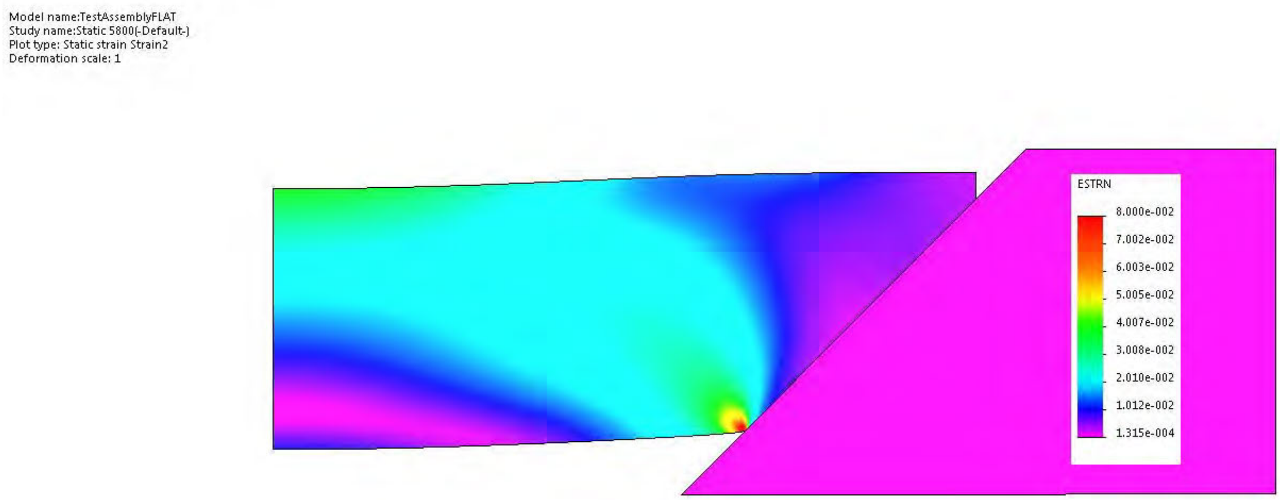

Fig. D1. Flat top, linear at 5800 psi.
The strain level is elevated in comparison to Fig. C2.

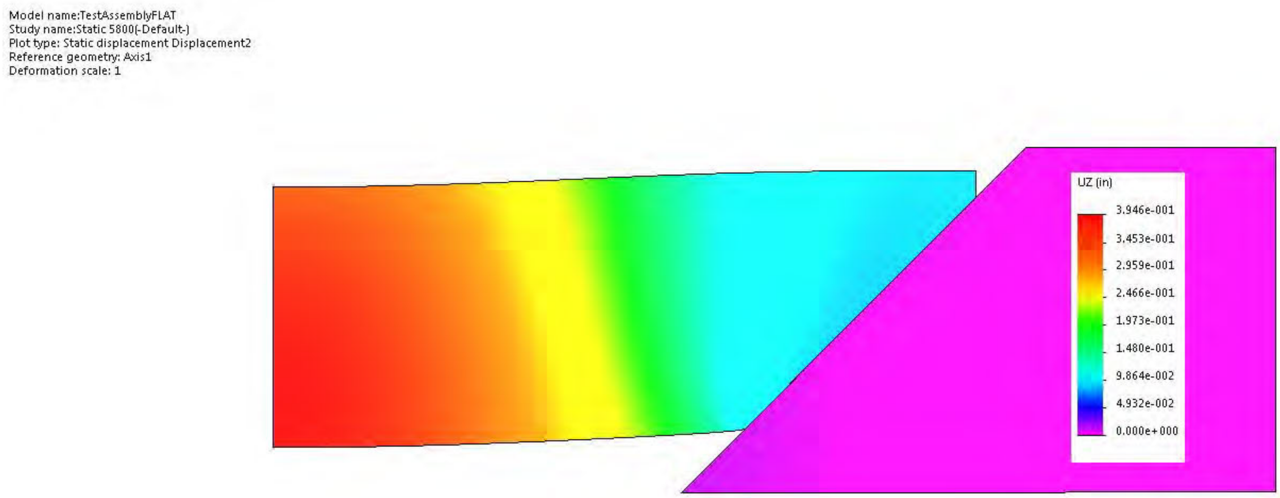

Fig. D2. Flat top, linear at 5800 psi.
The downwards deflection is almost twice the deflection of Fig. C3. The flat top design is significantly more flexible than the Cyclops design, which is consistent with the structure.

CONFIDENTIAL NTSB/USCG

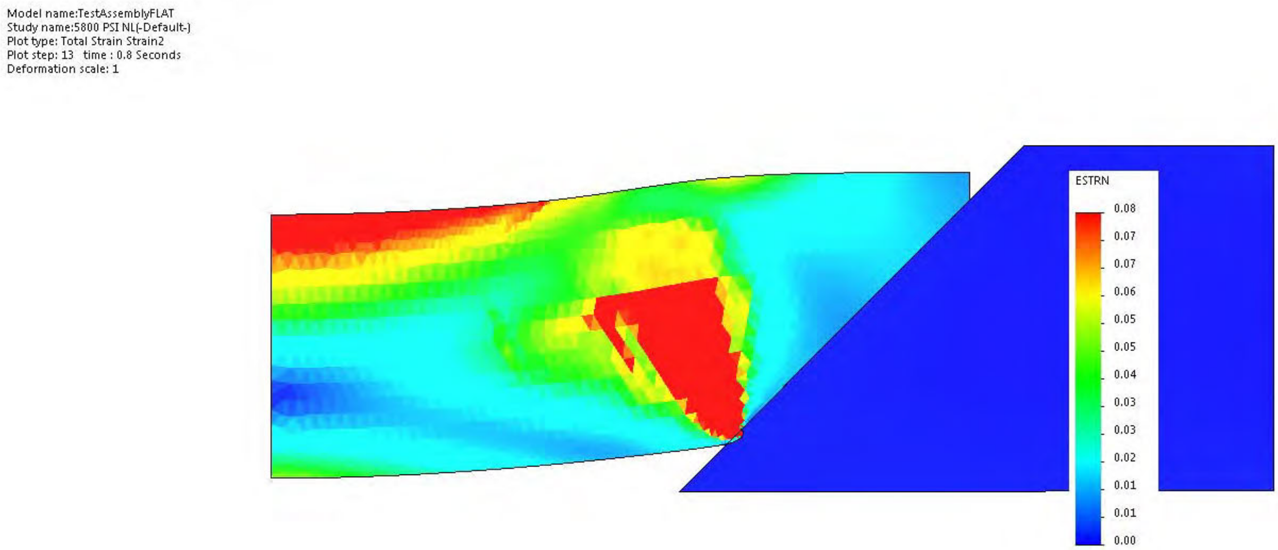

Fig. D3. Flat top window. Nonlinear at 5800 psi pressure. Strain levels and gradients indicate failure.

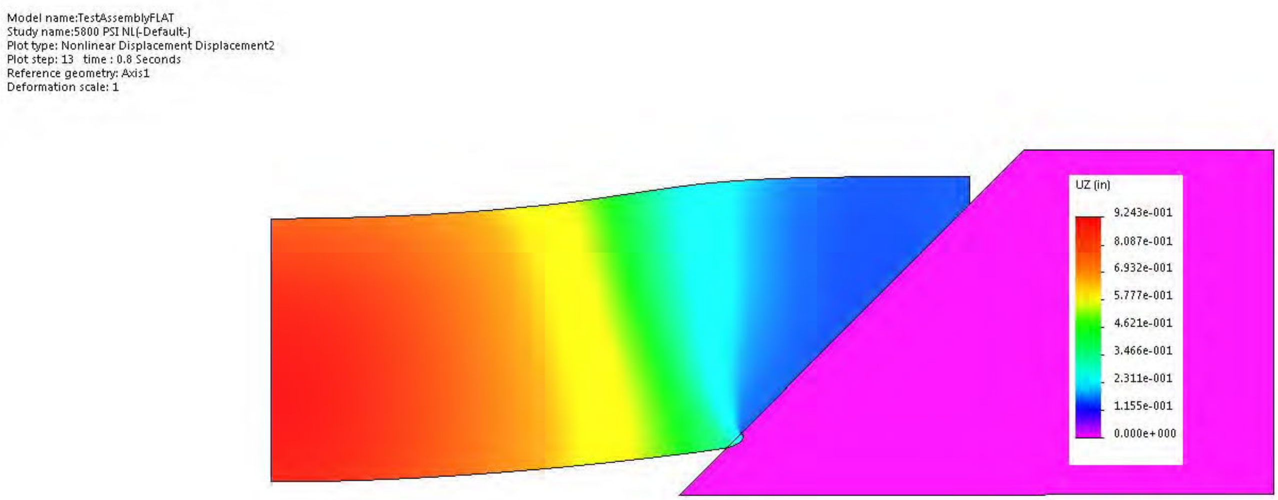

Fig. D4. Flat top window. Nonlinear deflection at 5800 psi pressure. Deflection is over 3 times the Cyclops design and is consistent with failure.

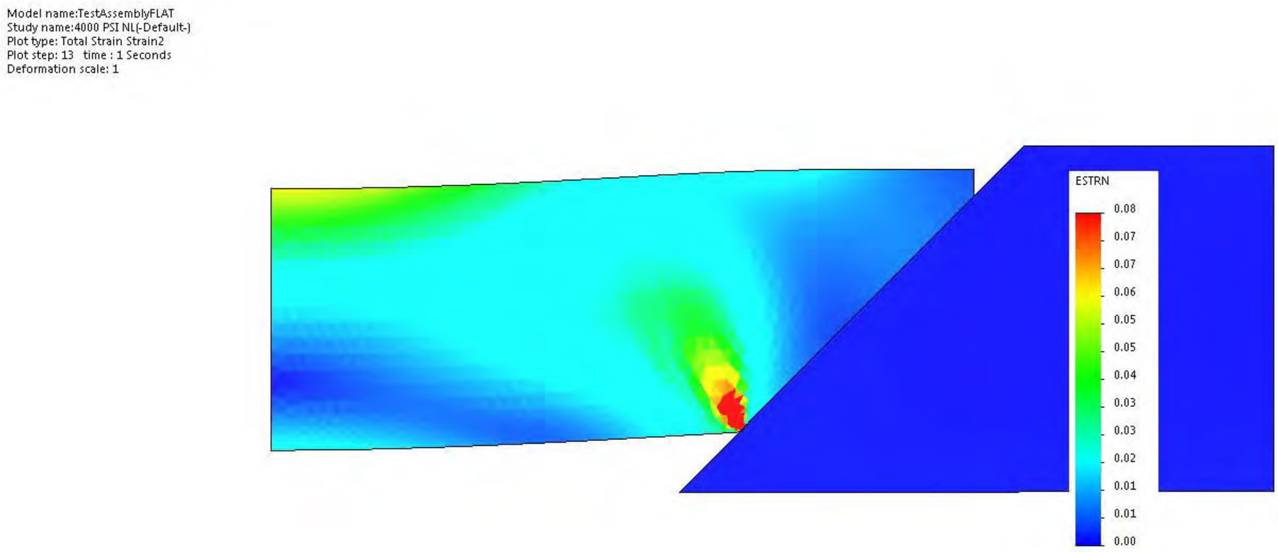

Fig. D5. Nonlinear flat top at 4000 psi. Strain profile is consistent with short cycle failure.

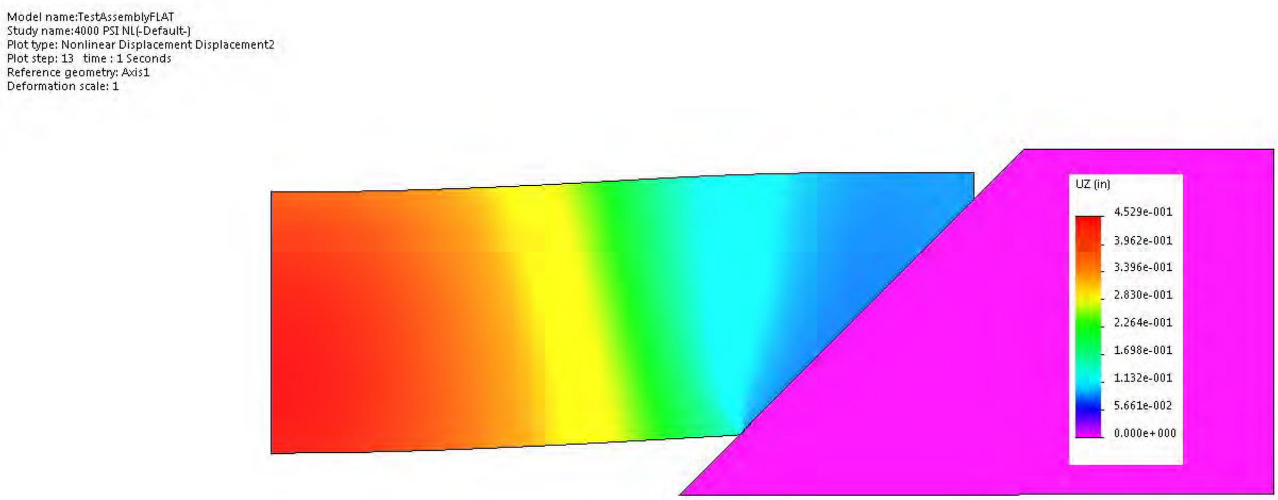

Fig. D6. Nonlinear flattop deflection at 4000 psi. Deflection is over twice the Cyclops design.

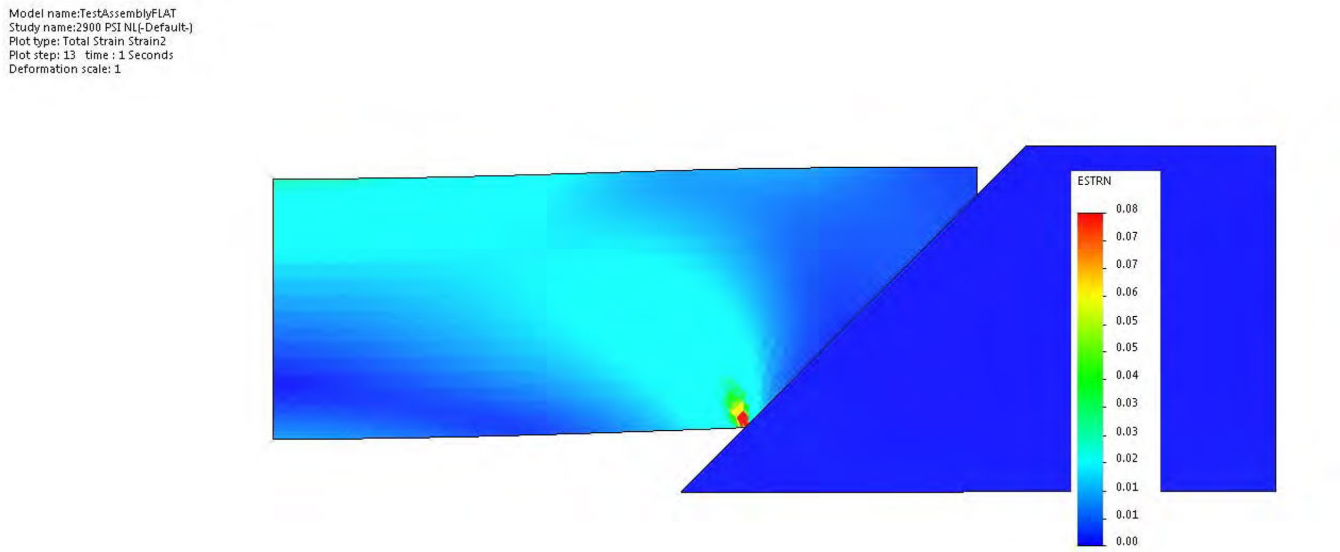

Fig. D7. Flatop strain at 2900 psi. Strain is potentially acceptable, although cyclic failure is possibly indicated.

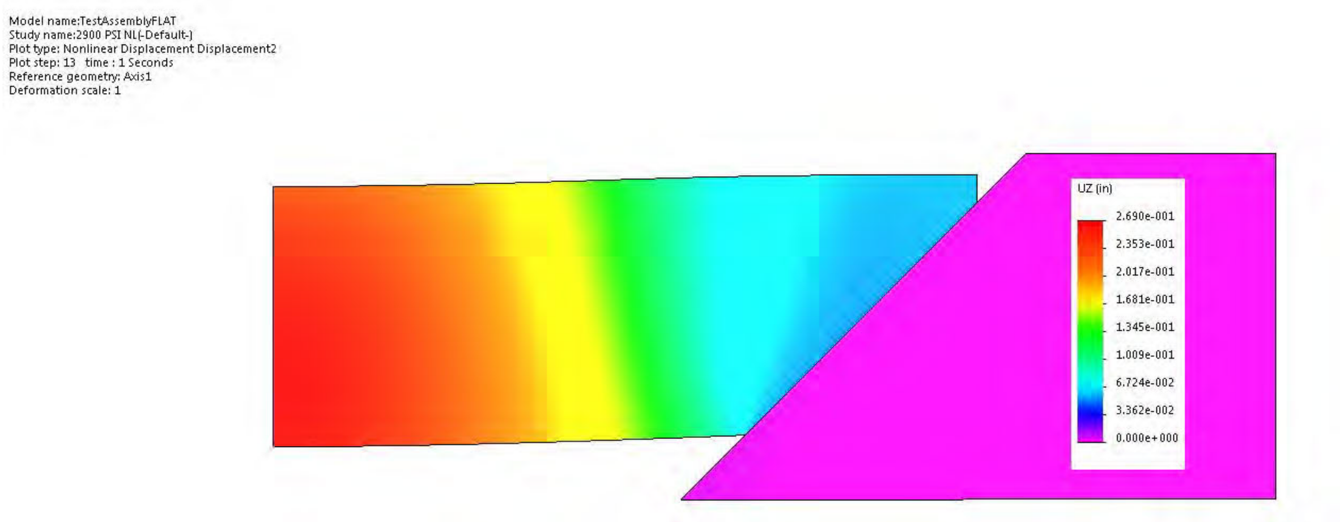

Fig. D8. Flatop deflection at 2900 psi. Downwards deflection is over twice the Cyclops design and is more than the Cyclops design at 5800 psi.

APPENDIX C

OceanGate Drawings
ASME Spherical Sector Window Design
FEA Models

CONFIDENTIAL NTSB/USCG

REV	DATE	DESCRIPTION	REVISED BY
--	2017/06/08	INITIAL RELEASE	[redacted]
A	2017/06/13	REFERENCE CHANGE LOG	
B	2017/10/10	REFERENCE CHANGE LOG	

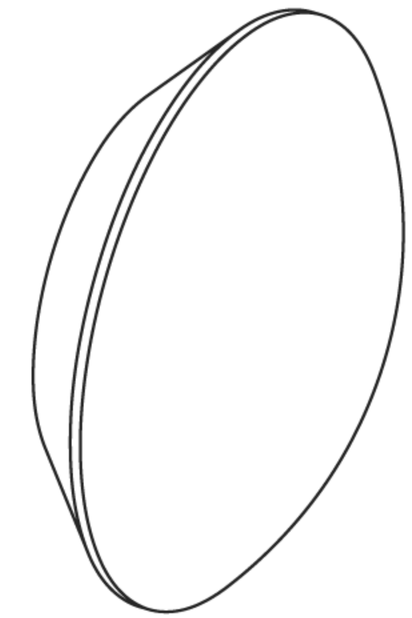

NOTES:
1. MATERIAL: ACRYLIC.
2. DENSITY: 0.049 lb/in^3.
3. VOLUME: 2175.590 in^3.
4. BUOYANCY: 80.591 lbf (IN .037 lb/in^3 WATER).
5. BREAK ALL SHARP EDGES.

1 PART MARK - IN ACCORDANCE WITH OCEANGATE.INSTRUCTION.0004 SECTION 5.6.

2 USED FOR DETERMINING α AND Ro ONLY. NOT PART OF END ITEM. ACTUAL TO BE REPORTED WITH CERTIFICATION.

3 DIMENSION TO BE SYMMETRIC ABOUT X AXIS.

NEXT [redacted]
1S-040[redacted]

[redacted]

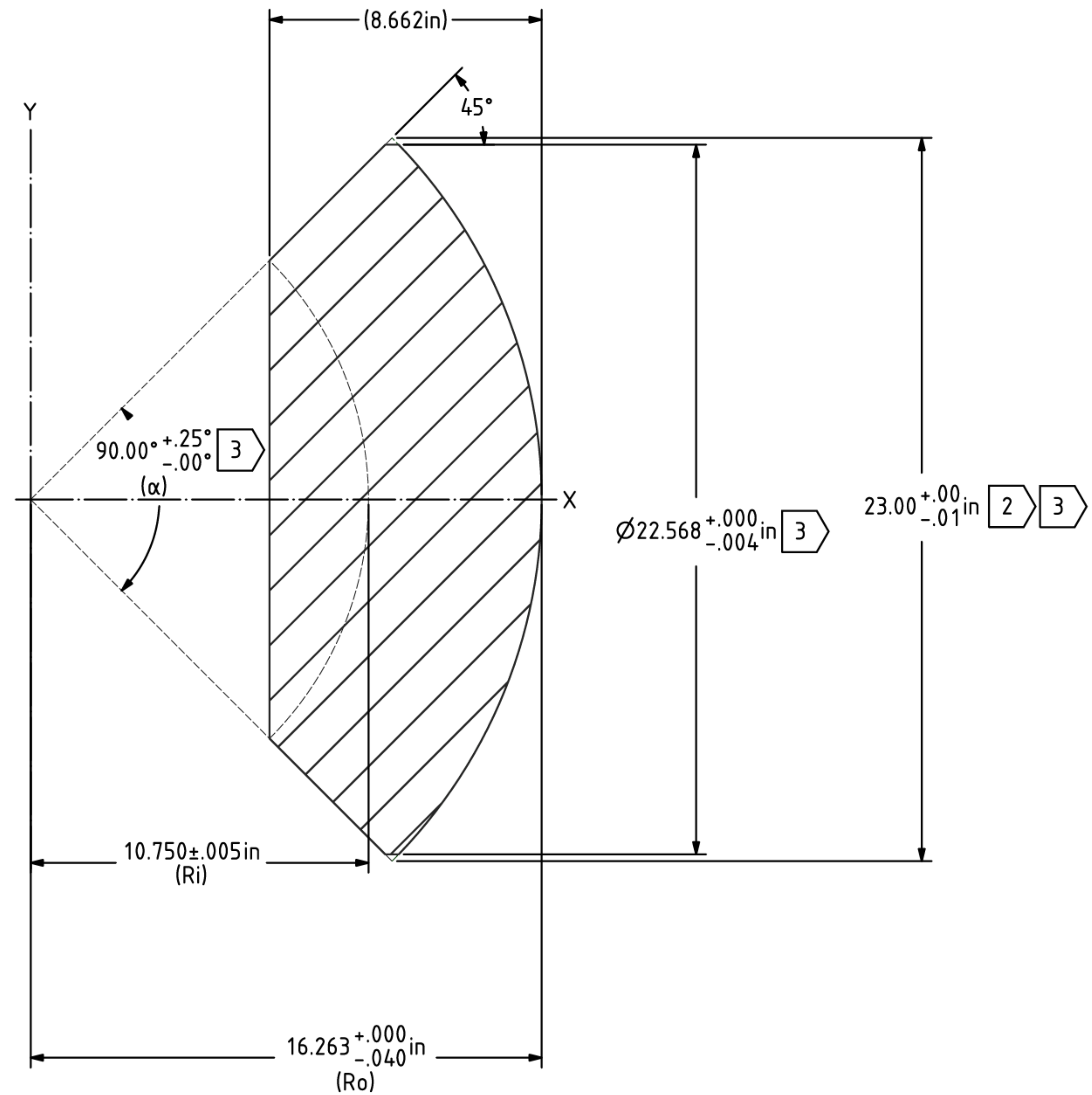

SIZE	DWG. NO.	REV
B	1S-040-MEC-000461	B
	SCALE: 1:10	SHEET 2 OF 2

STEP 1. Ensure the acrylic meets the following specification. The actual values will not be used in the calculations. This is a GO/NO GO screening for material properties.

Table 2-3.4-1 Specified Values of Physical Properties for Each Lot

Test Procedures	Physical Property		Specified Values	
			U.S. Customary Units	SI Units
ASTM D256 [Note (1)]	Izod notched impact strength		≥0.25 ft-lb/in.-min	≥13.3 J/m
ASTM D542	Refractive index		1.49 + 0.01	1.49 + 0.01
ASTM D570 [Note (1)]	Water absorption, 24 hr		≤0.25%	≤0.25%
ASME PVHO-1 method, para. 2-3.7(c)	Compressive deformation at 4,000 psi (27.6 MPa), 122°F (50°C), 24 hr		≤1.0%	≤1.0%
ASTM D638 [Note (1)]	Tensile:			
	(a) ultimate strength		≥9,000 psi	≥62 MPa
	(b) elongation at break		≥2%	≥2%
	(c) modulus		≥400,000 psi	≥2 760 MPa
ASTM D695 [Note (1)]	Compressive:			
	(a) yield strength		≥15,000 psi	≥103 MPa
	(b) modulus of elasticity		≥400,000 psi	≥2 760 MPa
ASTM D732 [Note (1)]	Shear, ultimate strength		≥8,000 psi	≥55 MPa
ASTM D785 [Note (1)]	Rockwell hardness		≥M scale 90	≥M scale 90
ASTM D790 [Note (1)]	Flexural ultimate strength		≥14,000 psi	≥97 MPa
ASTM D792 [Note (1)]	Specific gravity		1.19 ± 0.01	1.19 ± 0.01
ASME PVHO-1 method, para. 2-3.7(d)	Ultraviolet (290 nm–330 nm) light transmittance		≤5%	≤5%
ASME PVHO-1 method, para. 2-3.7(e)	Clarity, visually rated		Must have readability	Must have readability
ASTM D696	Coefficient of linear thermal expansion at		$\leq 10^{-5}$ (in./in. °F)	$\leq 10^{-5}$ (mm/mm °C)
	°F	°C		
	−40	−40	2.9	5.22
	−20	−29	3.0	5.40
	0	−18	3.2	5.76
	20	−7	3.4	6.12
	40	4	3.7	6.66
	60	16	4.0	7.20
	80	27	4.3	7.74
	100	38	4.7	8.46
	120	49	5.1	9.18
	140	60	5.4	9.72
ASTM D648	Deflection temperature of plastics under flexure at 264 psi (1.8 MPa)		≥185°F	≥85°C
ASME PVHO-1 method, para. 2-3.8	Total residual monomer:			
	(a) methyl methacrylate		≤1.6%	≤1.6%
	(b) ethyl acrylate			

GENERAL NOTE: The manufacturer shall certify that the typical physical properties of the acrylic satisfy the criteria in this Table.

NOTE: (1) These tests require testing a minimum of two specimens. For others, test a minimum of one specimen. Where applicable, use the sampling procedures described in para. 2-3.7. For other tests, use the sampling procedures described in the appropriate ASTM test methods. Where two specimens are required in the test procedure, the average of the test values shall be used to meet the requirements of the minimum physical properties of this Table.

STEP 2 Determine the Short Term Critical Pressure (STCP) by obtaining the correction factor (CF), multiply it by the design pressure, and use that "design pressure" for the charts. Assume **Di=15.2 inches** as shown in the original design, shown below..

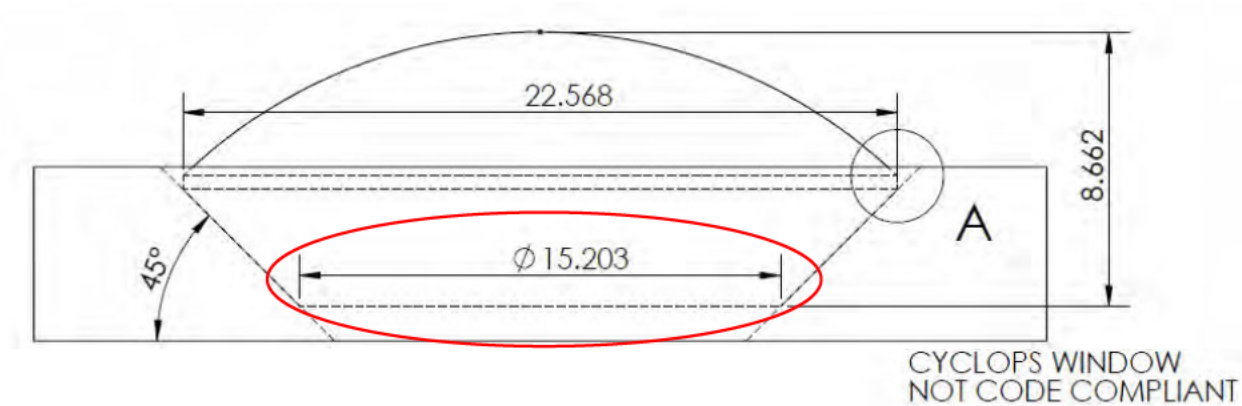

Table 2-2.3.1-3 Conversion Factors for Acrylic Spherical Sector Windows With Conical Edge, Hyperhemispherical Windows With Conical Edge, and NEMO-Type Windows With Conical Edge

Operational Pressure Ranges	Temperature, °F (°C)				
	50 (10)	75 (24)	100 (38)	125 (52)	150 (66)
N = 1 2,500 psi (17.2 MPa)	CF = 4	CF = 6	CF = 8	CF = 10	CF = 16 1,500 psi (10.3 MPa)
N = 2 5,000 psi (34.5 MPa)	CF = 4	CF = 6	CF = 8	CF = 10 3,500 psi (24.1 MPa)	3,000 psi (20.7 MPa)
N = 3 7,500 psi (51.7 MPa)	CF = 4				

GENERAL NOTES:
(a) The CFs in this Table apply only to STCPs plotted in Figures 2-2.5.1-6 and Figures 2-2.5.1-7 for spherical sector windows with conical edge and Figures 2-2.5.1-14 and 2-2.5.1-15 for hyperhemispherical windows with conical edge and NEMO-type windows with conical penetrations.
(b) Dotted lines refer to intermediate pressure ranges as indicated by the adjacent pressure figures.
(c) Interpolation between CFs is allowed.

Design pressure = 5800 psi

CF for 5800 psi = 4

STCP = 4 * 5800 psi = 23,200 psi (160 MPa) (Use 160 MPa due to graph units)

Comment: Using the typical design method, it is assumed the temperature at depth will be the window temperature. This is why there is no consideration for a temperature above 50F (10C). Subsequent studies address the insulating properties (Kemper, *Cross Heat Retention and Structural Integrity of Glassy Polymer Windows*, 2018). There are also significant shortfalls in the acrylic specification in Step 1, to include the minimum required elongation at break is less than the elastic limit, allowing for brittle design. (Kemper, *Shortfalls in Polymer Specifications for PVHOs*, 2019). Given there has not been a failure of a PVHO window that was designed, fabricated, and operated per ASME PVHO-1 and PVHO-2, there various shortfalls are addressed in the overall conservative assumptions built into the process. The shortfalls become pertinent when applying engineering techniques, including Finite Element Analysis (FEA). This method was developed experimentally in the 1960s and 1970s by the US Navy.

STEP 3 Determine the ratio, t/Di, from the design chart. Use a 90 degree cone.

Figure 2-2.5.1-7 Short-Term Critical Pressure of Spherical Sector Acrylic Windows — Part 2

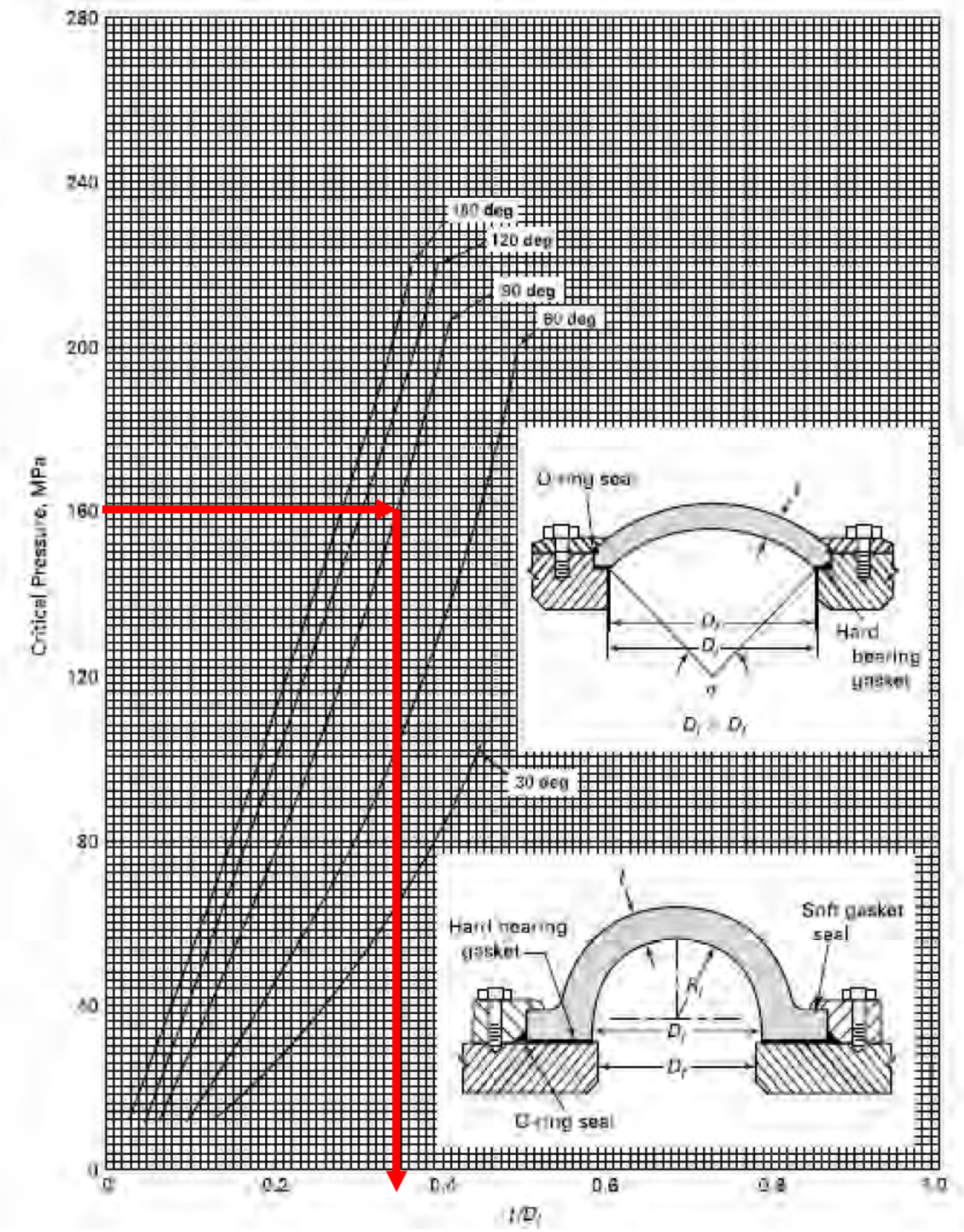

t/Di = 0.36

t = Di * (t/Di) = 15.2 * 0.36 = 5.47 inches, rounded up to 5.5 inches

Design complete for window. Detailed design for window seat is up to designer.

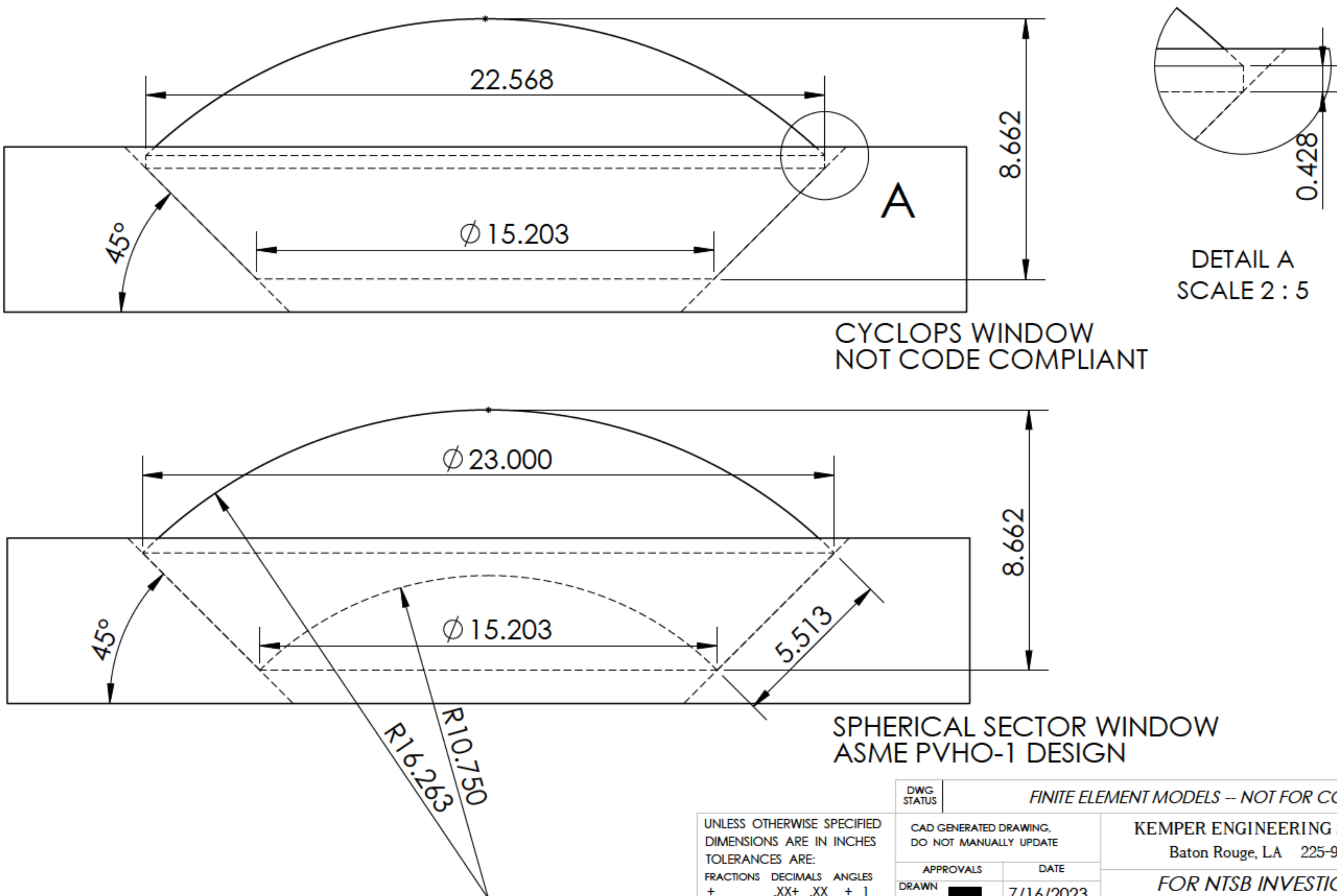

DETAIL A
SCALE 2 : 5

CYCLOPS WINDOW
NOT CODE COMPLIANT

SPHERICAL SECTOR WINDOW
ASME PVHO-1 DESIGN

DWG STATUS: FINITE ELEMENT MODELS -- NOT FOR CONSTRUCTION

UNLESS OTHERWISE SPECIFIED DIMENSIONS ARE IN INCHES
TOLERANCES ARE:
FRACTIONS + DECIMALS .XX+ .XX .XXX+.XXX ANGLES + 1

MATERIAL --

FINISH --

DO NOT SCALE DRAWING

CAD GENERATED DRAWING, DO NOT MANUALLY UPDATE

APPROVALS		DATE
DRAWN	[redacted]	7/16/2023
CHECKED	[redacted]	7/17/2023
RESP ENG		
MFG ENG		
QUAL ENG		

KEMPER ENGINEERING SVCS LLC
Baton Rouge, LA 225-923-2945

FOR NTSB INVESTIGATION
TITAN SUBMERSIBLE REVIEW MODELS

SIZE A | DWG. NO. NTSB-TITAN-1 | REV. 0
SCALE 1:5 | CAD FILE: NTSB-TITAN | SHEET 1 OF 2

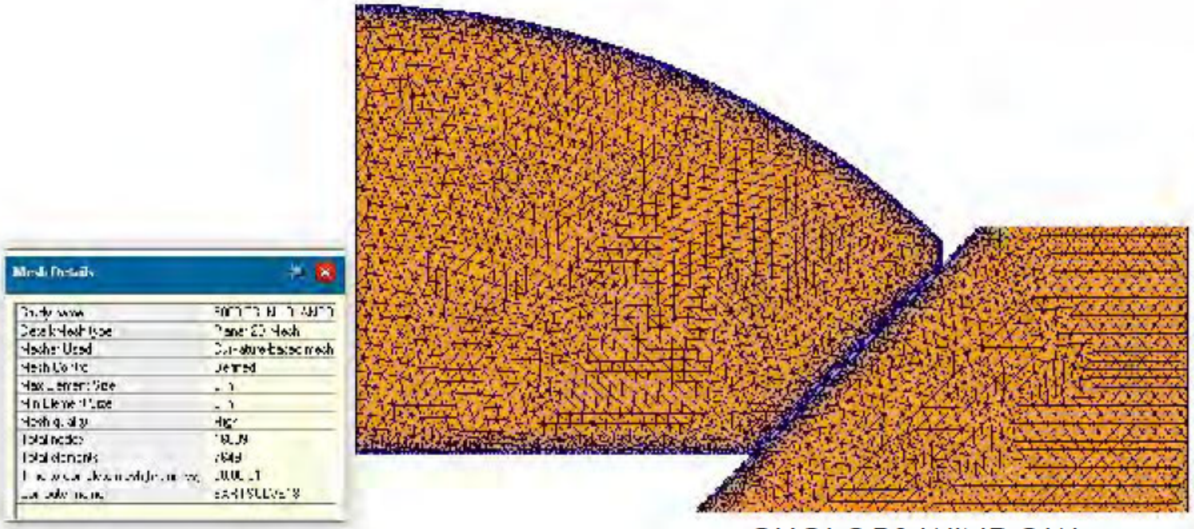

CYCLOPS WINDOW
NOT CODE COMPLIANT

MESH DATA FOR BOTH ANALYSES

AXYSYMETRIC ANALYSIS
(2D APPROXIMATION)
SAME SEAT FOR BOTH

NOMINAL MESH = 0.25 IN
REFINED SIZE = 0.05 IN

CONTACT ELEMENTS BETWEEN
WINDOW, SEAT ALLOWS MOVEMENT.
ASSUME FRICTION = 0

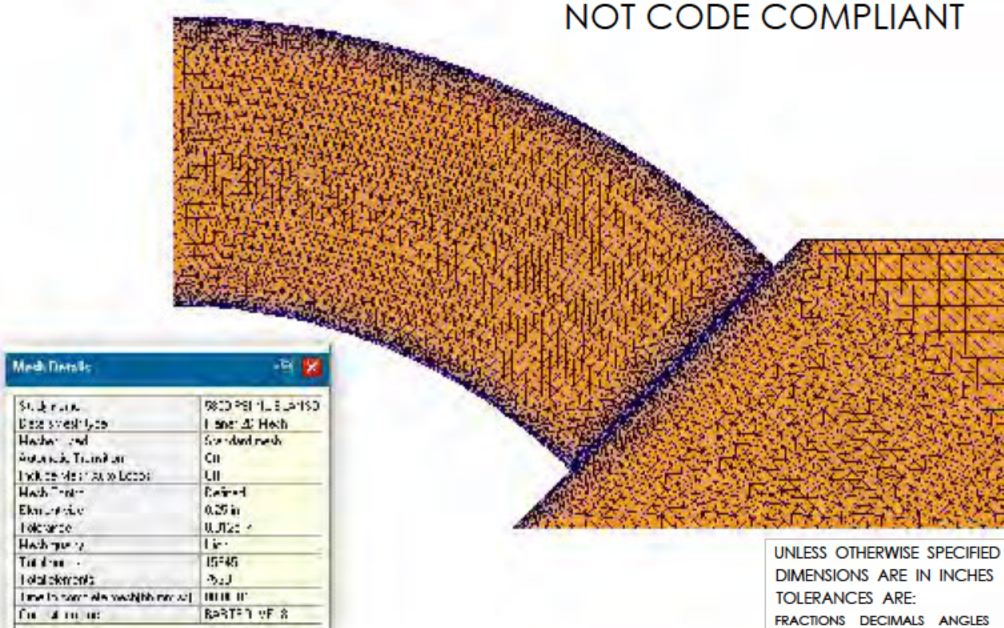

SPHERICAL SECTOR WINDOW
ASME PVHO-1 DESIGN

DWG STATUS	FINITE ELEMENT MODELS -- NOT FOR CONSTRUCTION

UNLESS OTHERWISE SPECIFIED
DIMENSIONS ARE IN INCHES
TOLERANCES ARE:
FRACTIONS + ; DECIMALS .XX+ .XX, .XXX+.XXX ; ANGLES + 1

MATERIAL --

FINISH --

DO NOT SCALE DRAWING

CAD GENERATED DRAWING, DO NOT MANUALLY UPDATE

APPROVALS		DATE
DRAWN	[redacted]	7/16/2023
CHECKED	[redacted]	7/17/2023
RESP ENG		
MFG ENG		
QUAL ENG		

KEMPER ENGINEERING SVCS LLC
Baton Rouge, LA 225-923-2945

FOR NTSB INVESTIGATION
TITAN SUBMERSIBLE REVIEW
MESH DATA

SIZE A | DWG. NO. NTSB-TITAN-2 | REV. 0
SCALE 1:5 | CAD FILE: NTSB-TITAN | SHEET 2 OF 2

APPENDIX D

FEA Results

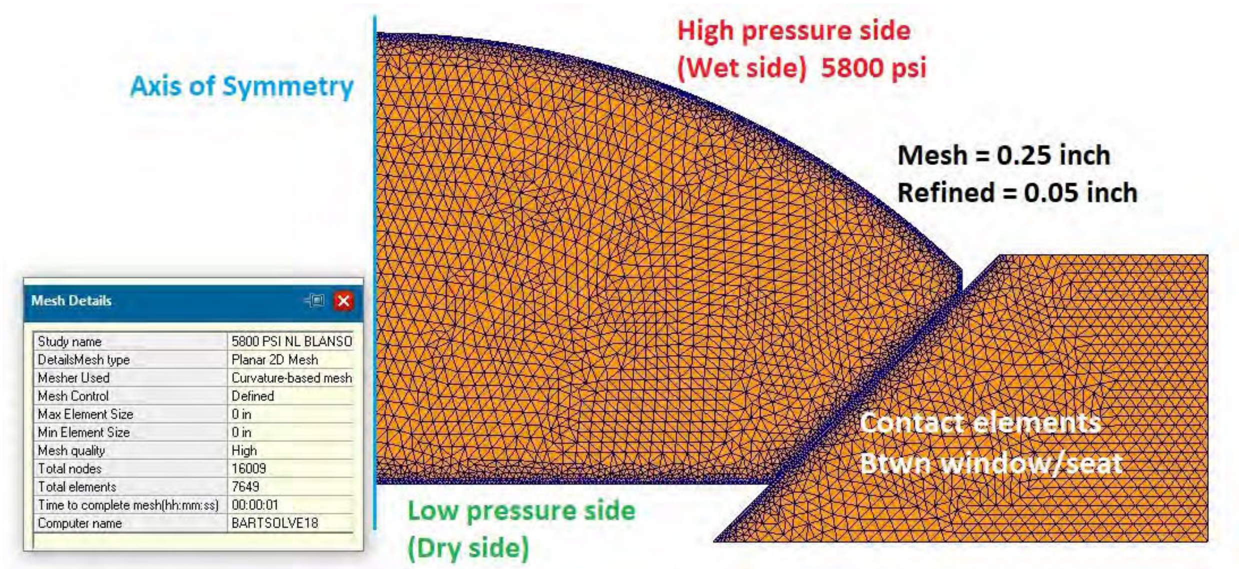

Fig. D1 Axisymmetrical Model

The analysis uses axisymmetrical 2D simplification. The analysis is a “design review” to assess whether it’s a prudent design. A number of key factors are neglected in the design process. These factors are typically ignored in the ASME PVHO-1 design process, which is highly conservative and is intended to have sufficient design margin that these issues do not impact the overall reliability of a window designed for a specific temperature and depth. US Customary units are used as they are the units provided in the original work. MIL-P 8184 acrylic is used as it was one of the defining materials used in developing the PVHO-1 design code and still meets the code requirements.

The Cyclops design was provided by [redacted] at Hydrospace in 2017. OceanGate wanted Hydrospace to fabricate their design, which does not comply with ASME PVHO-1 or any other known hyperbaric engineering design code. The media has described the window being “7 inches thick”, whereas the drawing provided by Hydrospace is 8.6 inches thick at the apex. It’s not certain to KES what the final embodiment of the window was, nor was the window seat design available to KES. The window seat is assumed to be rigid with respect to the window, to include no deformation. KES does not have the window seat design and cannot verify this assumption.

The Finite Element Analysis model shown here neglects the potential for imperfections in the window or seat or misalignment. The window seat is fixed, which neglects the potential for the forces on the thick seat causing rotation inwards about the head/seat joint. Contact elements allow the window to move with respect to the seat. The axisymmetric assumption does not account for potential local irregularities. The use of Finite Element Analysis (FEA) is not an approved method in the ASME code for windows as it is with metallic components; however, there is an ASME task group developing design-by-analysis code method for glassy polymers such as acrylics.

The model also assumes there is no creep or other form of permanent deformation from previous dives. Another assumption is uniform temperature. A significant shortcoming in the existing codes and standards is a uniform temperature assumption, given that acrylic acts as a thermal insulator rather than a conductor. This is significant because the typical design approach is to use 50 degrees F (10 degrees C) as the design temperature because it’s the typical temperature at depth for many submersibles. In typical pressure vessel work, peak pressure coincides with hottest temperature such that the allowable stress at peak load is the lowest one in the design cycle. This is not the case with submersibles or diving bells.

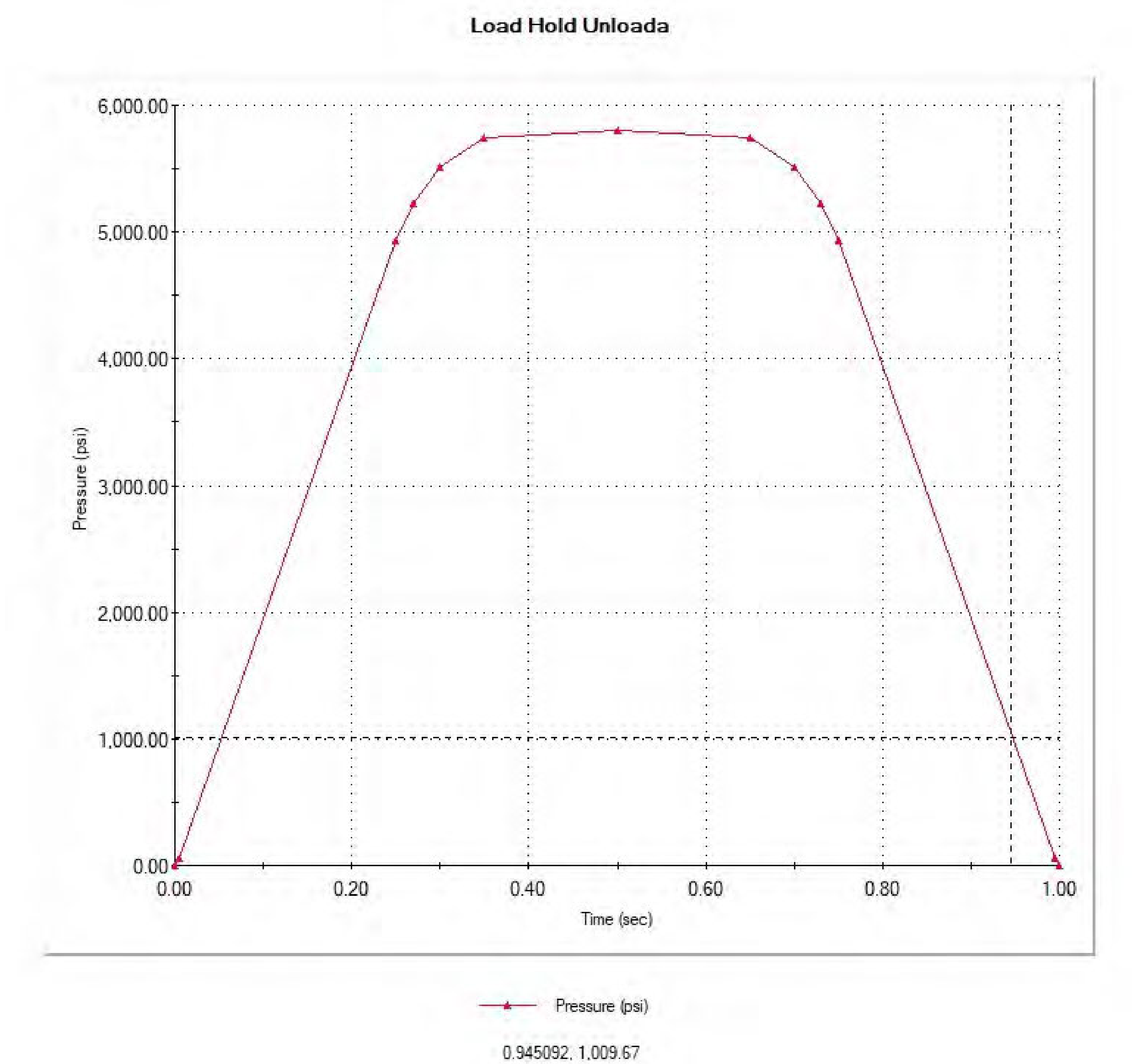

<u>Fig. D2. Load Cycle (Pseudo time)</u>
The analysis loads and unloads the pressure on the window. The intent is to assess whether there is residual strain (and stress), which would also be permanent deformation. The full cycle is a notional 1 second, which is simply a bookkeeping method for incrementing loads as opposed to a transient analysis where actual time is used. The peak load of 5,800 psi is at halfway through the cycle, or 0.5 seconds.

The unloading portion ceased at 0.95 seconds, which corresponds to 1000 psi pressure. This is due to the limitations of implicit nonlinear analysis, which cannot address radical changes in geometry. A likely reason for the failure to complete is the strain energy stored in the window caused the window to “spring back”, overcoming the 1000 psi pressure and no longer being a determinant solution.

The results will be for three points: Max load (0.5 seconds), Unloaded (0.95 seconds), and Loading (0.05 seconds). The more precise value of the time steps are 0.945 for unloaded and 0.490 for loading, so there the loading point is about 10% less pressure load than the unloading point.

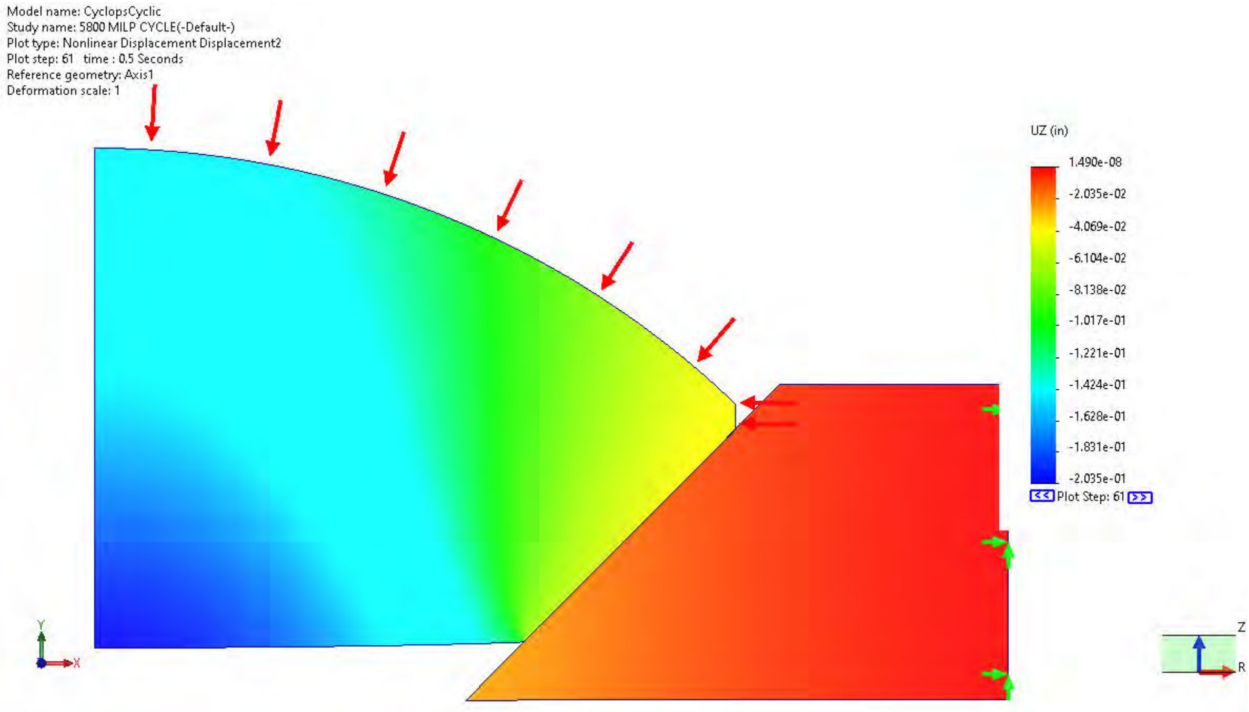

Fig. D3. Titan Window, MIL-P 8184, Time = 0.5 (Full load); Axial displacement (Cylindrical Coords)
This shows the inwards deflection at maximum pressure to be 0.204 inches. This is significant because interviews during OceanGate operations indicates the window would deflect up to "three-quarters of an inch", or over three times this amount. Note, the assumed temperature for the material is 75 degrees F (24 degrees C), so this would result in more deflection than the colder temperatures in the North Atlantic.

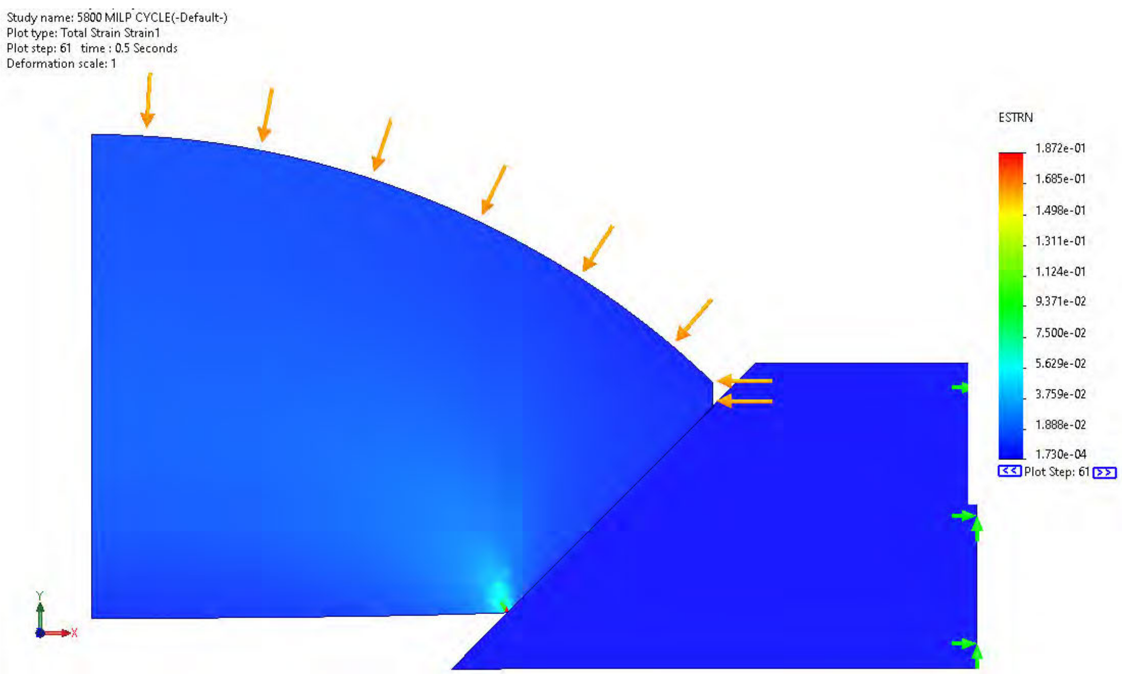

Fig. D4. Titan Window, MIL-P 8184, Time = 0.5 (Full load); Equiv. Strain (Full range)
This shows the peak strain is 18.8% in a primarily compressive loading. This is in excess of the typical strain for a conical frustrum window designed for 5,800 psi.

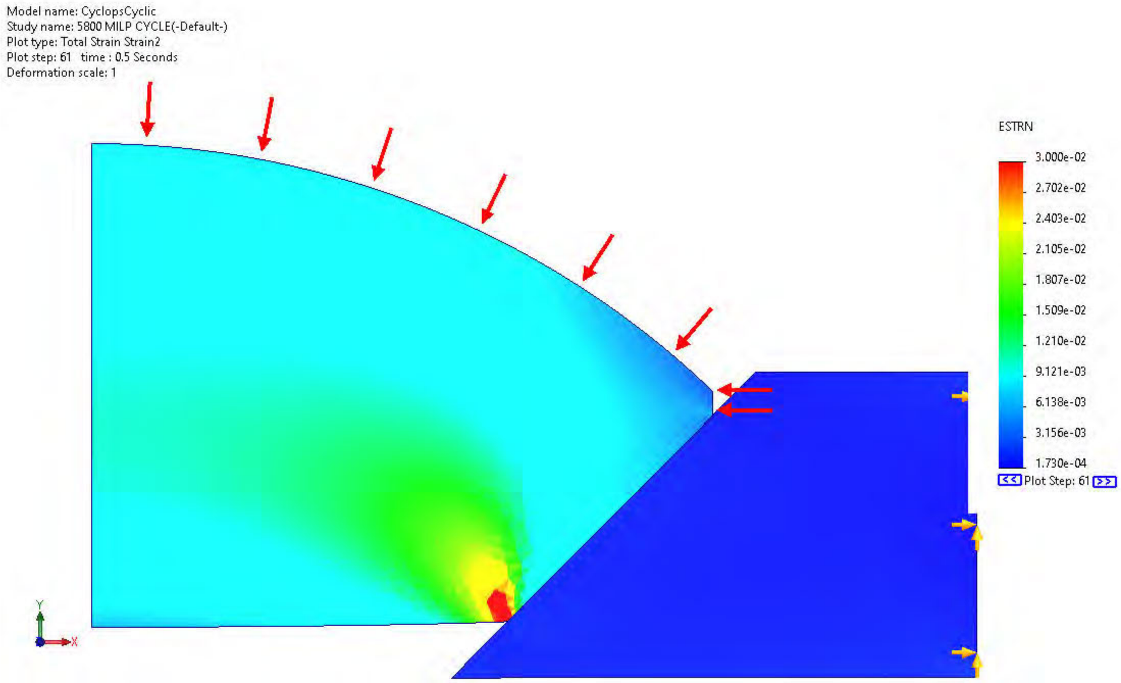

Fig. D5. Titan Window, MIL-P 8184, Time = 0.5 (Full load); Equiv. Strain (3% max)
This shows the red region approximates the plastic deformation. Acrylic has limited "spring back" above yield. The strain pattern is consistent with failure mode typical of a conical frustrum.

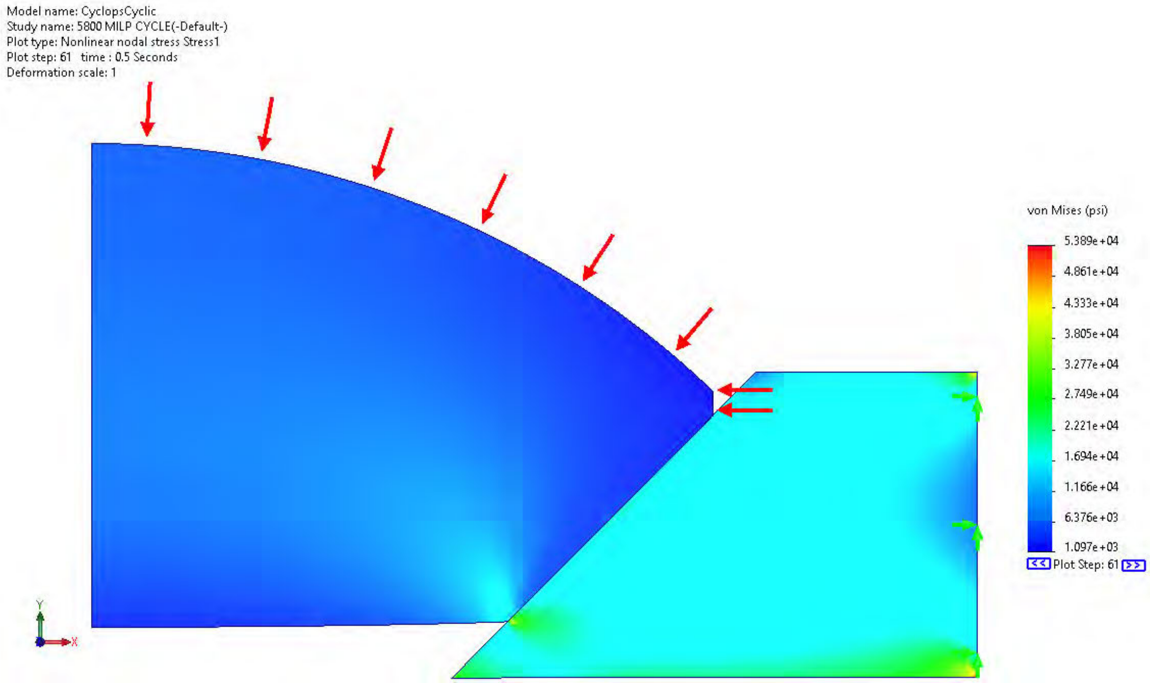

Fig. D6. Titan Window, MIL-P 8184, Time = 0.5 (Full load); Von Mises Stress (full range)
This shows the stress in the acrylic window and traditional steel window seat. Since there were no drawings for the titanium head and window seat, the usual method was used. The stresses in the window are well above yield. More significant is the stress in the window seat at the outside restraints. A significant moment force is created by the window wedging downwards. A detailed analysis of the window will require a detailed model of the head and window seat.

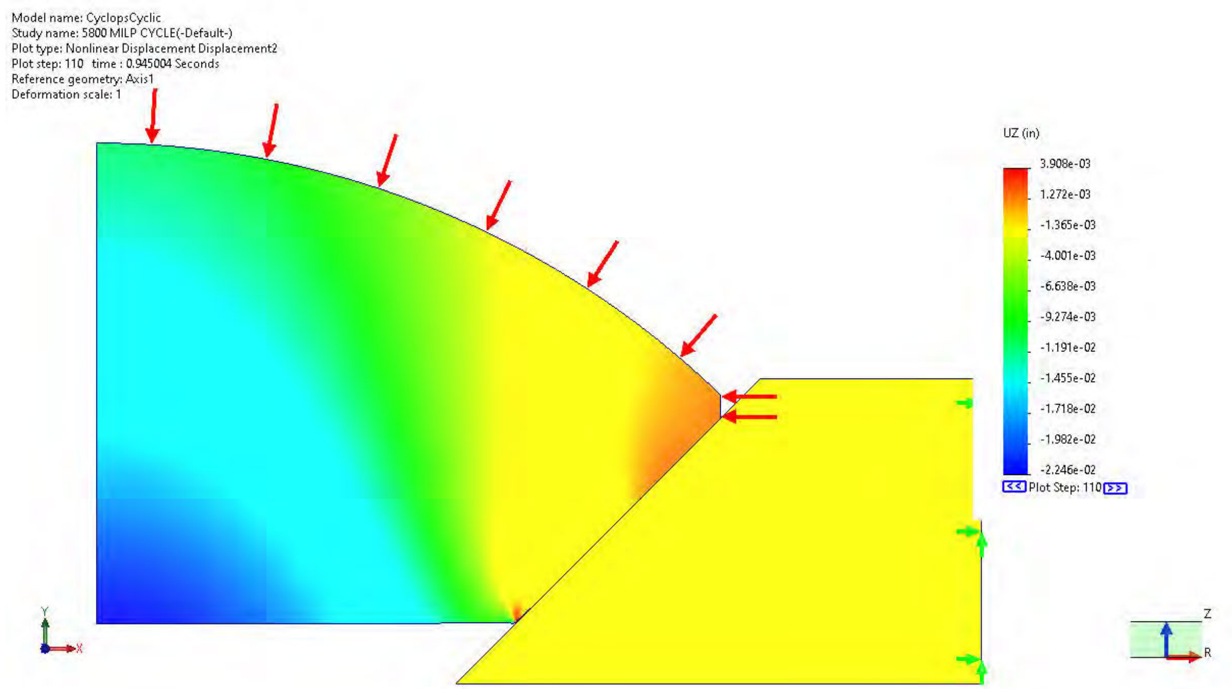

Fig. D7. Titan Window, MIL-P 8184, Time = 0.95 (Unloaded); Axial displacement (Cyl. Coords)
This shows the inwards deflection at of 0.0225. Since there is still a 1000 psi pressure, it's not full unloaded. The localized deflection in the lower corner of the window indicates material flow. There is also a positive peak value, showing a rebound above its starting point.

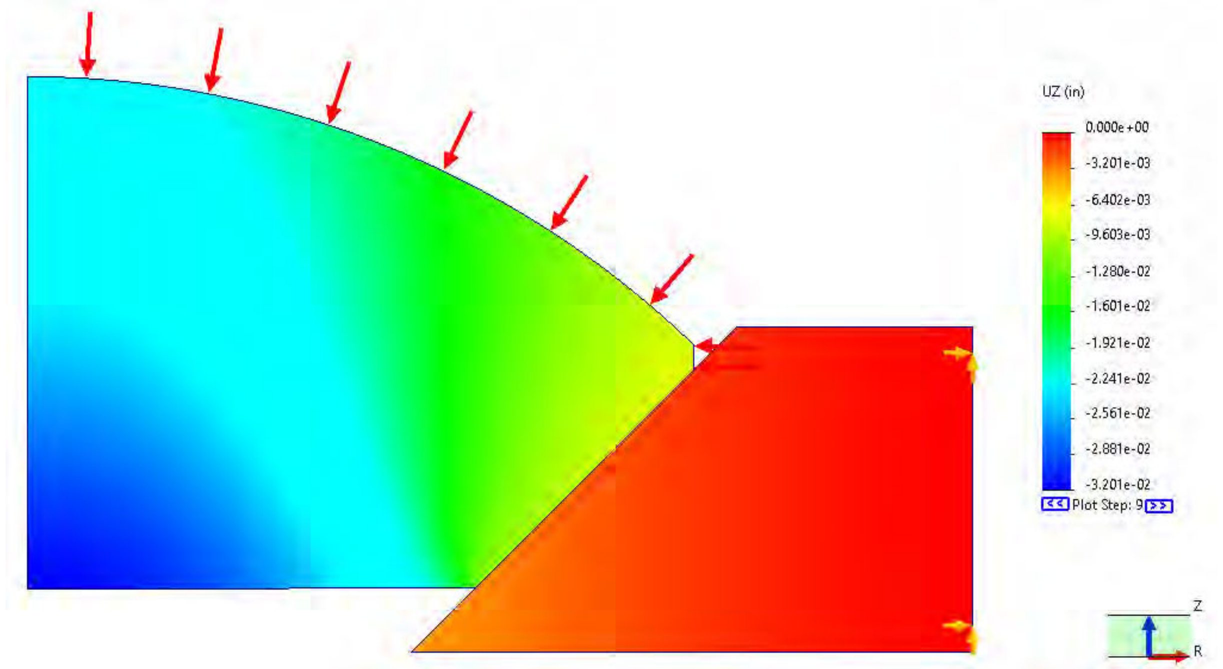

Fig. D8. Titan Window, MIL-P 8184, Time = 0.05 (Loading); Axial displacement (Cyl. Coords)
This shows 1000 psi in loading. This shows the inwards deflection of 0.032. There is no upwards deflection, nor is there localized deflection along the contact surface as there is in Fig. D7.

CONFIDENTIAL NTSB/USCG

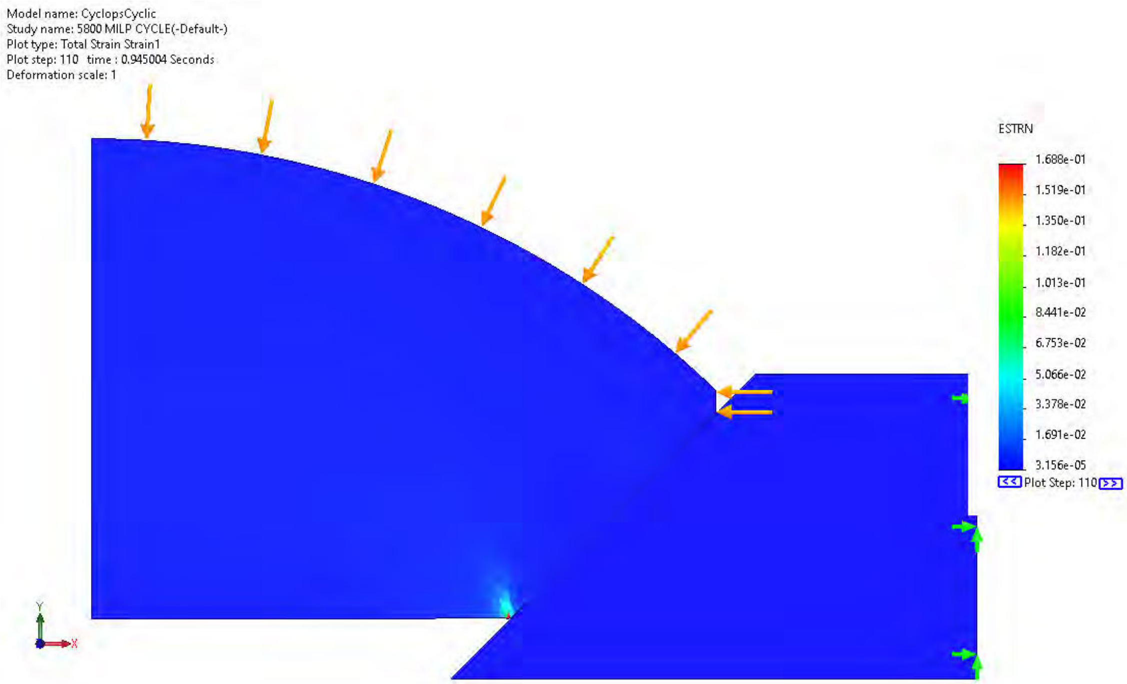

Fig. D9. Titan Window, MIL-P 8184, Time = 0.95 (Unloaded); Equiv. Strain (Full range)
This shows the peak strain is 16.9% in a primarily compressive loading. Any strain above 3% can be considered a permanent deformation.

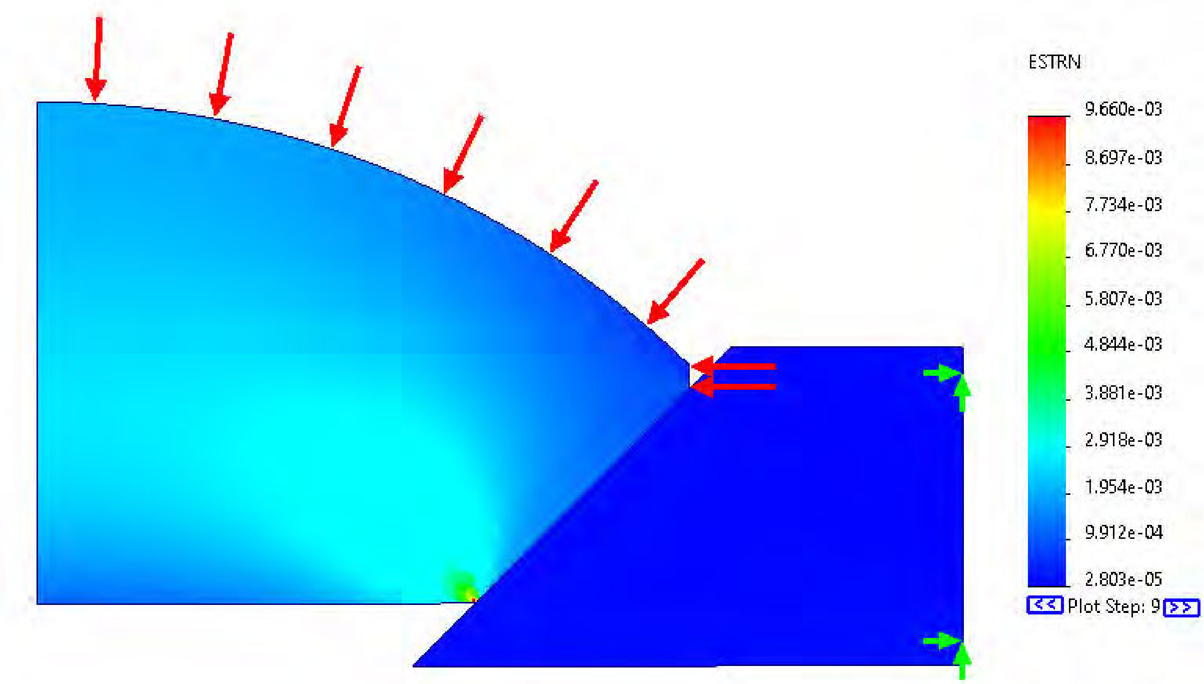

Fig. D10. Titan Window, MIL-P 8184, Time = 0.05 (Loading); Equiv. Strain (Full range)
This shows the peak strain is 0. 97% in a primarily compressive loading, localized in the lower outside corner of the window. This is well within the linear range and would result in no permanent deformation. Comparing to Figure 9, with the same pressure load, shows the effect of a full pressure cycle.

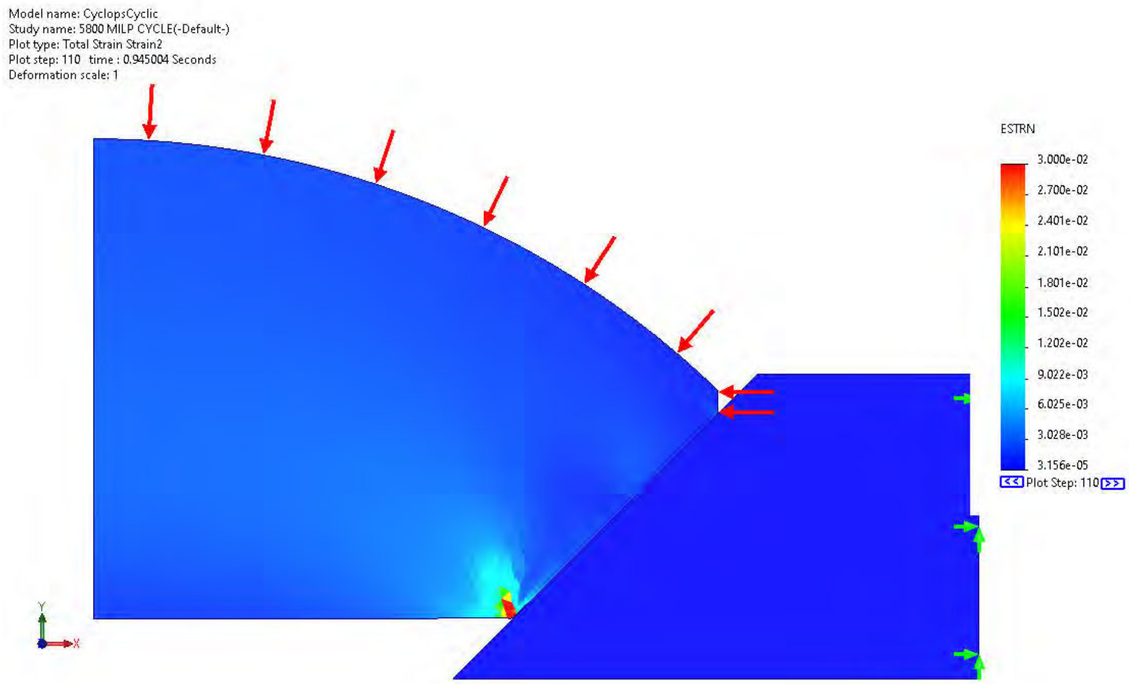

<u>Fig. D11. Titan Window, MIL-P 8184, Time = 0.95 (Unloaded); Equiv. Strain (3% max)</u>
This shows a significant portion of the outside lower corner of the window to have permanent deflection. While some residual strain along the corner is expected, this is a larger than what is experienced with a PVHO-1 conical frustrum designed for this pressure.

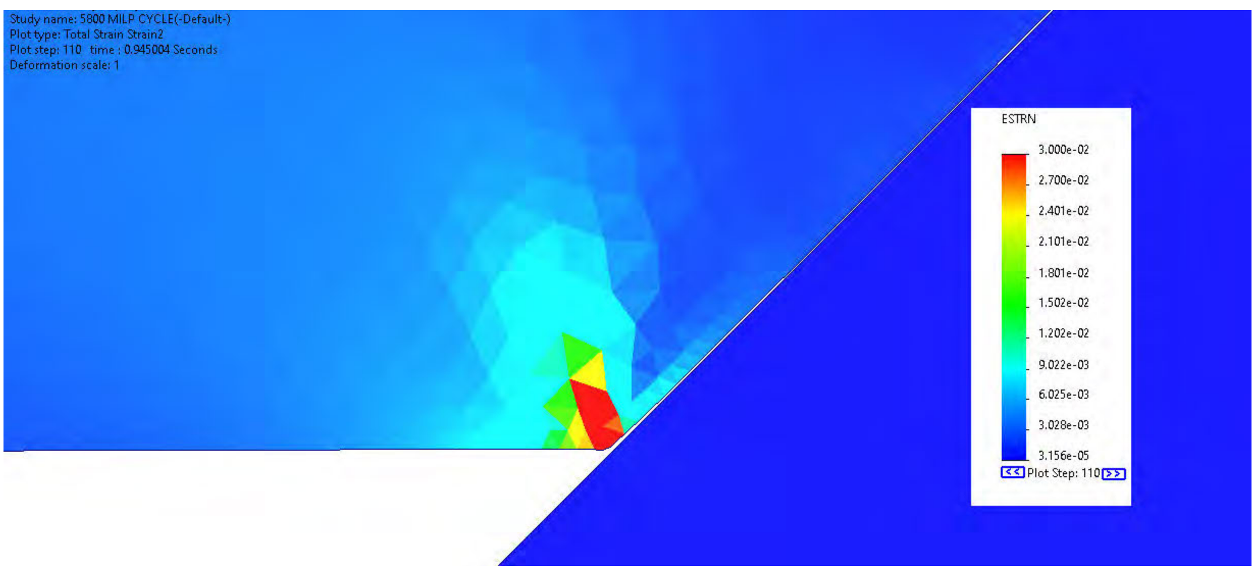

<u>Fig. D12. Titan Window, MIL-P 8184, Time = 0.95 (Unloaded); Equiv. Strain (3% max) Detail view</u>
This shows a close up of the outside lower corner of the window. There is a rounding of the corner that is often machined into this location in a conical frustrum. There is a visible gap between the window and window seat while the upper portion still maintains contact. This indicates a permanent change to the profile such that only the upper section of the window to be in initial contact with the window seat, potentially creating a ratcheting with each subsequent dive allowing progressive inwards deflection.

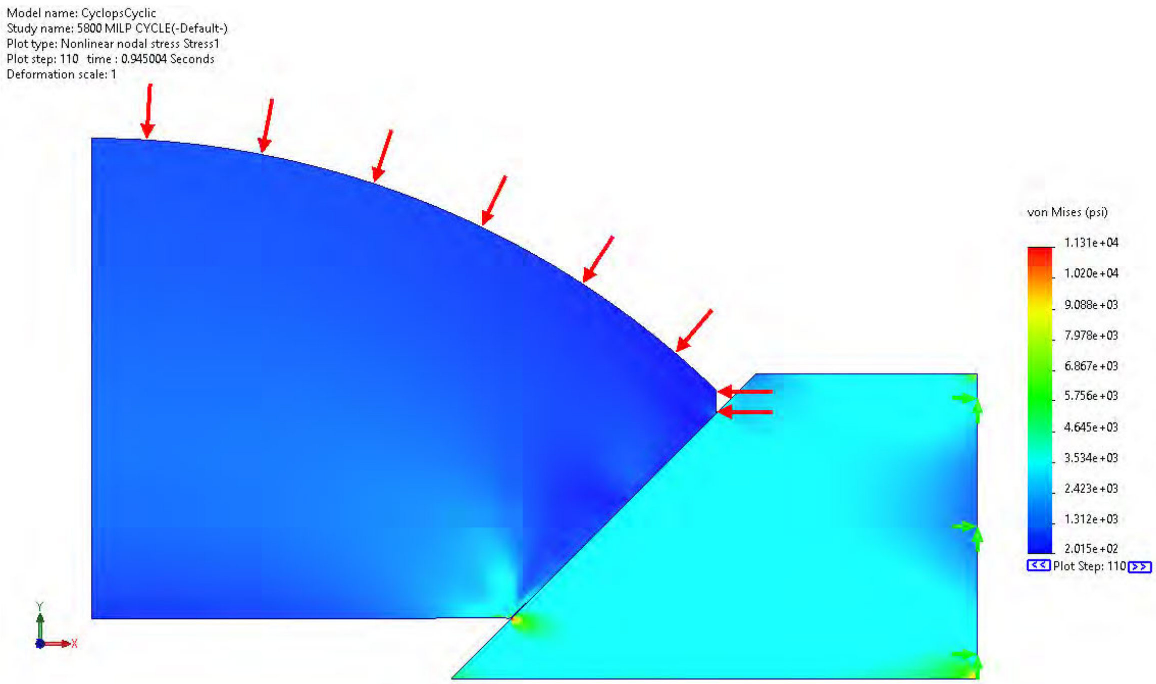

<u>Fig. D13. Titan Window, MIL-P 8184, Time = 0.95 (Unloading); Von Mises Stress (full range)</u>
This shows the stress in the acrylic window and traditional steel window seat. Peak stress is 11,310 psi, but in the acrylic window 3800 psi, well below the 9,000 psi yield strength. The strains shown in Fig. D11 are permanent but the stresses are largely relieved, with some residual stresses in the lower corner.

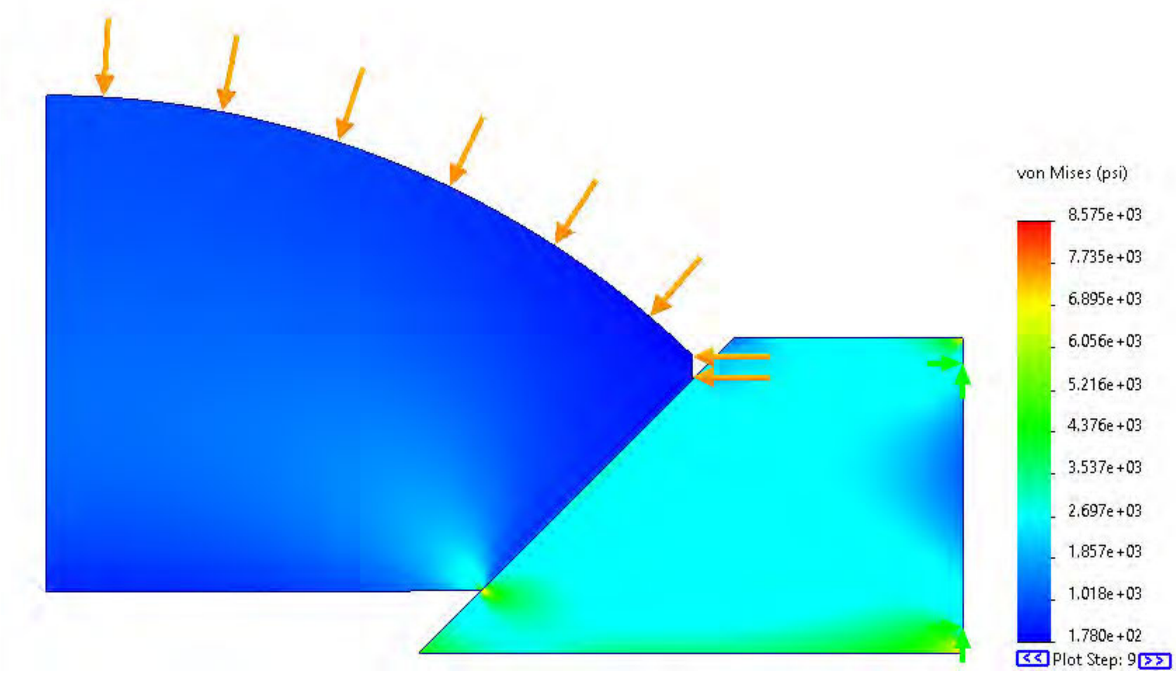

<u>Fig. D14. Titan Window, MIL-P 8184, Time = 0.05 (Loading); Von Mises Stress (full range)</u>
This shows the stress in the acrylic window and traditional steel window seat at around 1000 psi pressure loading. Peak stress is 8575 psi, or 25% less than Fig. 13. Stress in the window 2700 psi and is well below yield. This difference between Fig. D13 and D14 illustrates the nature of the residual stresses after one cycle.

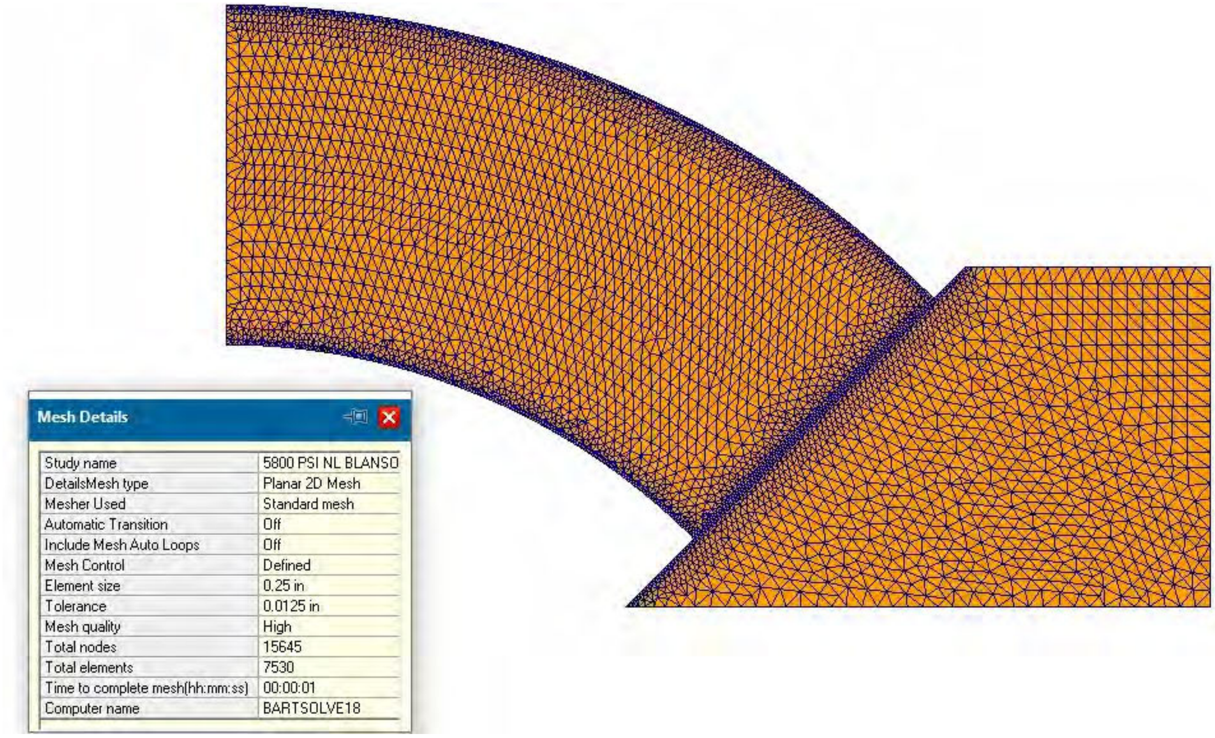

Fig. D15. Spherical Sector, MIL-P 8184, Mesh and model

It was offered by HydroSpace that a ASME PVHO-1 window would be safe and reliable. The summary report submitted to OceanGate was intended to start the conversation, where it analyzed the desired design as well as a conical frustrum, as the failure mode is driven by the section in contact with the seat. For completeness, the ASME design for a window meeting the 5800 psi pressure is presented here. This design uses the same window seat geometry. The design dimensions and ASME design process are shown in App. C. The analysis is an axisymmetric nonlinear model with contact elements to allow the window to slide along the window seat. The same material data is used as the previous model.

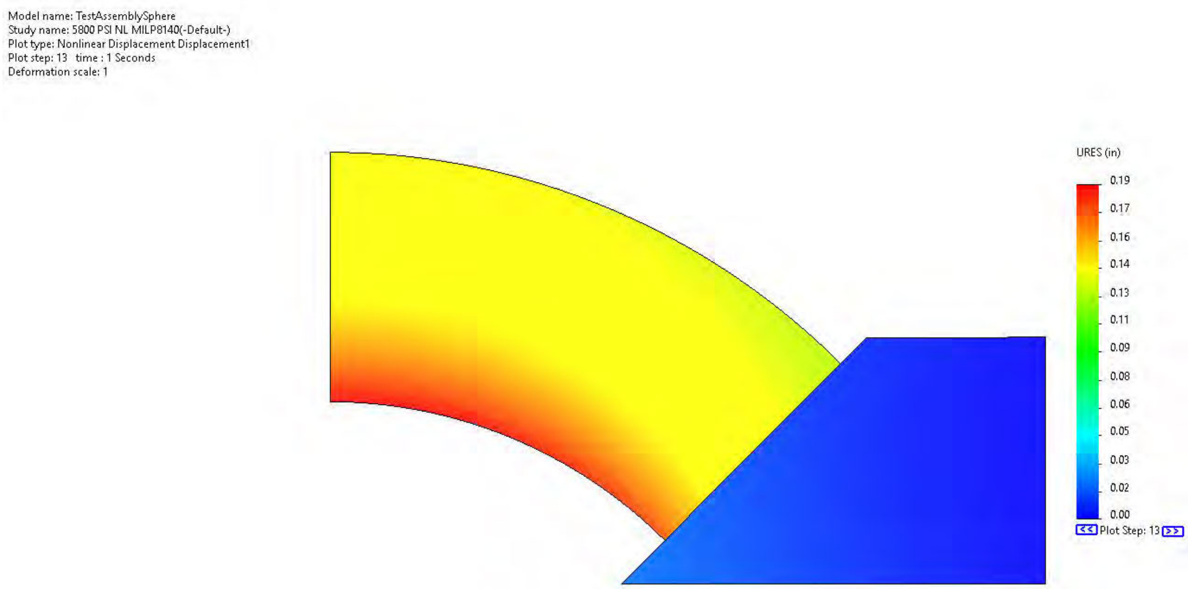

Fig. D16. Spherical Sector, MIL-P 8184, Deflection

Maximum deflection is 0.19 inches at the apex of the inner curved surface. This is comparable to the results in Fig. D3

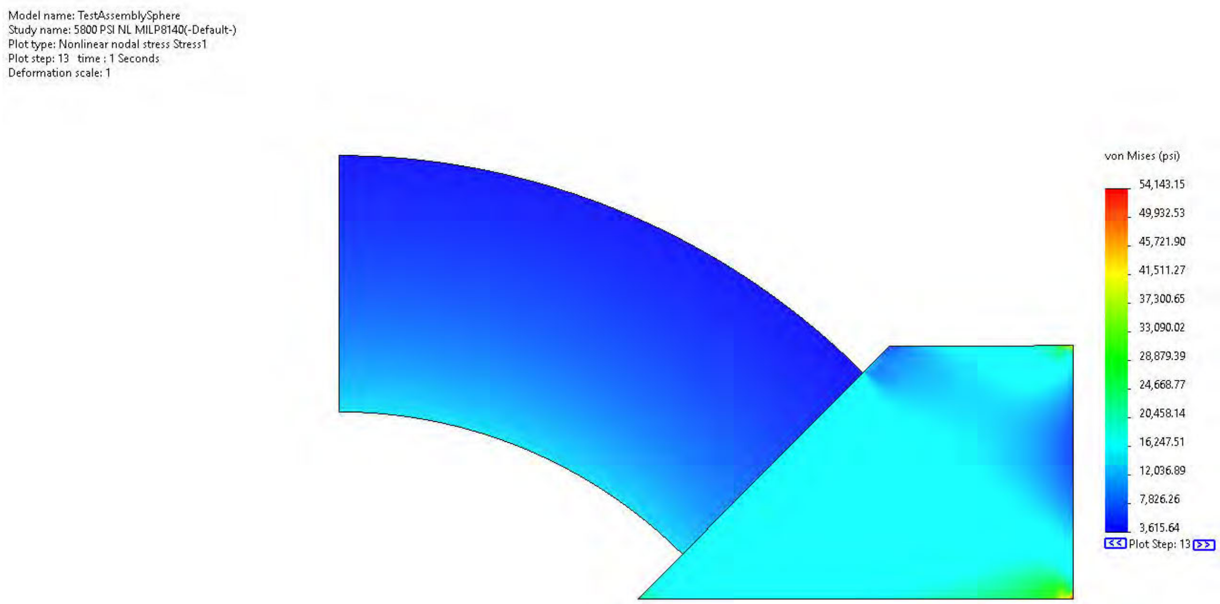

Fig. D17. Spherical Sector, MIL-P 8184, VM Stresses

The stress gradient in the window is generally radial, consistent with the geometry and past studies. Peak stress in the window is around 11500 psi, which is below the allowable peak of 13300 psi. Peak stress is in the window mount's lower outside corner, which reinforces the potential issues of the Titan window seat and hull cap.

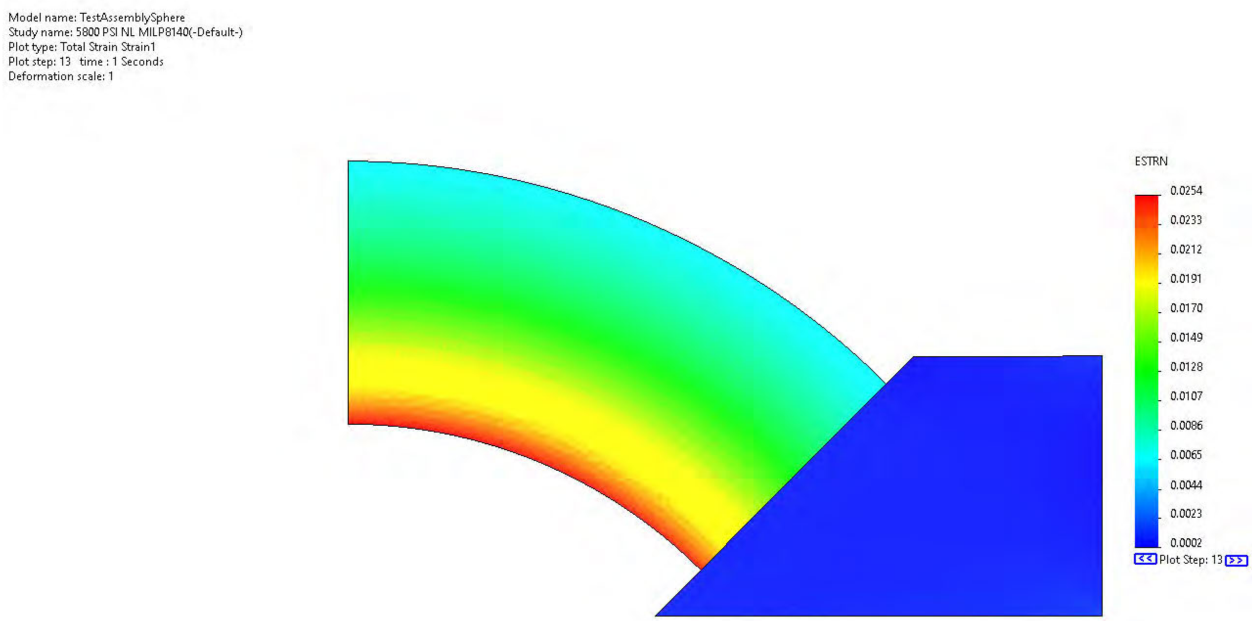

Fig. D18. Spherical Sector, MIL-P 8184, Equiv. Strain

The stress gradient in the window is generally radial, consistent with the geometry and past studies. Peak strain in the window is around 2.5%, which is below the allowable peak of 4.3%. Plastic materials are better gauged by comparing strain than stress since stresses above yield are common in polymers. These are values for 80F which is above the air and water temperatures for the final Titan dive.

CONFIDENTIAL NTSB/USCG

APPENDIX E

CV for [redacted] P.E., DFE

[redacted] III
Lt. Colonel, US Army (Retired)
Professional Engineer, Board Certified Forensic Engineer
P.E., RPEQ, IntPE, CPEng, DFE, CFEI
Fellow, ASME and NSPE
[redacted]

Education:

High School, 1983, Xaverian, Brooklyn, NY
BSME, May 1992, Louisiana State Univ., Baton Rouge, LA
Commissioned Army Reserves, Corps of Engineers (Distinguished Military Graduate)
US Army Corps of Engineers officer training through Command & General Staff College

Technical (selected items)

Finite Element Analysis, ANSYS OEM Course, Houston, TX. 1995
Accident Reconstruction, SAE Professional Educ. Center, Detroit, MI 1999
Base Camp Master Planning (US Army Corps of Engineers) Camp Shelby, MS 2005
Security Engineering & Blast Modeling (Protective Design Center, USACE) Baghdad, Iraq 2006
Supervisors Development Course (US Army) 2013
International Dynamics of Terrorism (INTAC) US Army Corps of Engineers, 2013
USACE Area Office University/Project Management, USACE, Winchester VA, 2013
"Train-the-Trainer" Kirk's Fire Investigation, NAFE 2018 Winter Conference, Phoenix AZ 2018
Counter-Explosive Hazards Planner's Course (US Counter Explosive Hazards Center), FT Wood MO 2018
Attack Site Forensic Investigation Course (National Ground Intelligence Center), FT Polk, LA 2019
Blaster's Course and Annual Conference on Explosives and Blasting Technique (ISEE) 2019
Advanced Surface and Subsurface Drilling Blasting (Mo. Univ. of Science & Technology) 2019
Computational Fluid Dynamics for Structural Designers & Analysts (NAFEMS) 2021
Fire Investigation Training Program (NAFI), New Orleans, 2022

Professional:

Registered Professional Engineer (Multiple jurisdictions)
Board Certified Forensic Engineer (NAFE Diplomate, #965S)
National Association of Fire Investigators (NAFI), Certified Fire and Explosion Investigator
Fellow, American Society of Mechanical Engineers (F.ASME)

- Member of the Pressure Vessel for Human Occupancy (PVHO) Codes and Standards (C&S) Committee
  Chair: Viewports Vice Chair: General Requirements Subcommittee
  Subcommittees: Submersibles, Diving Systems, Design & Piping, Viewports, General Requirements, Post Construction (PVHO2); Medical Systems
  Working Group: "Design by Analysis" for Glassy Polymers; Tunneling PVHOs
- Member, Mobile Uncrewed Systems, Verification & Validation C&S committees and subcommittees
- Active in the Safety Engineering & Risk Assessment Division (SERAD)

Fellow, National Society of Professional Engineers (NSPE)
2021-present NSPE Committee On Policy and Advocacy (COPA)
2019-present NSPE Software Certification Task Group
2018-2020 NSPE Taskforce on Emerging Technology
Senior Member, National Academy of Forensic Engineers (NAFE)
2020-present Editor-in-Chief, Journal of the National Academy of Forensic Engineers
2018-2020 Board of Directors Member as Vice President, Director
2017-present Peer review; Member of the Ethics committee
Member, Louisiana Engineering Society (LES) (State chapter of the NSPE)
President, Baton Rouge Area Section (2001-2002), plus other Section and State offices

Professional Work History:

2006-current Kemper Engineering Services, LLC. Baton Rouge, La.
•Position: VP of Engineering, Principal Engineer
•Principal Responsibilities: Lead engineer, responsible for all work by staff and contract employees. Also in charge of the company's Outreach & Engagement efforts
•Principal Technical Areas: Mechanical design, Machine design, Structural design, Vessel and Piping Design & Analysis, Marine Engineering, Failure Analysis, Blast Modeling, Security Engineering, Finite Element Analysis, Solid Modeling, Kinematic Modeling, Hydraulics, Computational Fluid Dynamics modeling, Reliability, FMEA and Fitness-For-Service studies, Design of Experiment, Accident Reconstruction, Project Management

1992-2020 US Army Reserves (Corps of Engineers Officer)
• Highest Rank: Lieutenant Colonel (Retired)
• Past assignments:
Engineer staff officer, Deployable Command Post, 412th Theater Engineer Command, Vicksburg, MS
Design Chief, Eastern European Infrastructure Development, 301st FEST, Boulder CO
Commander, 475th Engineer Detachment (Explosive Hazards Coordination Cell), Vicksburg MS
Battalion Commander, 2-411th Log. Spt. Bn., 181st Infantry Brigade (1st Army Div West) Ft. McCoy, WI
Officer In Charge for USACE Resident Office, Gardez AFG. Responsible for construction in 5 provinces, $350M.
Team Chief, US SOUTHCOM response team of the USACE Contingency Response Unit, Washington DC
Observer/Controller-Trainer, then O/C-T Team Chief. 1st Group, 1st Brigade, 75th Div., Houston TX
Plans Officer, 420th Engineer Brigade, Bryan Texas
Lead Engineer (FCCME), Det. 8, 412th Engineer Command supporting 130th Engineer Brigade, Balad, Iraq
Mechanical Eng. (FCCME) Det. 1, 412th Engineer Command supporting SETAF, US Army Europe
Mechanical Eng. (FCCME), 412th Engineer Command, Vicksburg, MS. AOR: Republic of Korea
Company Commander, A/489th Engineer Battalion (Corps)(Mech), Hot Springs, Ark
Acting Commander, XO, Platoon Leader, 285th Engineer Company (Combat Spt. Equipment) Baton Rouge, La

1997-2005 Kemper Imageering, Inc. Baton Rouge, La.
•Position: Vice President and Principal Engineer
•Principal Responsibilities: Lead engineer, responsible for all work by staff and contract employees.
•Principal Technical Areas: Mechanical design, Machine design, Structural design, Vessel and Piping Design & Analysis (API and ASME), Failure Analysis, Blast Modeling and Analysis, Finite Element Analysis, Solid Modeling, Kinematic Modeling, Computational Fluid Dynamics, Reliability, FMEA, Project Management
Also a paid consultant for CDI Engineering, Baton Rouge, La 2000-2003.

1992-1997 KnightHawk Engineering, Inc., Baton Rouge, LA
• Position: Mechanical Engineer (EIT), later Marketing Director
• Principal Technical Areas: Pipe Stress, Piping & Vessel Design and Modifications (ASME & API), Hydraulics, Finite Element Analysis, Structural Design and Analysis, Machine Design, Kinematics, Field Work, Project Mgt..
Other Responsibilities: Technical Editing, Marketing, Presentations, Photography.

1990-1992 Self-Employed/College Student, Baton Rouge, LA
• Freelance photographer for Baton Rouge Morning Advocate and State Times, Associated Press, various magazines. Freelance writer and graphic designer.
• Self-financed 100% of tuition, books, fees, plus most living expenses. Sr. Cadet, USAR.

1988-1990 U.S. Army, Fort Bragg, NC
• 82nd Airborne Division Public Affairs Office. Assistant NCO in charge, Darkroom Supervisor, Primary Trainer for new personnel. Co-ordinated and executed print and video coverage. Performed photogrammetry analysis for intelligence section. Participated in training as a "player" in urban warfare, combined arms operations, live fire exercises, airborne operations, and air assault operations as well as amphibious operations with the US Marine Corps. Worked with other units, to include 24th Inf. Div., 10th Mtn. Div, Special Forces, and PsyOps.
• The Paraglide. (Post newspaper, circ. 25,000.) Staff writer/photographer, Features Editor, Darkroom Supervisor.

1987-1988 Freelance Journalist, Writer, Photographer

1983-1986 US Army cadet

Licenses and Certifications:

Certifications

Certified Fire & Explosion Investigator (CFEI) #23392-15345
National Association of Fire Investigators (7/21/2022)
Diplomate of Forensic Engineering (DFE) (Board-certified Forensic Engineer) #965S
The Council of Engineering & Scientific Specialty Board (CESB) Initial 2017, Senior Grade 2019
Anti-Terrorism Officer (AT Level 2, 3)
Department of Defense (7/10/2006, 18/03/2015)
Combat Life Saver (Tactical Combat Casualty Care)
US Army; Camp Shelby, MS (7/27/2005) and Ft. McCoy (5/4/2013)
HAZMAT and Safety In Transportation
US Army Ordnance Corps (8/15/2005)
Construction Quality Management for Contractors
US Army Corps of Engineers (1/25/2004)

Professional Engineer (P.E.)

Alabama (#39546-E, 10/01/2020)
Colorado (#57870, 9/15/2020)
Louisiana (#27736, 1/28/1998) Initial license
Illinois (#62072210, 04/06/2020)
Mississippi (#3188, 08/17/2020)
Missouri (#2022020011, 6/2/2022)
Nevada (#28008, 8/10/2020)
North Carolina (#054730, 7/29/2022)
Texas (#85022, 3/26/1999)
Washington (#20117178, 9/21/2020)

International Engineer

International Board of Forensic Engineering Sciences (#0043, 09/15/2022)
Engineers Australia, National Engineering Register #8606293
Chartered Professional Engineer (CPEng)
International Professional Engineer (IntPE) (Australia)
Asia-Pacific Economic Cooperation (APEC) Engineer
Member of the Institution of Engineers Australia (MIEAus)
Registered Professional Engineer of Queensland (RPEQ) (#26396, 08/13/2021)

Professional Memberships

American Academy of Forensic Sciences (AAFS)
Army Engineer Association (Life Member)
American Society of Civil Engineers (ASCE)
Institution of Engineers Australia (EA)
American Society of Testing and Materials (ASTM)
International Association of Fire Investigators (IAFI)
Institute of Electrical and Electronics Engineers (IEEE)
International Society of Explosives Engineers (ISEE)
International Studies Association (ISA)
Marine Technology Society (MTS)
The International Association for the Engineering Modelling, Analysis and Simulation (NAFEMS)
National Association of Fire Investigators (NAFI)
National Fire Protection Association (NFPA)
Society of Automotive Engineers (SAE)
Society of American Military Engineers (SAME)
Society of Naval Architects and Marine Engineers (SNAME)

CONFIDENTIAL NTSB/USCG

Engineering and Technical Experience:

Machine Design and Kinematics

-Evaluation of human/machine interactions, to include object manipulation, equipment operation, or impact.
-Design or evaluation of crane systems for fabrication yard, tractor crawler cranes, and hydraulic cranes.
-Design of lifting plans including modeling loads on hardware.
-Design of mechanical, mechanical/hydraulic, and mechanical/electrical power transmissions.
-Design of downhole tools.
-Design of K12-L0 vehicle barrier (impact and blast resistance).
-Design of novel vehicle arresting fence system.
-Design of novel subsurface oil recovery system.
-Conceptual design of recycling process, leading to an award of a patent.
-Design, evaluation and redesign of arresting cable and supports.
-Design, analysis, and review of tools, products, equipment, and controls for safety, ergonomics, and reliability
-Design, evaluation and modeling of elevators, walkways, conveyors, and manlifts.
-Design, evaluation and redesign of engines, pumps, fans, and compressors.
-Evaluation and redesign of process agitators and associated equipment.
-Evaluation, design, and redesign of skid-mounted systems and enclosures for equipment, including for lifts
-Evaluation and redesigns of bearings, linkages and power transmissions.
-Design of consumer products, leading to award of patents
-Equipment shock and impact, blast & ballistics
-Welding, fastener, shaft, cam, and spring design and analysis.

Failure Analysis

-Root cause analysis of a failed telescoping platform support in mineshaft.
-Root cause analysis of thermally-induced localized failure of water jacket on a reactor.
-Root cause analysis of a failed piping and pressure vessels.
-Root cause analysis of cracked tubing in heat exchanger, failed furnace tubing, failed process piping.
-Root cause analysis of failed power transmission (gears, linkages) with subsequent redesign.
-Root cause analysis of critical underperformance of water system
-Root cause analysis of failure of protective structures in blast and fragment loading
-Root cause analysis for failed marine and diving equipment.
-Root cause analysis for failed lifting equipment (booms, pad eyes, hooks, links, slings, wire ropes)
-Root cause analysis of biotech cartridge system used in testing biological samples
-Analysis of failed vehicle arresting system prototype with subsequent redesign.
-Analysis of failed bolting on process equipment mounts and structural supports.
-Analysis of failed welds on structural members subjected to upset loads.
-Analysis of failed welds within equipment and with equipment mounts.
-Root cause analysis of failed structural members.

Safety, Reliability, and Fitness-For-Service

- Failure Modes Effects Analysis for a variety of static and rotating equipment, vehicles/airframes, and systems
-Piping, pressure vessels, and saturation diving systems (API 579/ASME FFS1 and ASME PVHO)
-Evaluation of a new offshore pipeline laying system.
-Evaluate of tunneling equipment, including "dry diving" pressure vessel
-Evaluation of control systems for ergonomics, safety, and functional logic for industrial equipment.
-Lead investigator for safety reviews (through U.S. Army)
-Reliability study for increasing a compressor's service pressure.
-Reliability study for electro-mechanical controls for movable barriers
-Reliability study for electro-mechanical controls for life support of medical equipment
-Evaluation of equipment and walkways for ergonomic factors and compliance with safety standards.
-Evaluation of a several vehicle arresting barriers, to include predicting response and correlating with test data.
-Reliability study of incorrectly made modifications on API 650 vessel for compliance with API 653 repairs.
-Evaluation of agitators on vessel heads, including non-standard structural supports, composite material heads
-Reliability studies for weapons systems, to include fatigue analysis per HP White Protocols
-Reliability study for a new 55 cubic yard clamshell crane bucket design for 3rd party review.
-Evaluation of supports, clearances, & operation envelopes for equipment lifts, lifting items, and cranes

- U.S. Patents 8919622, 8919623 "Hands Free Beverage Carrier That Attaches To A Person's Clothing Or A Wearable Accessory" (Co-Inventor), both granted 30 Dec. 2014

- Patent, Republic of Ireland, "Total Municipal Solid Waste (MSW) recovery facility including power generation capability." Grant Number 84128, grant date 8 Feb. 2006. IE20010276A1, 2002.

IP Development: Developed drawings and other support for client seeking patents. Researched existing patents to assist clients in developing new IP. Examined claims of alleged IP infringement.

Peer Reviewed Papers *(* indicates associated presentation)*

Scheduled for Nov. 2024 at ASME Int'l Mechanical Engineering Congress and Exposition

[redacted] (2023) "Deterministic Methods for Verification, Validation, and Uncertainty Quantification in Engineering Code Applications." IMECE2023-114382 *Proceedings of the ASME Int'l Mechanical Engineering Congress and Exposition*, Oct. 29-Nov. 2 2023, New Orleans, LA.

[redacted] (2023) "Review of Life Limitations For Acrylic Windows In Pressure Vessels." IMECE2023-114381 *Proceedings of the ASME Int'l Mechanical Engineering Congress and Exposition*, Oct. 29-Nov. 2 2023, New Orleans, LA.

Kemper, B., P. LaPlante [redacted] Certification." IMECE2023-114381 *Proceedings of the ASME Int'l Mechanical Engineering Congress and Exposition*, Oct. 29-Nov. 2 2023, New Orleans, LA.

Published as of 1 Sept. 2023

Kemper, B. [redacted] Validation, and Uncertainty Quantification 2023 (VVUQ2023), Baltimore, MD, USA, May 2023. DOI: 10.1115/VVUQ2023-108506

[redacted] (2023)* "Evolving Methods for Design by Analysis for Glassy Polymers in Marine Applications." Offshore Technology Conference, Houston, Texas, USA, May 2023. DOI: 10.4043/32369-MS

[redacted] "Artificial Intelligence and Stochastic Terrorism – Should it be done?" 1st Workshop for Assured Autonomy, Artificial Intelligence, and Machine Learning, *Proceedings of the 33rd Int'l Symposium on Software Reliability Engineering*. (Charlotte, NC) DOI 10.1109/ISSREW55968.2022.00091

[redacted] "Attempting to Establish Design Margins for Glassy Polymers in Critical Structural Service." *Proceedings of the ASME 2021 International Mechanical Engineering Congress and* Exposition. (Vol. 13) Safety *Engineering and Risk Analysis* DOI: 10.1115/IMECE2021-71836

[redacted] (2021)*. "Computational Fluid Dynamics Modeling of a Commercial Diving Incident." *Journal of the National Academy of Forensic Engineers*, 38(1). DOI: 10.51501/jotnafe.v38i1.66

[redacted] (2021)*. "Validation of Modern Finite Methods For Glassy Polymers Using Historical Studies." *Proceedings of ASME Pressure Vessel and Piping Conference, 2021* (Virtual) DOI: 10.1115/PVP2021-62146

[redacted] (2021) "Failure Modes for Acrylic Polymers in Section VIII Pressure Vessels." *Proceedings of ASME Pressure Vessel and Piping Conference, 2021* (Virtual), DOI: 10.1115/PVP2021-62148

[redacted] 2020)*. "Misapplication of Pressure Vessel Codes in Forensic Applications." *Journal of the National Academy of Forensic Engineers*, 37(1). DOI: 10.51501/jotnafe.v37i1.67

[redacted] (2020) "Developing 'Design By Analysis' methodology for windows for Pressure Vessels for Human Occupancy." *ASCE-ASME Journal of Risk and Uncertainty in Engineering Systems Part B: Mechanical Engineering*, Volume 6, Issue 3, Sept. 2020. DOI: 10.1115/1.4046742

[redacted] (2019) "Blast Modeling for Facility Security Management." *Proceedings of the 45th Annual Conference on Explosives and Blasting Techniques*, Jan. 27-30, 2019. International Society of Explosives Engineers.

[redacted] (2013)*. "Criteria For Eliminating Cyclic Limit For PVHO Flat Disc Windows." *Joint ASME/USCG Workshop on Marine Technology & Standards*. DOI: 10.1115/MTS2013-0323 [redacted] (2013)*. "Jurisdictional Acceptance of Non-ASME Pressure Vessels for Human Occupancy". *Joint ASME/USCG Workshop on Marine Technology & Stds*. DOI: 10.1115/MTS2013-0322

[redacted] (2007)* "Risk Mitigation and Reliability Lessons Learned From Iraq". *Volume 14: Safety Engineering, Risk Analysis and Reliability Methods*. ASME, 2007 DOI: 10.1115/imece2007-42142

[redacted] (2004) "Evil Intent and Design Responsibility." *Science and Engineering Ethics*, 10(2), 303--309. Opragen Publishing, 2004. DOI:10.1007/s11948-004-0026-4

[redacted] (2002)* "Application of Annealed Cables for Vehicle Arresting Barriers." *Proceedings of the ASME 2002 International Mechanical Engineering Congress and Exposition. Safety Engineering and Risk Analysis*. pp. 61-66. ASME. DOI: 10.1115/IMECE2002-32464

Select Conference Papers, Publications and Presentations *(*associated presentation)*

"Industry Leaders' Perspectives and Outlook of Systems and Software Engineering for the Industrial Engineering Community" Ben Amaba, Sonatype; Leon McGinnis, Georgia Tech University, Atlanta, GA; Dr. Phil Laplante, Penn State University;, Dr. Jeff Daniels, Lockheed Martin Corporation; Cliff DeBerry, Memphis Light Gas and Water; Bart Kemper, Kemper Engineering Services, LLC; Andrei Popa, Chevron Technical Center; Kent Welter, NuScale Power; Eren Yilmaz, Black and Decker, Winspyre. Moderator: [redacted], Kemper Engineering Service. Institute of Industrial & Systems Engineering (IISE) Annual Meeting, New Orleans, La. May 2023

"Security and the Infrastructure Design." Part of the panel discussion "Complexity & Security: Theorizing Within and Beyond Limits", International Studies Association Annual Conference, Montréal, Canada. March 2023

"Don't Do That! Lessons learned in forensic engineering." 27th Louisiana Joint Engineering Societies Conference. Lafayette, La. Feb. 2023

[redacted] "The Perils of Using Linear Analysis for Metal Component Failures" *Proceedings of American Academy of Forensic Scientists 75th Annual Scientific Meeting,* Feb. 16-17, 2023. (Orlando, Fl.)

[redacted] "Advancing Towards Design By Analysis for Glassy Polymers". *Proc. of 19th Submarine Symp*, Marine Technology Society. Nov. 30-Dec.2, 2022 (New Orleans, La.)

[redacted] "Simulation Triad for Evaluating Use of Engineering Simulation." *Proceedings of American Academy of Forensic Scientists 74th Annual Scientific Meeting,* Feb. 21-25, 2022. (Seattle, Wa.)

"Throwing the Flag: Guidelines for Assessing Engineering Simulation." National Academy of Forensic Engineers Winter Meeting, Tucson, Az. Jan. 6, 2022

[redacted] "THE ALEXANDER Research Submersible". OCEAN SHOTS, National Academy of Sciences. Sept. 15, 2021

"COVID-19 Engineering Mitigations and Liability" with Curt Freedman, PE. National Academy of Forensic Engineers Summer Conference, Providence, Rhode Island. July 31 2021

"Modern Capabilities of Forensic Engineering and Technical Expertise." Presented to the Uzbekistan Republic's *Suleymanova Centre Of Forensic Expertise*, in collaboration with the UN Office on Drugs and Crime (UNODC) and the American Academy of Forensic Sciences (AAFS). June 30, 2021

[redacted] "Fatal Hyperbaric Treatment Explosion Investigation Incorporating Engineering Simulations with Verification & Validation." *Proceedings of American Academy of Forensic Scientists 73rd Annual Scientific Meeting* Feb. 15-19, 2021. (Virtual)

[redacted] "Developing 'Design by Analysis' Methods for Glassy Polymers for Pressure Vessels." Poster, Pressure Vessel track. *ASME International Mechanical Congress & Exposition*. Nov. 16-19, 2020 (Virtual)

[redacted] "Debarkation Syndrome as a Technology-Induced Neurological Condition." Poster, Biomedical track. *ASME International Mechanical Congress & Exposition*. Nov. 16-19, 2020 (Virtual)

"Design by Analysis for Glassy Polymer Structures." *Underwater Intervention 2020*. New Orleans, La. Feb. 2020

"Debarkation Syndrome and Commercial Submarines." [redacted] *17th Manned Underwater Vehicles Symposium*. New Orleans, La. Feb. 2020

"Introduction to Forensic Engineering and the National Academy of Forensic Engineers." 24th Louisiana Joint Engineering Societies Conference. Lafayette, La. Jan. 2020

CONFIDENTIAL NTSB/USCG

[redacted] "NEMO joint design in ASME PVHO Code". *16th Manned Underwater Vehicles Symp.*, Marine Technology Society, New Orleans, La. Feb. 2019. DOI: 10.13140/RG.2.2.24600.85768/1

[redacted] "Shortfalls in polymer specifications for PVHOs." *Proceedings of Underwater Intervention 2019*. New Orleans, La. Feb. 2019. DOI: 10.13140/RG.2.2.32884.60807/1

[redacted] "Heat Retention and Structural Integrity of Glassy Polymer Windows," 15th Manned Underwater Vehicle Symp., Marine Tech. Soc., New Orleans, LA, Feb. 2018 DOI: 10.13140/RG.2.2.36321.02405

[redacted] "Truck Bombs and Standoff: Using Blast Modeling for Installation Threat Management." Engineer, The Professional Bulletin of Army Engineers, Sept-Dec. 2017

"Forensic Investigation of Oxygen Chamber Fire". ASME PVHO Codes & Standards, San Diego, CA Feb. 2017.

"Design of Undersea Viewports for Pressures over 10,000 PSI." With Linda Cross, EI. 14th Manned Underwater Vehicles Symposium, Underwater Intervention, New Orleans, February 2017 DOI: 10.13140/RG.2.2.10758.27204

"Use of Finite Element Analysis in Designing Acrylic Structures for Fatigue and Stress." With [redacted] 13th Manned Underwater Vehicles Symposium, , New Orleans, February 2016. DOI: 10.13140/RG.2.2.26146.12482/2

"Contracting Engineering & Construction in Expeditionary Environments." 20th Louisiana Joint Engineering Societies Conference. Lafayette, La. Jan. 2016

"Novel Subsurface Oil Recovery System Concept." With Krista Kemper. Underwater Intervention 2013, New Orleans La, Jan. 2013.

[redacted] "US Coast Guard Acceptance of Non-ASME Pressure Vessels for Human Occupancy." *Proceedings of Underwater Intervention 2012*. Published by the Marine Technology Society, Jan. 2012.

[redacted] "Mitigating Potentially Weaponized Natural Phenomena." *Responder Rundown Newsletter*. CBRNE Resource Network. Dec. 2011.

"Introduction to Engineering Codes & Standards" Presented to the LSU Mechanical Engineering Senior Capstone Design course. 2010 - 2012, 2015 Also University of Louisiana (Lafayette), 2015-2022, Southern University (Baton Rouge) 2022

[redacted] "HE Sorbent/Barrier Belt Independent Technical Review". May 2010 Report number: ONX100510. DOI: 10.13140/RG.2.2.32411.36646

"Performance Based Standards: The New Approach" 14th JESC, Jan. 2010 in Lafayette, La.

"Introduction to Security Engineering." 13th Joint Engineering Societies Conference, Jan. 2009 in Lafayette,, La.

"Engineering Lessons Learned in Iraq." 11th Joint Engineering Societies Conference, Jan. 2007 in Baton Rouge, La. as well as to the Baton Rouge Section of ASME December, 2008.

[redacted] "More Than Management." *Engineer, the Professional Bulletin of Army Engineers*, July-Sept. 2006

[redacted] "Building a Construction Management Section for Iraq." *Army Engineer Magazine*, July-August 2006.

"Using Advanced Engineering Software in Forward Deployed Areas" US Armed Forces Base Camp Design Workshop, May 2005 at the United States Military Academy, West Point NY.

"Evil Intent and Design Responsibility." Ethics in Engineering Conference, Oct. 15, 2003, New Orleans, La; 7th Joint Eng. Soc. Conf., Feb. 2004, Baton Rouge, La.; US Base Camp Design Workshop, West Point NY April 2004.

"Professional Licensure and Ethics." Regional speaker for the National Council of Examiners for Engineering and Surveying (NCEES), 2001-2003. Exam review and validation May 2002.

"The New Professional Engineer Exam." Presented to the Baton Rouge Section of ASME Nov. 2002.

Selected and participated in reviewing and validating the U.S. national Principles and Practice Examination for Mechanical Engineering. (NCEES, Atlanta, Ga. May 2002.)

"Professional Licensure and Ethics." Regional speaker for the National Council of Examiners for Engineering and Surveying (NCEES), 2001-2003.

"Engineering Applications of Animation." Feb. 1999, 4th Louisiana Joint Engineering Societies Conference, New Orleans, La.

Committee Publications:

Emerging Technology: A Public Regulatory Policy Guide. Member of the Emerging Technology Task Force. National Society of Professional Engineers. September 2020.

ASME PVHO-1-2019 Safety Standard for Pressure Vessels for Human Occupancy (An American National Standard). Main committee member and member of all subcommittees. American Society of Mechanical Engineers, NY NY, 2019. Also co-authored the 2012, 2016 versions.

ASME PVHO-2-2019 Safety Standard for Pressure Vessels for Human Occupancy: In Service Guidelines (An American National Standard). Main committee member and member of the Post-Construction subcommittees. American Society of Mechanical Engineers, NY NY, 2019. Also co-authored the 2012, 2016 versions.

Journal of the National Academy of Forensic Engineers. ISSN: 2379-3252 Editor In Chief, 2020-current; Associate Editor, Peer Reviewer 2017-2020

Guidelines for Engineering Standards of Practice for the Design of Mechanical Systems, Louisiana State Board of Registration for Professional Engineers and Land Surveyors (LAPELS). January 2012.

STP-PT-047 Principles of Safety and Performance for Medical Hyperbaric Chambers: Guidelines for Regulatory Submissions. Member of the ASME PVHO Subcommittee on Medical Hyperbaric Systems. June 30, 2011

SeaSteading Engineering Report Part 1: Assumptions & Methodology. Primary author: Eelco Hoogendoorn. Technical Review: Miguel Pardo, Bart Kemper, Alexia Aubault, Michael Santos. February, 2011

Cited as Primary Source:

UK Patent GB2600490A, "Oil capturing apparatus" [redacted] 04 May 2022

[redacted] "Artificial Intelligence in Critical Infrastructure Systems" in *Computer*, vol. 54, no. 10, pp. 14-24, 2021. doi: 10.1109/MC.2021.3055892

[redacted] "How Small Arms Capabilities Shape Decisions at Battalion and Brigade Level". DTIC Accession Number ADA56719 Report date 27 Sept. 2012.

[redacted] "Developing Base Camps to Support Military Operations Worldwide". *Proceedings from the 2005 ASEM National Conference*, Virginia Beach, VA

Select Conferences:

4th Annual International Scientific and Practical Conference (Kyiv Scientific Research Institute of Forensic Expertise), Kyiv, UKR, 2022
1st Workshop for Assured Autonomy, Artificial Intelligence, and Machine Learning, Charlotte NC 2022
US Decade of the Ocean Launch (National Academies of Sciences, Engineering, Medicine), Virtual, 2021
7th World Congress of Biomechanics, Boston, MA 2014
Offshore Technology Conference, Houston, TX 2011, 2012, 2023
US Armed Forces Base Camp Design Workshop, West Point NY 2004, 2005
2nd International IED Defeat Workshop, Fort Irwin CA 2005
Ethics and Social Responsibility in Engineering and Technology, New Orleans LA 2003

American Academy of Forensic Scientists
Annual Scientific Conference of AAFS; 2021-2023
American Society of Industrial Security
Physical Security: Advanced Applications and Technology; 2005
American Society of Mechanical Engineers
International Mechanical Engineering Conference and Exposition; 2002, 2007, 2020, 2021
Pressure Vessel and Piping Conference; 2021
Joint ASME/USCG Workshop on Marine Technology & Standards; 2008, 2013
Verification, Validation, and Uncertainty Quantification; 2021, 2023
International Studies Association

ISA Annual Meeting: 2023 (Montréal, CAN)

International Society of Explosives Engineers

Annual Conference on Explosives and Blasting Techniques; 2019

Louisiana Engineering Society

Joint Engineering Societies Conference; 1995-2001, 2004, 2007-2011, 2016, 2020, 2023

Marine Technology Society

Submarine Symposium (co-located with Underwater Intervention); 2012-13, 2016-20, 2022

National Academy of Forensic Engineers

Winter Conference; 2017-2023

Summer Conference; 2021

Honors and Recognitions:

Fellow, National Society of Professional Engineers (April 2023)

Dudley Hixon-Bobby Price National Professional Achievement Award, Louisiana Engineering Society (Feb. 2023)

Fellow, American Society of Mechanical Engineers (March 2022)

ASME Certificate of Acclamation for contributions for the Safety Standard PVHO-1: 2016 (October, 2016)

2007 Army Engineer of the Year; Top Ten Federal Engineer of the Year (NSPE's Federal Engineer of the Year recognition program, presented 22 Feb. 2007 at the National Press Club, Washington DC)

Young Engineer of the Year, Baton Rouge Chapter of the LES, Feb. 2000

Chrome Shaft Award. Presented by the LSU Mechanical Engineering Faculty. May 1992.

Military awards include: Bronze Star (w/Oak Leaf Cluster), Meritorious Service Medal (w/2 Oak Leaf Clusters), Army Commendation Medal (w/Oak Leaf Cluster), Humanitarian Service Medal, NCO Development Ribbon, Combat Action Badge, Basic Parachutist Badge